Report No.: SIR-95-017
Revision No.: 0
Project No.: ANO-10Q
File: ANO-10Q-402
February 1995

Flaw Acceptance Standards for Arkansas Nuclear One Unit 1 Reactor Pressure Vessel Weld Inspections

Prepared for:

Entergy Operations

Prepared by:

Structural Integrity Associates
San Jose, California

Prepared by: _____ Date: 2/22/95
N. G. Cofie

Reviewed by: _____ Date: 2/22/95
A. F. Deardorff

Approved by: _____ Date: 2/22/95
N. G. Cofie

Table of Contents

List of Tables

List of Figures

1.0 INTRODUCTION

In preparation for the second ten-year in-service inspection (ISI) of the reactor pressure vessel at Arkansas Nuclear One Unit 1 (ANO-1) during the February 1995 outage (1R12), Entergy Operations Inc. contracted with Structural Integrity Associates (SI) to develop flaw acceptance diagrams for the shell-like regions of the vessel to allow for rapid evaluation of flaws in the case that flaw indications are found during the vessel examinations. Similar previous evaluations were performed during the first ten-year ISI interval by Babcock and Wilcox in Reference 1. However, the Reference 1 report considered only inside surface flaws and it is only valid up to the second ten-year ISI. The present analysis updates the Reference 1 evaluation such that the flaw acceptance diagrams can be used until the end of plant life. In addition, it also addresses both surface and subsurface flaws and incorporates new flaw and materials evaluation methodologies that have been developed since the Reference 1 report was published.

This report contains a definition of acceptable flaw sizes that can be used during the vessel inspection to perform rapid assessment of flaw indications. These flaw acceptance guidelines are provided in graphical format in the appendices of this report and are based on the methods contained in ASME Section XI [2]. The evaluation methods have been supplemented by more sophisticated evaluation techniques, where Section XI, Appendix A, may not be completely definitive for the evaluation (e.g., for cladding stress intensity factors). An evaluation of vessel materials and thicknesses has resulted in a conservative grouping of potentially-flawed locations to limit the number of flaw evaluations to a manageable number. Thus, the graphical acceptance standards included herein are intended to be conservative but need not serve as the only basis for performing Section XI flaw evaluations.

Section 2.0 of this report describes the methods of analysis and the assumptions that have been made in conducting the analysis. Reading and understanding the information included therein is important to understand the limitations inherent in conducting an evaluation of all possible flaws that might exist in the vessel.

Section 3.0 presents an evaluation of the specific materials and welds for the ANO-1 reactor vessel and shows how they were grouped to limit the number of evaluations conducted. The design input (stresses, load cases, etc) that forms the basis for the analysis is included.

Section 4.0 presents and describes the results. Section 5.0 summarizes the findings and restates the limitations with respect to the results presented in this report.

2.0 EVALUATION METHODOLOGY

2.1 Overview of Section XI Evaluation Procedures

The rules for evaluation of flaws in reactor vessels are contained in IWA-3000, IWB-3500 and IWB-3600 of Section XI of the ASME Boiler and Pressure Vessel Code [2]. Appendix A of Section XI provides specific methodology that may be used for detailed fracture mechanics evaluations. The following provides an overview of the Section XI evaluation approach.

In the first step of vessel flaw evaluation, the indications from vessel inspections must be characterized per the requirements of Section XI Article IWA-3000. This requires that the indications be bounded by a rectangular shape with depth (**a** for surface flaws and **2a** for subsurface flaws) and length (ℓ) that will completely contain the suspected material flaw. Closely adjacent flaws must be linked together based on criteria contained in IWA-3000. Similarly, flaws closely adjacent to the base metal surface must be assumed to be surface flaws, based on criteria presented in the code.

The next step in the vessel flaw evaluation is to compare the flaw with the evaluation standards included in Table IWB-3510-1. This table provides the size of allowable planar flaws that may be accepted without further evaluation. Table IWB-3510-1 defines allowable sizes for surface and subsurface flaws as a function of wall thickness, flaw aspect ratio ($\mathbf{a}/\ell$) and flaw depth ratio (**a/t**), where **t** is the base metal thickness.

If the indication is larger than may be accepted by IWB-3510-1, then additional analytical evaluation is allowed per IWB-3600. These evaluations are based on the total wall thickness including cladding. Again, flaws located closely adjacent to the surface must be evaluated

as surface flaws based on criteria in IWB-3000. Flaws located completely within the vessel cladding are acceptable with no further evaluation. Key points of the evaluation include:

- The criteria allow acceptance by specifying a factor of safety on either the size of the critical flaw, or a factor of safety on the stress intensity factor.

- Separate evaluations are required for Normal/Upset and Emergency/Faulted conditions, with different factors of safety for each.

- Additional consideration is given to areas near structural discontinuities (e.g., for welds near a flange) by allowing alternate factors of safety for low-pressure operating conditions.

Appendix A of Section XI provides a detailed procedure for vessel flaw evaluation. To perform the analysis, the following factors must be considered:

- The flaw must be characterized and resolved into a shape that can be evaluated. This includes determination of the depth ratio (a/t) and the aspect ratio (a/ℓ) of the flaw. For subsurface flaws, the eccentricity ratio (e/t) must be determined, where e is the distance from the center of the vessel wall (including cladding) to the center of the flaw.

- Stresses and the temperature at the location of the flaw must be determined for all loading conditions.

- The flaw stress intensity factor and critical crack size must be calculated, either by using the equations, charts, and tables of Appendix A of Section XI or through use of other more sophisticated, documented analytical techniques.

- The material properties must be defined at the location of the flaw, including the effects of irradiation.

- The crack growth that can occur during the evaluation interval must be determined (e.g., to the next inspection or to the end of life).

- The flaw size at the end-of-evaluation period must be less than that allowed by Section XI.

- The primary stress limits of the original design code Section III, (NB-3000) must also be met assuming a local area reduction of the pressure-retaining membrane that is equal to the area of the characterized flaws.

2.2 Specific Details of Evaluation Methodology

2.2.1 Stress Intensity Factors

Appendix A of Section XI provides a basic methodology for evaluating vessel flaws. However, there is limited guidance for the determination of stress intensity factors for cracks extending through cladding. In addition, the guidelines are very limited for determining the stress intensity at the surface for surface flaws. The following describes how the stress intensity factors were determined for the ANO-1 RPV evaluation.

Appendix A Methods

For all stresses, except for those due to cladding for an internal surface flaw, the methods of Appendix A are used for the deepest point of surface flaws and for subsurface flaws.

Surface Stress Intensity Factors (except for cladding)

For surface stress intensity factors for surface flaws, M_m and M_b, as defined in Appendix A of Section XI, have been determined based on the Raju/Newman membrane and bending

solutions [3] for the worst case of internal and external cracks for a vessel with thickness-to-radius ratio of 0.1. For flaws with an aspect ratio (a/ℓ) of zero, the surface stress intensity factor is assumed to be zero since an infinitely long crack does not have a surface point. The so-determined surface stress intensity factor is applied at the cladding-to-base metal interface for the vessel inside surface.

Cladding Stress Intensity Factor

For cladding stresses for a long inside-surface flaw, the stress intensity factor at the deepest point of the flaw is determined by integration of the stress over the crack face for an edge-cracked plate using the methods from Tada and Paris [4].

$$\overline{K_I} = \frac{2}{\sqrt{\pi a}} \int_o^a m(x) \cdot \sigma(x)\, dx \qquad (1)$$

where: $\sigma(x)$ = cladding stress distribution in cladding and base metal as a function of distance (x) from clad surface

a = crack depth

$$m(x) = \frac{3.52(1-a^*)}{(1-t^*)^{1.5}} - \frac{4.35 - 5.28a^*}{(1-t^*)^{0.5}} \qquad (2)$$

$$+ \left[\frac{1.3 - 0.3(a^*)^{1.5}}{(1-(a^*)^2)^{0.5}} + 0.83 - 1.76a^*\right] \cdot \left[1-(1-a^*)t^*\right]$$

where: $a^* = x/a$

$t^* = a/t$

t = wall thickness

As shown in a paper by Kuo, Deardorff, and Riccardella, [5], this solution yields a stress intensity factor that has reasonable comparison to "exact" solutions, but is unrealistic and increases significantly for deep-wall cracks in a pressure vessel. Thus, it is assumed that the

deep-wall stress intensity factor increases by no more than described by the following:

For $a \leq a_{min}$,

$$K_I' = \overline{K_I} \tag{3}$$

For $a > a_{min}$

$$K_I' = \text{lesser of } \overline{K_I}$$

or

$$\overline{K_{I,min}} \sqrt{\frac{a}{a_{min}}} \tag{4}$$

where:

$\overline{K_{I,min}}$ = minimum $\overline{K_I}$ in base material

a = crack depth size

a_{min} = a at $\overline{K_{I,min}}$

To account for the flaw aspect ratio, the stress intensity factor is corrected using the shape factor of Appendix A of Section XI for the crack.

$$K_I = K_I' \left(\frac{Q_o}{Q} \right)^{0.5} \tag{5}$$

where: Q_o = shape factor for flaw with aspect ratio of $(a/\ell) = 0$

Q = shape factor for flaw with aspect ratio (a/ℓ) being evaluated

The stress ratio (the other factor affecting Q) is determined based on membrane plus bending stress ($\sigma_m + \sigma_b$) for the flaw, exclusive of the cladding stresses at the crack. Since

a ratio is being determined, this approach is reasonable.

The stress intensity factor at the cladding surface is not evaluated. However, the stress intensity factor for the cladding-to-base metal interface location is evaluated as if it were at the surface. The cladding stress intensity factor (determined by Equation 1 above) for a flaw depth equal to the thickness of the cladding (with the same aspect ratio as the deeper flaw being evaluated) is determined. It is then modified based on the ratio between the membrane stress intensity correction factors for the surface (using the Raju/Newman, M_m) and the crack tip (using the Appendix A, M_m). Although not rigorously derived, this formulation is believed to be conservative for this analysis.

For flaws with aspect ratio of zero ($a/\ell = 0$), there is no surface crack. Therefore the stress intensity factor due to cladding at the "surface" is evaluated as zero.

2.2.2 Fracture Toughness

The fracture toughness, K_{Ia} or K_{Ic}, is obtained from Section XI Appendix A. The analyzed vessel wall local fracture toughness, at the location of the associated crack stress intensity factor, is determined with consideration of local temperature (as a function of wall depth), initial RT_{NDT}, local fluence, margins and chemistry factors in accordance with the methods of Regulatory Guide 1.99 Revision 2 [6]. The approach is as follows:

$$ART = RT_{NDT,i} + RT_{NDT}\ Shift + Margin \qquad (6)$$

where:

ART = Adjusted Reference Temperature, °F

$RT_{NDT,i}$ = initial RT_{NDT}, °F

Margin = required margin = $2\sqrt{\sigma_i^2 + \sigma_\Delta^2}$, °F

(RT_{NDT} Shift, σ_i, and σ_Δ are defined below)

The margin is determined based on the standard deviation of the initial RT_{NDT} (σ_i) and that of the RT_{NDT} shift (σ_Δ). The standard σ_Δ is 28°F for welds and 17°F for base metal

[6], except that σ_Δ need not exceed 0.5 times the computed shift in RT_{NDT}.

$$RT_{NDT}\ \text{Shift} = (CF) \cdot (FF) \tag{7}$$

where:

CF = chemistry factor, °F

FF = fluence factor, dimensionless

$$FF = f^{(0.28 - 0.1 \log_{10}(f))} \tag{8}$$

where:

f = local fluence, neutrons/cm^2 x 10^{19} (E>1MeV)

The local fluence, f, at any position in the wall may be calculated from:

$$f = f_{surf}\, e^{-0.24x} \tag{9}$$

where:

f_{surf} = fluence at inside surface, neutrons/cm^2 x 10^{19} (E>1MeV)

x = distance from inside surface, inches

The fluence at the surface is a function of time:

$$f_{surf} = \frac{f_{ref}}{EFPY_{ref}}\ x\ EFPY \tag{10}$$

where:

f_{ref} = reference surface fluence , neutrons/cm^2 x 10^{19} (E>1MeV)

$EFPY_{ref}$ = effective full power years associated with f_{ref}

EFPY = effective full power years for evaluation

This allows the adjusted reference temperature to be calculated for the beltline region at any depth, at any time, and for each specific weld or plate being evaluated. For regions not in the beltline region, there is no shift in RT_{NDT}.

2.2.3 Crack Growth Considerations

A conservative estimate of the crack growth for determining allowable subsurface and outside surface flaws is based on the crack-growth curve for air of Section XI Appendix A, using the latest formulations from the 1992 Edition with 1993 Addenda. A conservative estimate of the number of cycles to the end of the evaluation period is made. For inside surface flaws, the water curve-growth is used. In all cases, the crack growth is based on R = 1.0, where R is the ratio of the minimum crack tip stress intensity factor to the maximum stress intensity factor (K_{min}/K_{max}). The stress intensity factor at the allowable flaw size for each flaw is used in this evaluation. For flaws accepted by the evaluation standards of Table IWB-3500-1, there is no requirement to consider crack growth.

2.2.4 Subsurface Flaw Size Considerations

For subsurface flaws, the maximum allowable size that does not have to be considered as a surface flaw per the requirements of Table IWB-3510-1 or Figure IWB-3610-1, as applicable, is determined based on flaw eccentricity as follows:

$$\left(\frac{a}{t}\right)_{max} = \frac{0.5 - |e/t|}{1.4} \qquad (11)$$

where:

t = thickness of vessel base material (for IWB-3500 evaluation), or total thickness of vessel wall including cladding (for IWB-3600 / Appendix A evaluation)

e = flaw eccentricity, measured from center of vessel wall, (determined with or without cladding as appropriate), negative if toward inner vessel wall

2.2.5 Definition of Allowable Flaw Size and Shape

In evaluating hypothetical flaws, such as evaluated herein, one is faced with the problem of determining the size of the allowable flaw. In some cases, larger flaws may be acceptable as compared to smaller flaws. This is especially true when there is a large bending component to the throughwall stress distribution, the fracture toughness through the wall is not constant due to irradiation embrittlement and/or if cladding stresses are a significant contribution to the stress intensity factor. Also, if the surface stress intensity factor is controlling, a flaw with a smaller aspect ratio (more extent of flaw length) may be acceptable when a similar depth flaw with less flaw length would not be acceptable. There are several choices that can be made in choosing the allowable flaw size at a location:

- **Option 1**: Accept the largest flaw with the smallest aspect ratio that is acceptable. In this case, a larger flaw (depth and/or length) may be acceptable whereas a smaller flaw would not be acceptable. This is analogous to evaluating an actual flaw by assuming a larger bounding flaw size or length.

- **Option 2**: The most conservative approach is to determine the minimum flaw size that is acceptable for the flaw aspect ratio being evaluated.

- **Option 3**: In some cases, the surface stress intensity may control the allowable flaw depth, especially when cladding stresses are being evaluated or if the surface fracture toughness is low. However, a longer flaw (e.g., $a/l = 0$) might be acceptable. For this option, the acceptable flaw size is based on the smallest acceptable flaw depth (as in Option 2) but the aspect ratio can be assumed to be smaller (the flaw is assumed to be longer) than for the actual aspect ratio being evaluated.

In the evaluations included in this report, the first option has been chosen since the stress intensity factor solution for surface stresses and cladding are believed to be quite conservative.

The stress intensity factor within the cladding does not have to be evaluated for acceptability. Thus, the allowable inside surface flaw size will always be at least equal to the cladding thickness plus that allowed by the acceptance standards of IWB-3500.

2.3 Analysis Implementation

The analysis presented within this report has been prepared using a computer program developed and verified by SI for this specific purpose. APPENDA (standing for Appendix A Analysis) [7] is a computer program written to perform reactor pressure vessel flaw evaluation in accordance with Appendix A of Section XI and Subarticle IWB-3600 of Section XI of the ASME Boiler and Pressure Vessel Code [2]. It uses the methodology described above, and determines allowable inside surface, outside surface and subsurface flaws. It is intended to provide a rapid assessment of all possible flaws so as to allow construction of flaw acceptance diagrams that may be used to provide guidance in reactor vessel inspections.

APPENDA performs an evaluation to determine the acceptable size of surface and subsurface flaws in accordance with the requirements of ASME Code Section XI, Appendix A and subarticle IWB-3600 [2]. In addition, the acceptability of relatively smaller flaws is evaluated in accordance with Section XI, Table IWB-3510-1 [2] for planar flaws. The program output includes the acceptable flaw size for the complete range of flaw aspect ratios and flaw eccentricities (for subsurface flaws). Key features include:

- Ability to include an arbitrary stress distribution for pressure, bending, thermal and residual stresses, including load multiplier factors for each,

- Evaluation of cladding stresses, with several methods to handle the effects of the cladding stresses at the surface for inside surface flaws,

- Ability to evaluate flaws based either on the maximum acceptable size, minimum acceptable size, or the minimum acceptable size assuming a smaller aspect ratio, a/l.

- Consideration of normal/upset condition, emergency/faulted condition or regions near local discontinuities (per IWB-3613 (a)).

- Automatic determination of the wall fracture toughness distribution given initial material properties and accumulated surface fluence at the end of the evaluation period.

- Conservative assessment of flaw growth to the end of the evaluation period.

A separate utility program MAPPA (standing for Multiple Appendix A analysis) provides an evaluation of multiple input cases and determines the controlling loading condition (or combination of conditions) for a number of individual evaluations using APPENDA.

3.0 BASIS OF ANO-1 VESSEL EVALUATION

3.1 Grouping of Locations

The reactor vessel plates, forgings and welds at ANO-1 are shown in Figure 3-1. The circled number designation used in this figure is consistent with that used in the Reference 1 flaw evaluation.

As shown in Figure 3-1, locations were defined as the following:

1. Nozzle Belt to Upper Shell Weld
2. Upper Shell Longitudinal Weld
3. Upper Shell to Lower Shell Weld
4. Lower Shell Longitudinal Weld
5. Lower Shell to Transition Forging Weld
6. Transition Forging between Vessel Shell and Bottom Vent
7. Transition Forging to Lower Shell Weld
8. Vessel Flange to Nozzle Belt Weld
9. Upper Nozzle Belt
10. Nozzle (Corner Crack)
11. Nozzle Belt to Nozzle Belt Weld
12. Nozzle (Vessel Side)
13. Upper Shell
14. Lower Shell
15. Upper Head to Closure Flange Weld
16. Lower Nozzle Belt
17. Upper Head
18. Lower Head

The evaluation in this report is limited to the shell welds and as such the nozzle-to-vessel welds (#10 and #12) were not considered. It should be noted that the nozzle welds are remote from the belt-line region and are unaffected by irradiation effects. Hence the Reference 1 flaw acceptance diagrams may be used for these locations, subject to recognition that the materials evaluation used for the current evaluation is probably more conservative.

Material properties for all the RPV plates and welds have been assembled in Reference 8 based on data collected during a site visit to ANO. Using this information, these locations have been identified by variations in fluence, initial RT_{NDT} and geometry in Table 3-1.

For the purpose of reducing the magnitude of the analytical computations, these locations have been combined to form nine groups. These groupings have been selected based on similarities in geometry, material data, stresses or thicknesses in the surrounding plate and/or weld material, as shown in Table 3-1. Referring to Figure 3-1, these groups have been combined starting from the top of the vessel (upper head). For each region, the surrounding material has been examined for the worst case, i.e., irradiation effects, stresses and/or initial RT_{NDT}. A description of each group and reasoning for their grouping is as follows:

Group A

Head Flange Weld and Adjacent Shells

This group includes the upper head shell (Mk# 24), upper head to closure flange weld, and closure flange. Material properties and stresses for the upper head to closure flange weld have been used to represent all materials in this group.

Group B

Upper Flange Weld and Adjacent Shells

This group includes the closure flange, vessel flange to nozzle belt weld (Weld 01-001), and upper nozzle belt shell (Mk #86). The material properties and stresses for Weld 01-001 have been used to represent all materials in this group.

Group C

Nozzle Belt to Nozzle Belt Weld and Adjacent Welds/Shells

This group includes the upper nozzle belt shell (Mk #86), the weld between the upper and lower nozzle belts, and the lower nozzle belt shell (Mk #87). For this group the material is unirradiated with no chemistry factors or fluences considered.

Group D

Beltline Shells (I)

The group represents two irradiated shells in the beltline region: Lower shells (Mk #A2, heat C5114) and lower nozzle belt shell (Mk #87). Because the irradiation effects are greater for the lower shell (with higher fluence and chemistry factor) and margin terms are greater, this material has been selected as representative for this grouping. Note that the other heat of the lower shell has been included in Group E. Maximum stresses are found at the nozzle belt to upper shell weld (01-003). Therefore, these stresses have been used to evaluate this grouping.

Group E

Beltline Shells (II)

The lower shell (Mk #A2, heat C5120) and upper shells 13-1, 13-2 (Mk #A1, heats C5120 and C5114) have been grouped together to form Group E, due to the irradiation effects for these materials. The higher chemistry factor of 123°F which exists for the upper and lower shells has been used for this group. Stresses found at the nozzle belt to upper shell weld have been used to evaluate this group.

Group F

Upper Shell to Lower Shell Weld

This group represents the upper shell to lower shell weld (Weld 01-004). This weld has been evaluated separately due to the relatively large chemistry factor. Maximum stresses are found at the nozzle belt to upper shell weld (Weld 01-003). Therefore, these stresses have been used to evaluate this group.

Group G

Beltline Welds

This group includes upper shell longitudinal welds, nozzle belt to upper shell weld, and lower shell longitudinal welds (Welds 01-007, 01-008, 01-003, 01-009, and 01-010). Weld 01-003 possesses the highest chemistry factor (167°F), therefore this was conservatively used for this group. Margins of 12.5°F and 20°F were used. Maximum stresses are found at the nozzle belt to upper shell weld (Weld 01-003). Therefore, these stresses have been used to evaluate this group.

Group H

Lower Shells/Welds (I)

The lower shell to lower head transition forging weld (Weld 01-005) and lower head transition forging (Mk #36) have been grouped together to form Group H. For this group, the lower shell to lower head transition forging weld (Weld 01-005) irradiation effects have been used, as well as the margin terms. Stresses for Weld 01-005 have been used for this group.

Group I

Lower Shells/Welds (II)

This group includes the lowerhead transition forging (Mk #36), lowerhead transition forging to lower shell weld (Weld 01-006), and lower head shell (Mk #6). Material properties for the lower head shell (Mk #6) have been used with an initial RT_{NDT} of 10°F and a margin shift of 10°F.

3.2 Vessel Geometry and Materials

The geometric details of the ANO-1 vessel are shown in Figures 3-2 through 3-5. The dimensions in these figures were assembled based on information contained in the drawings from References 9 through 11. Although small discrepancies were observed in the vessel wall thicknesses in these drawings, the smallest thickness at a given location was

conservatively used when these minor discrepancies were noted.

The vessel plate material is either A533, Class 1, Grade B. The vessel flange material and nozzles are A-508-64, Class 2. The vessel stud bolts were fabricated from A540 Grade B23 steel. Material properties for these materials were obtained from the existing vessel Stress Report [12] for use in the present evaluation as presented in Table 3-2.

3.3 Loadings and Loading Conditions

In the Reference 1 evaluation, the steady state leak test, slightly above normal operating conditions (temperature and pressure) was evaluated. In addition, heatup (at full pressurized conditions) was considered for the upper head closure flange, and cooldown (at zero or some other low pressure) was considered for all other locations. This choice of conditions was chosen to maximize the internal surface tensile stresses since only inside surface flaws were considered in the flaw evaluation. For the current evaluation, several other loading conditions will be evaluated since surface (both inside and outside) as well as subsurface flaws are being evaluated.

3.3.1 **Boltup at Ambient Conditions**

This is chosen to evaluate the stresses near the upper closure welds at a uniform through-wall temperature of 70°F. Boltup produces significant compressive stresses on the inside surface, but there are corresponding tensile stresses on the outside surface. Since the analysis is to consider both internal and external flaws, and also subsurface flaws, this may be a bounding condition. The decreased safety factors associated with local discontinuities (IWB-3613) are considered when this case is considered by itself.

3.3.2 Heatup at Cold Conditions

This condition is chosen at 100°F above boltup or 170°F, assuming the reactor has heated up at the Technical Specification limit of 50°F/hr for two hours, establishing the thermal gradients in the vessel [13]. The limit of 527 psi pressure for the "Hydrostatic Heatup and Cooldown" in Reference 13 is used. The vessel temperatures are determined based on a reactor fluid temperature of 170°F. This condition may be limiting for some of the outside surface weld locations, since the fracture toughness may be lower than the upper shelf value of 200 $\sqrt{ksi\text{-}in^2}$. (Heatup at colder conditions is not considered because significant time is required to establish a steady state stress gradient that would exhibit maximum tension at the outside surface).

3.3.3 Heatup at Warm Conditions

This condition is similar to the above, except that the conditions at 220°F vessel fluid temperature and 822 psig are chosen. Although the material fracture toughness should be higher, ... may be offset by the higher pressure stresses, such that this condition could control.

3.3.4 Heatup at Hot Conditions

This condition is chosen at the end of heatup with a fluid temperature of 603°F. This condition may be controlling for some of the outside surface locations. A vessel pressure of 2300 psig for the leak test is used (1.06 times the nominal operating pressure). The vessel heatup rate is taken as 50°F/hr.

3.3.5 Leak Test

This condition is the same as above, except that the vessel wall temperature will be uniform

at 603°F with no throughwall thermal stresses. This condition may be limiting for some locations.

3.3.6 **Cooldown at 100°F/hr**

This case is chosen based on the maximum pressure for the cooldown transient at the lowest temperature condition [13]. Cooldown is expected to produce inside surface tensile stresses. In addition, cladding-induced stresses play an important part at lower temperatures. This cooldown rate is only allowed with the vessel > 280°F, so this lower bound temperature is chosen for the vessel fluid [13]. The maximum pressure for "Hydrostatic Heatup and Cooldown" is taken as 1382 psig.

3.3.7 **Cooldown at 50°F/hr**

This is similar to the above except the vessel fluid temperature is taken as 150°F and the pressure is taken as 461 psig. (For the flange region, the lower safety factors permitted by IWB-3613 are used).

3.3.8 **Cooldown at 25°F/hr**

This is similar to the above except that the vessel fluid temperature is taken as 70°F and the pressure is taken as 388 psig.

3.4 Stresses and Stress Evaluation

3.4.1 Operating Stresses

In performing the evaluations, the possibility of using previous stress analyses in Reference 1 and also the existing stress report [12] was explored. It was observed that detailed through-wall stress information in either of these references was not available at the critical

locations of the vessel for flaw evaluation. As such, an axisysmmetric finite element model was developed for the purpose of determining the operating stresses in the vessel.

The finite element model of the vessel is shown in Figure 3-6. The model was developed using the ANSYS computer software [14]. The model was generated using isoparametric finite elements for the vessel. No clad material was included in the model. The upper shell flange and the upper head were not physically connected in the model, but rather they shared common coincident nodal locations. In the thermal analysis, the coincident nodes were coupled such that they have the same temperature. For stress analysis, the upper head is connected to the flange by a number of gap elements. These gap elements started from the inner diameter and ran approximately to the end of the raised seating face between the flange and the head. The bolt holes in the flange were not modeled but were accounted for by modifying the stiffness of the material at that location based on area reduction of the holes. The materials properties are presented in Table 3-2.

The following basic loading conditions were determined from the Stress Report [12]:

- Gasket loads of 400 kips and 407.6 kips were applied to the mating flange surfaces at the inner and outer gasket grooves.

- A spring load of 6×10^3 kips was applied during heatup and a value of 3×10^3 kips was applied during cooldown. For isothermal conditions, the average value was used.

- The boltup load of 84×10^3 kips was applied for 70°F isothermal conditions.

Five basic stress cases were run using this model to determine the stress response. Several other load cases can be derived from these basic load cases.

Load Case 1 - Bolt-up at 70°F

In this load case, the cold bolt-up load was applied to the flange. In addition to the bolt-up load, the spring and gasket loads were applied. The bolt load was applied to the model by the use of a 2-D spar element available in the ANSYS library.

Load Case 2 - Bolt-up at 603°F

This case is similar to Load Case 1 above except the vessel was maintained at 603°F. Bolt loads decreased slightly.

Load Case 3 - Bolt-up plus Pressure at 603°F

This case simulates the leak test. It is similar to Load Case 2 except that a pressure of 2242 psig was applied to the inside surface of the vessel. The pressure force was also applied between the top head and the upper shell flange to the first gasket.

Load Case 4 - Heatup Transient

The initial temperature of the transient was 350°F with a heatup rate of 50°F per hour to a temperature of 603°F. Stress analysis was performed at the instant 603°F was reached. An internal pressure of 2242 psig was applied during the transient with the bolt and gasket loads used in Load Case 1 also applied.

Load Case 5 - Cooldown Transient

The initial temperature of the transient was 603°F with a cooldown rate of 100° F/hour to temperature of 287°F. In this case, a pressure of 175 psig was applied.

Individual load case stresses derived from the above basic load cases are shown in Tables 3-3 through 3-11 for the various groups of the vessel. The computed stresses were extrapolated into the vessel cladding region for purposes of the flaw evaluation. More details of the thermal and stress analyses are provided in Reference 14.

3.4.2 Weld Residual Stresses

For purposes of the fracture mechanics analysis, it was also assumed that weld residual stresses could be present at all locations. A cosine-shaped distribution was assumed in the base metal with a maximum surface tensile stress of 8 ksi [15]. The 8 ksi stress was conservatively extended into the cladding for purposes of evaluation. Since residual stresses may be beneficial in reducing the stress intensity factors, evaluations were also conducted without residual stresses so that the controlling condition could be determined.

3.4.3 Cladding Stresses

Cladding stresses were determined using Structural Integrity Associates computer software PIPE-TS2 [16] which determines thermal stresses in a bi-metallic cylinder. The cladding in a reactor pressure vessel is at its maximum tensile value at cold ambient temperature conditions because of the relative thermal expansion coefficients for alloy steel and stainless steel. It was assumed that the cladding tensile stress at 70°F was nominally 35 ksi (in tension), slightly higher than the minimum yield strength for stainless steel (30 ksi) obtained from the ASME Code material property tables. This stress level is conservative, especially when one considers that some additional yielding would have occurred during the original vessel cold hydrotest that would tend to reduce the cladding residual stress below the yield value at ambient conditions. Table 3-10 shows the cladding-induced stresses used in this analysis for the cladding and the base metal. Because the hoop and axial stresses are nearly identical, the cladding axial stress distribution was conservatively used in all cases. It was also assumed that the cladding stresses determined for the cylindrical model would be applicable for the spherical and the flanged regions.

For use in computing the flaw shape factor, Q, the reactor vessel material, A533 Class 1 Grade B has a specific minimum yield strength of 50 ksi [11] at ambient conditions. For other cases, the yield strength was determined based upon the maximum temperature existing at the section being analyzed.

Table 3-1
Grouping of Locations

	Region	Type	Description	ID	t [in]	Initial Trtndt F	Fluence n/cm²	Chemistry Factor F	Margin σΔ F	Margin σI F
	UH	Shell	Upper Head	Mk #24	6.625	10	NA	NA	NA	NA
	15	Weld	Upper head to Closure Flange		6.625	-5	NA	NA	NA	20
	VF	Shell	Vessel Flange	Mk #7	12	10	NA	NA	NA	0
Group	**A**				**6.625**	**-5**	**NA**	**NA**	**NA**	**20**
		Shell	Closure Flange	Mk #7	12	10	NA	NA	NA	0
	8	Weld	Vessel Flange to Nozzle Belt	01-001	12	-5	NA	NA	NA	20
	9	Shell	Upper Nozzle Belt	Mk #86	12	10	NA	NA	NA	0
Group	**B**				**12**	**-5**	**NA**	**NA**	**NA**	**20**
	9	Shell	Upper Nozzle Belt	Mk #86	12	10	NA	NA	NA	0
	11	Weld	Nozzle Belt to Nozzle Belt	01-002	12	-5	NA	NA	NA	20
	16	Shell	Lower Nozzle Belt (1)	Mk #87	12	30	NA	NA	12	0
Group	**C**				**12**	**-5**	**NA**	**NA**	**NA**	**20**
	16	Shell	Lower Nozzle Belt	Mk #87	8.4375	30	7.41E+18	31	12	0
	14-2	Shell	Lower Shell	Mk #A2 (C5114)	8.4375	17	9.75E+18	106	17	10
Group	**D (2)**				**8.4375**	**17**	**9.75E+18**	**106**	**17**	**10**
	13-1	Shell	Upper Shell	Mk #A1 (C5120)	8.4375	-10	9.75E+18	123	17	5
	13-2	Shell	Upper Shell	Mk #A1 (C5114)	8.4375	-10	9.75E+18	106	17	5
	14-1	Shell	Lower Shell	Mk #A2 (C5120)	8.4375	-10	9.75E+18	123	17	5
Group	**E**				**8.4375**	**-10**	**9.75E+18**	**123**	**17**	**5**
	3	Weld	Upper Shell to Lower Shell	01-004	8.4375	-5	9.75E+18	195	12.5	20
Group	**F**				**8.4375**	**-5**	**9.75E+18**	**195**	**12.5**	**20**
	2	Weld	Upper Shell Longitudinal	01-007	8.4375	-5	7.22E+18	150	12.5	20
	2	Weld	Upper Shell Longitudinal	01-008	8.4375	-5	7.22E+18	150	12.5	20
	1	Weld	Nozzle Belt to Upper Shell	01-003	8.4375	-5	7.41E+18	167	12.5	20
	4	Weld	Lower Shell Longitudinal	01-009	8.4375	-5	7.61E+18	150	12.5	20
	4	Weld	Lower Shell Longitudinal	01-010	8.4375	-5	7.61E+18	150	17	10
Group	**G**				**8.4375**	**-5**	**7.41E+18**	**167**	**12.5**	**20**
	14-1	Shell	Lower Shell	Mk #A2 (C5120)	8.4375	-10	9.75E+18	123	5	5
	14-2	Shell	Lower Shell	Mk #A2 (C5114)	8.4375	17	9.75E+18	106	17	10
	5	Weld	Lower Shell to Transition Forging	01-005	5	-5	5.46E+16	165	4	20
	6	Shell	Transition Forging	Mk #36	5	10	NA	NA	NA	0
Group	**H (3)**				**5**	**-5**	**5.46E+16**	**165**	**4**	**20**
	6	Shell	Transition Forging	Mk #36	5	10	NA	NA	NA	0
	7	Weld	Transition Forging to Lower Head	01-006	5	-5	NA	NA	NA	20
	LH	Shell	Lower Head	Mk #6	5	10	NA	NA	NA	10
Group	**I**				**5**	**10**	**NA**	**NA**	**NA**	**10**

Notes:

1. For this grouping, it has been assumed that this portion of the Lower Nozzle Belt (Mk #86) region is unirradiated.
2. Plate 14-2 has been selected to represent Group D due to the higher fluence.
3. Although the other regions in this grouping possess a larger fluence, weld 01-005 has been selected to represent this region due to its larger overall radiation shift.

Table 3-2

Material Properties of ANO-1 Vessel

Properties	Material	Temperature, °F											
		70	100	150	200	250	300	350	400	450	500	550	600
E, psi	RPV Material SA-533 Cl 1 GrB SA-508-44-Cl 2	2.99E+07	2.98E+07	2.97E+07	2.95E+07	2.93E+07	2.91E+07	2.89E+07	2.86E+07	2.83E+07	2.80E+07	2.77E+07	2.74E+07
α, in/in		6.12E-06	6.18E-06	6.28E-06	6.38E-06	6.49E-06	6.59E-06	6.69E-06	6.79E-06	6.89E-06	7.00E-06	7.10E-06	7.20E-06
k, Btu/in² s		6.12E-04	6.08E-04	6.02E-04	5.96E-04	5.90E-04	5.84E-04	5.78E-04	5.72E-04	5.65E-04	5.59E-04	5.53E-04	5.47E-04
C, Btu/lb °F		0.104	0.107	0.111	0.115	0.118	0.12	0.123	0.125	0.126	0.128	0.13	0.133
ρ, lb/in³		0.28385	0.28385	0.28351	0.2831	0.28275	0.28235	0.282	0.28166	0.28125	0.2809	0.28049	0.28015
E, psi	Bolt Material SA540 Gr B23	2.99E+07	2.99E+07	2.97E+07	2.95E+07	2.93E+07	2.90E+07	2.87E+07	2.83E+07	2.78E+07	2.74E+07	2.68E+07	2.63E+07
α, in/in		6.09E-06	6.17E-06	6.30E-06	6.42E-06	6.54E-06	6.66E-06	6.77E-06	6.88E-06	6.99E-06	7.10E-06	7.20E-06	7.31E-06
k, Btu/in² s		5.09E-04	5.06E-04	5.00E-04	4.95E-04	4.89E-04	4.83E-04	4.78E-04	4.72E-04	4.67E-04	4.61E-04	4.56E-04	4.50E-04
C, Btu/lb °F		0.104	0.107	0.111	0.115	0.118	0.12	0.123	0.125	0.126	0.128	0.13	0.133
ρ, lb/in³		0.28409	0.28385	0.28351	0.2831	0.28275	0.28235	0.282	0.28166	0.28125	0.2809	0.2805	0.28015

Note: To simulate bolt holes in the flange, the values of g, E, k and C were multiplied by 0.517 in the local cross-section area occupied by the Bolt Hole.

Table 3-3

Stresses for Group A

Axial Stresses

Distance From I.D. (in)	Stresses (ksi)					
	Bolt-Up @T=70°F	Pressure 2242 psi	Heatup 50°F/hr		Cooldown 100°F/hr	
			Stress	Temp.	Stress	Temp.
0	-22.071	16.255	-3.830	589.00	5.816	311.29
0.187	-20.916	15.706	-3.821	589.00	5.557	311.29
0.188	-20.910	15.703	-3.034	589.00	5.555	311.29
0.845193	-16.850	13.772	-2.518	581.44	4.645	323.74
1.50633	-12.960	12.812	-1.781	574.74	3.427	334.89
2.171318	-9.123	12.359	-1.067	568.99	2.172	344.55
2.84007	-5.222	12.269	-0.423	564.22	0.976	352.66
3.512498	-1.191	12.458	0.140	560.42	-0.117	359.19
4.188518	3.087	12.901	0.616	557.61	-1.088	364.11
4.868048	7.720	13.633	0.999	555.79	-1.941	367.39
5.551008	12.820	14.740	1.348	554.98	-2.769	369.00
6.237318	18.640	16.440	1.731	555.20	-3.666	368.87
6.926903	25.360	19.510	2.537	556.48	-5.196	366.95

Hoop Stresses

Distance From I.D. (in)	Stresses (ksi)					
	Bolt-Up @T=603°F	Pressure 2242 psi	Heatup 50°F/hr		Cooldown 100°F/hr	
			Stress	Temp.	Stress	Temp.
0	-0.276	9.301	-18.163	589.00	28.124	311.29
0.187	0.254	9.206	-18.048	589.00	27.112	311.29
0.188	0.257	9.206	-17.560	589.00	27.107	311.29
0.845193	2.120	8.872	-15.317	581.44	23.551	323.74
1.50633	3.868	8.881	-13.034	574.74	19.967	334.89
2.171318	5.607	9.059	-10.987	568.99	16.709	344.55
2.84007	7.367	9.370	-9.164	564.22	13.772	352.66
3.512498	9.146	9.795	-7.563	560.42	11.149	359.19
4.188518	10.940	10.314	-6.158	557.61	8.852	364.11
4.868048	12.760	10.940	-4.963	555.79	6.878	367.39
5.551008	14.580	11.670	-3.959	554.98	5.223	369.00
6.237318	16.410	12.530	-3.174	555.20	3.898	368.87
6.926903	18.520	13.800	-2.501	556.48	2.802	366.95

Table 3-4

Stresses for Group B

Axial Stresses

Distance From I.D. (in)	Stresses (ksi)					
	Bolt-Up @T=70°F	Pressure 2242 psi	Heatup 50°F/hr		Cooldown 100°F/hr	
			Stress	Temp.	Stress	Temp.
0	-14.527	10.709	-16.250	590.53	25.818	309.95
0.187	-13.764	10.630	-15.780	590.53	24.661	309.95
0.188	-13.760	10.630	-15.105	590.53	24.655	309.95
1.3875	-11.080	10.128	-11.078	576.06	18.085	335.09
2.5875	-8.361	9.430	-7.147	563.26	11.717	357.53
3.7875	-5.576	8.652	-3.671	552.08	6.041	377.24
4.9875	-2.871	7.927	-0.734	542.48	1.212	394.26
6.1875	-0.212	7.258	1.694	534.42	-2.797	408.59
7.3875	2.437	6.636	3.653	527.88	-6.029	420.26
8.5875	5.101	6.047	5.181	522.82	-8.536	429.31
9.7875	7.765	5.490	6.316	519.22	-10.366	435.74
10.9875	10.310	4.905	7.082	517.07	-11.520	439.59
12.1875	12.800	4.340	7.497	516.36	-12.073	440.87

Hoop Stresses

Distance From I.D. (in)	Stresses (ksi)					
	Bolt-Up @T=603°	Pressure 2242 psi	Heatup 50°F/hr		Cooldown 100°F/hr	
			Stress	Temp.	Stress	Temp.
0	-1.043	15.788	-20.45	590.53	32.35	309.95
0.187	-0.787	15.726	-19.73	590.53	31.11	309.95
0.188	-0.786	15.725	-18.93	590.53	31.11	309.95
1.3875	0.112	15.326	-14.32	576.06	23.48	335.09
2.5875	1.008	14.879	-9.96	563.26	16.35	357.53
3.7875	1.902	14.423	-6.18	552.08	10.10	377.24
4.9875	2.749	13.998	-2.97	542.48	4.75	394.26
6.1875	3.569	13.596	-0.31	534.42	0.30	408.59
7.3875	4.374	13.207	1.83	527.88	-3.29	420.26
8.5875	5.172	12.834	3.46	522.82	-6.05	429.31
9.7875	5.966	12.474	4.61	519.22	-7.98	435.74
10.9875	6.726	12.113	5.30	517.07	-9.11	439.59
12.1875	7.465	11.771	5.54	516.36	-9.46	440.87

Table 3-5

Stresses for Group C

Axial Stresses

Distance From I.D. (in)	Stresses (ksi)					
	Bolt-Up @T=70°F	Pressure 2242 psi	Heatup 50°F/hr		Cooldown 100°F/hr	
			Stress	Temp.	Stress	Temp.
0	1.295	8.177	-15.280	597.46	26.140	301.06
0.187	1.224	8.131	-14.687	597.46	24.223	301.06
0.188	1.224	8.131	-14.162	597.46	24.212	301.06
0.845193	0.977	7.972	-10.196	584.33	17.474	324.71
1.50633	0.734	7.811	-6.459	572.73	11.191	345.83
2.171318	0.494	7.654	-3.235	562.63	5.697	364.39
2.84007	0.257	7.496	-0.504	536.36	0.987	380.40
3.512498	0.022	7.339	1.747	533.16	-2.932	393.89
4.188518	-0.212	7.182	3.535	531.25	-6.061	404.86
4.868048	-0.446	7.027	4.858	530.62	-8.406	413.35
5.551008	-0.681	6.871	5.751	553.98	-9.966	419.38
6.237318	-0.917	6.718	6.203	546.74	-10.766	422.98
6.926903	-1.154	6.562	6.228	540.88	-10.804	424.17

Hoop Stresses

Distance From I.D. (in)	Stresses (ksi)					
	Bolt-Up @T=70°F	Pressure 2242 psi	Heatup 50°F/hr		Cooldown 100°F/hr	
			Stress	Temp.	Stress	Temp.
0	0.700	17.257	-14.82	597.46	28.24	301.06
0.187	0.674	17.166	-14.71	597.46	26.16	301.06
0.188	0.674	17.166	-15.20	597.46	26.15	301.06
0.845193	0.583	16.845	-10.92	584.33	18.85	324.71
1.50633	0.494	16.533	-6.92	572.73	12.11	345.83
2.171318	0.407	16.228	-3.47	562.63	6.25	364.39
2.84007	0.322	15.943	-0.57	536.36	1.25	380.40
3.512498	0.239	15.665	1.81	533.16	-2.89	393.89
4.188518	0.157	15.396	3.69	531.25	-6.20	404.86
4.868048	0.077	15.137	5.10	530.62	-8.69	413.35
5.551008	-0.003	14.886	6.04	553.98	-10.37	419.38
6.237318	-0.081	14.644	6.54	546.74	-11.27	422.98
6.926903	-0.159	14.402	6.62	540.88	-11.38	424.17

Table 3-6

Stresses for Groups D, E, F and G

Axial Stresses

Distance From I.D. (in)	Stresses (ksi)					
	Bolt-Up @T=70°F	Pressure 2242 psi	Heatup 50°F/hr		Cooldown 100°F/hr	
			Stress	Temp.	Stress	Temp.
0	-	9.663	-8.051	599.00	15.558	298.26
0.187	-	9.696	-8.082	599.00	15.141	298.26
0.188	-	9.631	-8.383	599.00	14.318	298.26
1.030268	-	9.922	-6.205	592.46	10.576	310.23
1.874535	-	10.150	-4.077	586.66	6.991	320.97
2.718302	-	10.370	-2.187	581.58	3.774	330.44
3.562069	-	10.590	-0.540	577.21	0.943	338.65
4.405837	-	10.810	0.880	573.54	-1.492	345.59
5.249604	-	11.030	2.070	570.55	-3.532	351.25
6.093371	-	11.260	3.020	568.25	-5.176	355.65
6.937149	-	11.480	3.750	566.61	-6.419	358.78
7.780911	-	11.700	4.230	565.63	-7.250	360.65
8.624673	-	11.890	4.470	565.30	-7.646	361.26

Hoop Stresses

Distance From I.D. (in)	Stresses (ksi)					
	Bolt-Up @T=70°F	Pressure 2242 psi	Heatup 50°F/hr		Cooldown 100°F/hr	
			Stress	Temp.	Stress	Temp.
0	-	23.453	-6.95	599.00	13.68	298.26
0.187	-	23.436	-6.93	599.00	13.27	298.26
0.188	-	23.400	-7.34	599.00	12.43	298.26
1.030268	-	23.240	-5.17	592.46	8.70	310.23
1.874535	-	23.060	-3.08	586.66	5.20	320.97
2.718302	-	22.900	-1.27	581.58	2.15	330.44
3.562069	-	22.740	0.29	577.21	-0.49	338.65
4.405837	-	22.590	1.59	573.54	-2.72	345.59
5.249604	-	22.450	2.63	570.55	-4.53	351.25
6.093371	-	22.310	3.45	568.25	-5.94	355.65
6.937149	-	22.170	4.03	566.61	-6.94	358.78
7.780911	-	22.050	4.38	565.63	-7.54	360.65
8.624673	-	21.920	4.50	565.30	-7.74	361.26

Table 3-7

Stresses for Group H

Axial Stresses

Distance From I.D. (in)	Stresses (ksi)					
	Bolt-Up @T=70°F	Pressure 2242 psi	Heatup 50°F/hr		Cooldown 100°F/hr	
			Stress	Temp.	Stress	Temp.
0	-	19.515	-12.493	599.79	18.924	294.20
0.187	-	18.840	-11.816	599.79	18.974	294.20
0.188	-	18.840	-12.204	599.79	18.969	294.20
0.688131	-	18.710	-9.127	596.75	14.400	299.61
1.188262	-	18.700	-6.620	594.00	10.470	304.48
1.688393	-	18.500	-4.370	591.55	6.628	308.87
2.188524	-	18.290	-2.150	589.39	3.246	312.73
2.688655	-	18.110	0.030	587.54	-0.078	316.04
3.188786	-	18.050	2.120	586.01	-3.336	318.80
3.688917	-	18.220	4.200	584.78	-6.573	321.00
4.189048	-	18.590	6.200	583.85	-9.655	322.66
4.689179	-	19.350	8.430	583.29	-13.080	323.67
5.18931	-	21.060	10.850	583.03	-16.764	324.14

Hoop Stresses

Distance From I.D. (in)	Stresses (ksi)					
	Bolt-Up @T=70°F	Pressure 2242 psi	Heatup 50°F/hr		Cooldown 100°F/hr	
			Stress	Temp.	Stress	Temp.
0	-	17.167	-7.75	599.79	12.61	294.20
0.187	-	16.440	-7.02	599.79	12.67	294.20
0.188	-	16.440	-7.82	599.79	12.67	294.20
0.688131	-	16.300	-6.26	596.75	10.08	299.61
1.188262	-	16.270	-4.72	594.00	7.68	304.48
1.688393	-	16.150	-3.35	591.55	5.45	308.87
2.188524	-	16.080	-2.11	589.39	3.47	312.73
2.688655	-	16.030	-0.99	587.54	1.68	316.04
3.188786	-	15.980	0.06	586.01	0.02	318.80
3.688917	-	15.990	1.04	584.78	-1.53	321.00
4.189048	-	16.040	1.93	583.85	-2.92	322.66
4.689179	-	16.160	2.77	583.29	-4.22	323.67
5.18931	-	16.530	3.55	583.03	-5.41	324.14

Table 3-8

Stresses for Group I

Axial Stresses

Distance From I.D. (in)	Stresses (ksi)					
	Bolt-Up @T=70°F	Pressure 2242 psi	Heatup 50°F/hr		Cooldown 100°F/hr	
			Stress	Temp.	Stress	Temp.
0	-	17.276	-4.172	600.46	8.109	292.85
0.187	-	17.341	-4.236	600.46	7.771	292.85
0.188	-	17.210	-4.410	600.46	7.117	292.85
0.688058	-	17.560	-3.310	598.10	5.316	297.11
1.188116	-	17.910	-2.310	595.99	3.700	300.91
1.688174	-	18.260	-1.390	594.15	2.219	304.25
2.188231	-	18.610	-0.570	592.56	0.894	307.14
2.688289	-	18.940	0.150	591.23	-0.271	309.58
3.188347	-	19.270	0.770	590.14	-1.292	311.58
3.688404	-	19.600	1.310	589.30	-2.171	313.13
4.188462	-	19.940	1.760	588.71	-2.914	314.25
4.68852	-	20.320	2.110	588.36	-3.502	314.94
5.188577	-	20.700	2.410	588.24	-4.003	315.17

Hoop Stresses

Distance From I.D. (in)	Stresses (ksi)					
	Bolt-Up @T=70°F	Pressure 2242 psi	Heatup 50°F/hr		Cooldown 100°F/hr	
			Stress	Temp.	Stress	Temp.
0	-	16.629	-7.57	600.46	12.98	292.85
0.187	-	16.647	-7.59	600.46	12.67	292.85
0.188	-	16.610	-7.95	600.46	12.06	292.85
0.688058	-	16.710	-6.93	598.10	10.43	297.11
1.188116	-	16.840	-5.97	595.99	8.91	300.91
1.688174	-	16.970	-5.10	594.15	7.53	304.25
2.188231	-	17.090	-4.33	592.56	6.32	307.14
2.688289	-	17.220	-3.66	591.23	5.24	309.58
3.188347	-	17.340	-3.07	590.14	4.31	311.58
3.688404	-	17.470	-2.58	589.30	3.52	313.13
4.188462	-	17.590	-2.16	588.71	2.86	314.25
4.68852	-	17.710	-1.82	588.36	2.34	314.94
5.188577	-	17.820	-1.57	588.24	1.94	315.17

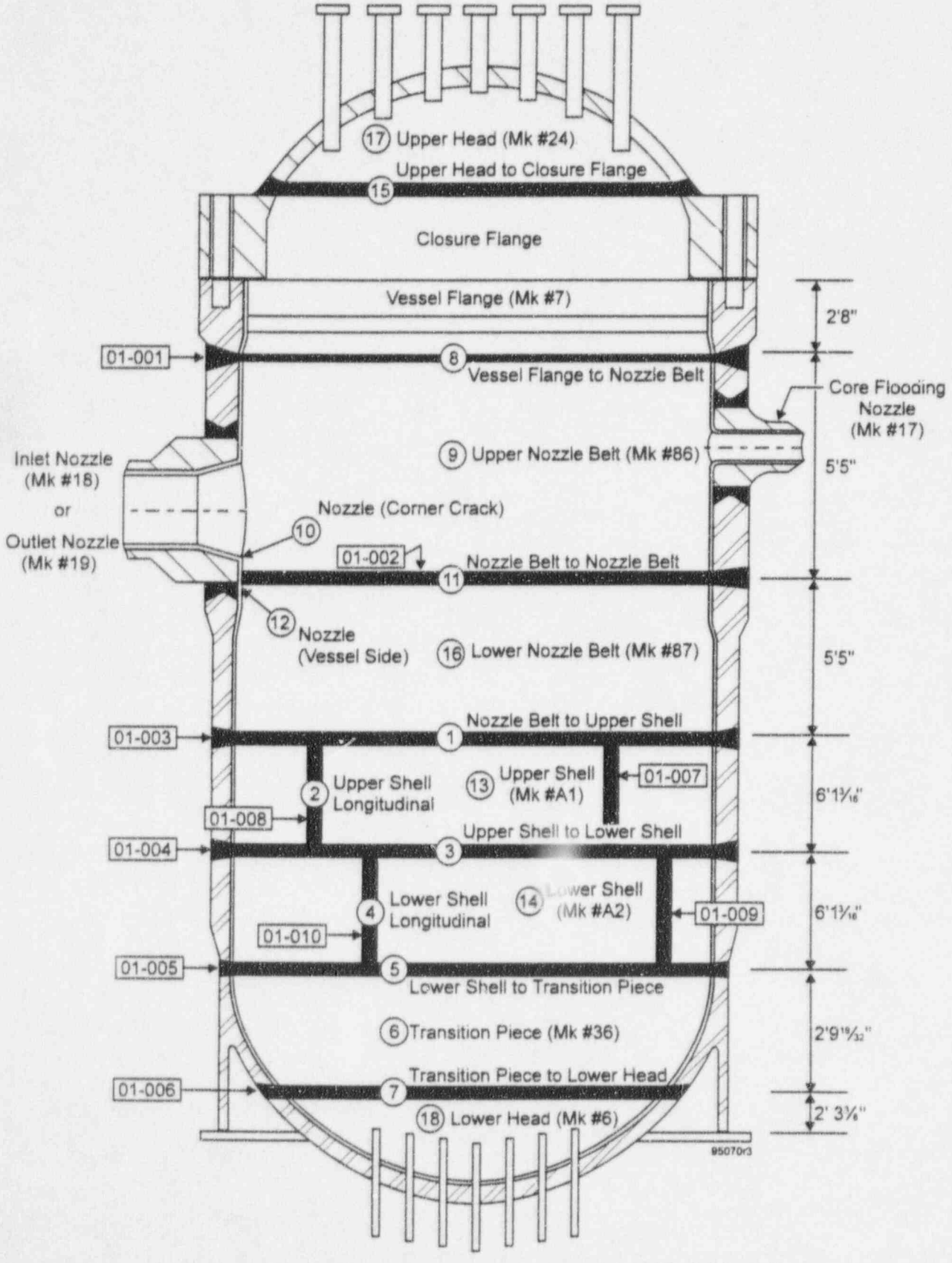

Figure 3-1. Plates and Weld Locations of ANO-1 Vessel

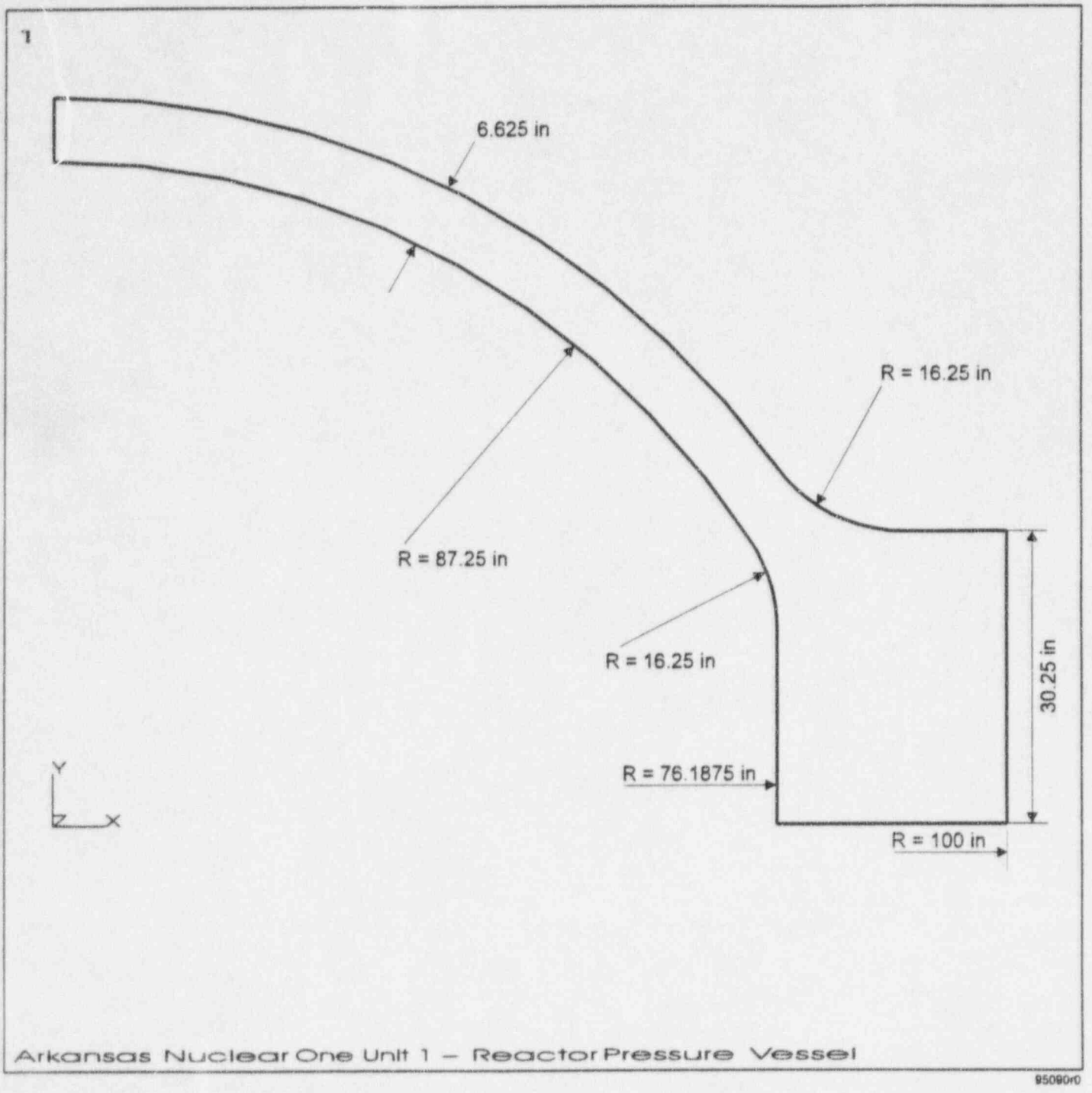

Figure 3-2. Vessel Geometry at ANO-1 - Top Head Region

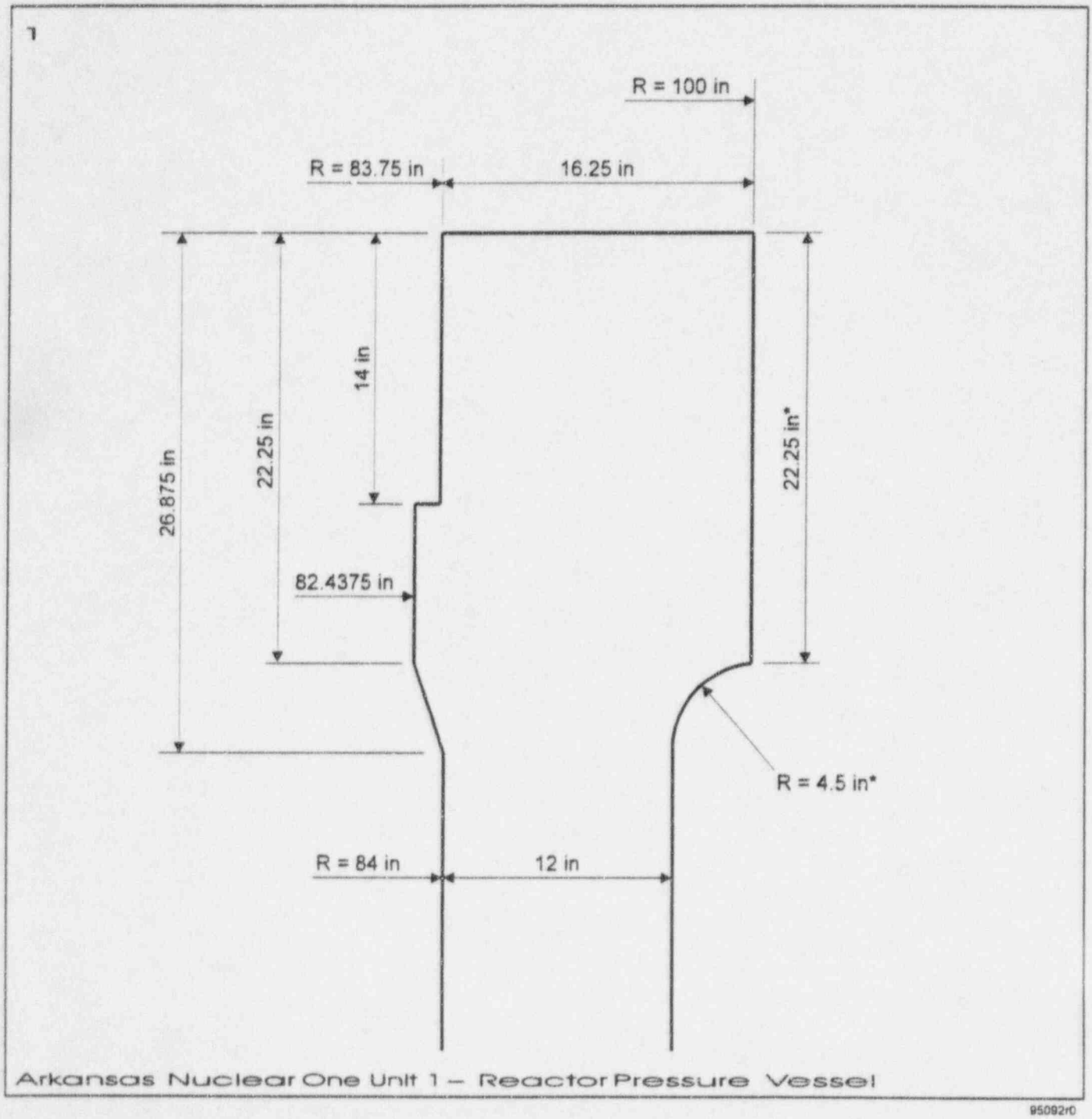

Figure 3-3. Vessel Geometry at ANO-1 - Flange Region

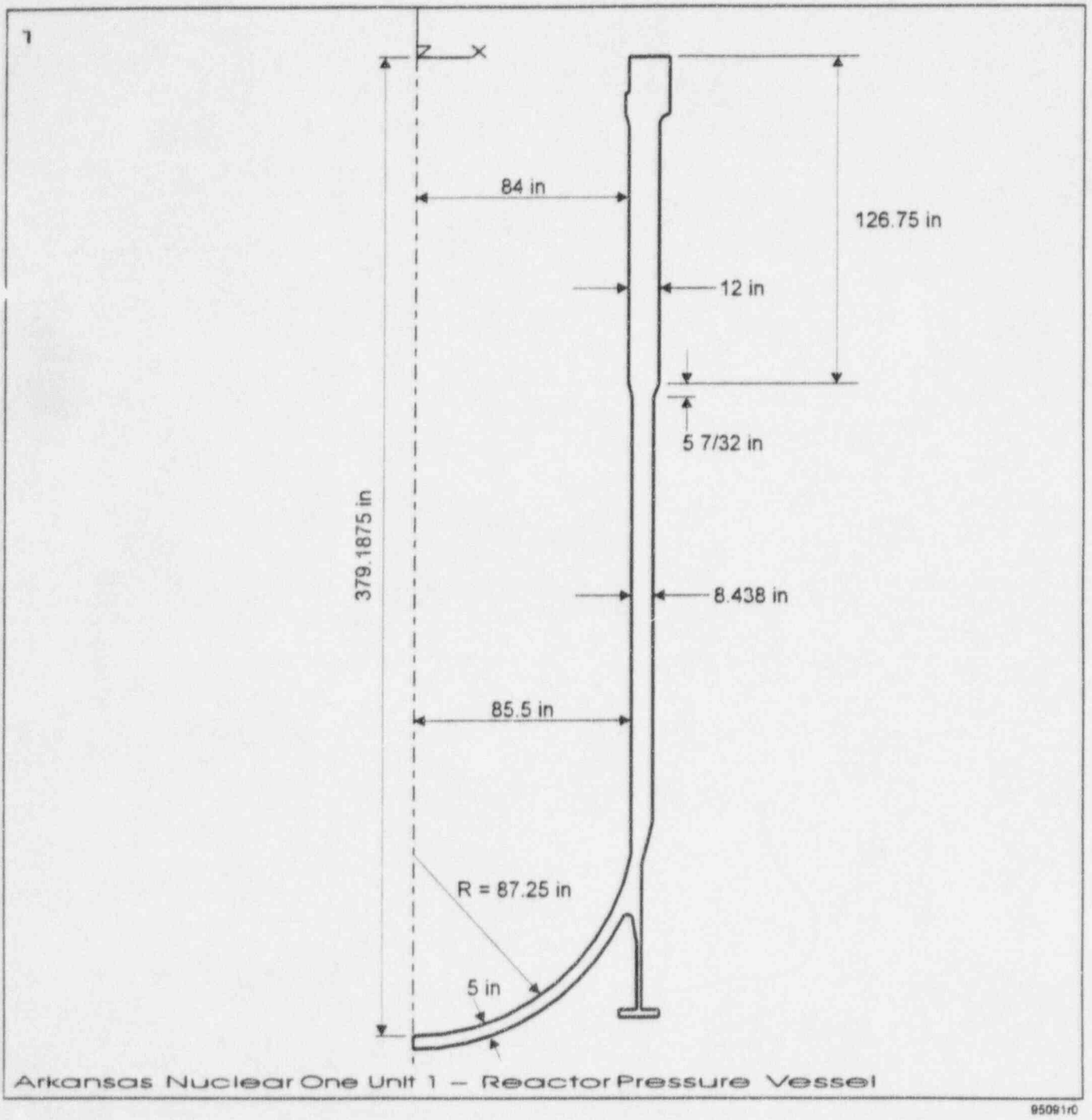

Figure 3-4. Vessel Geometry at ANO-1 - Beltline and Bottom Head Regions

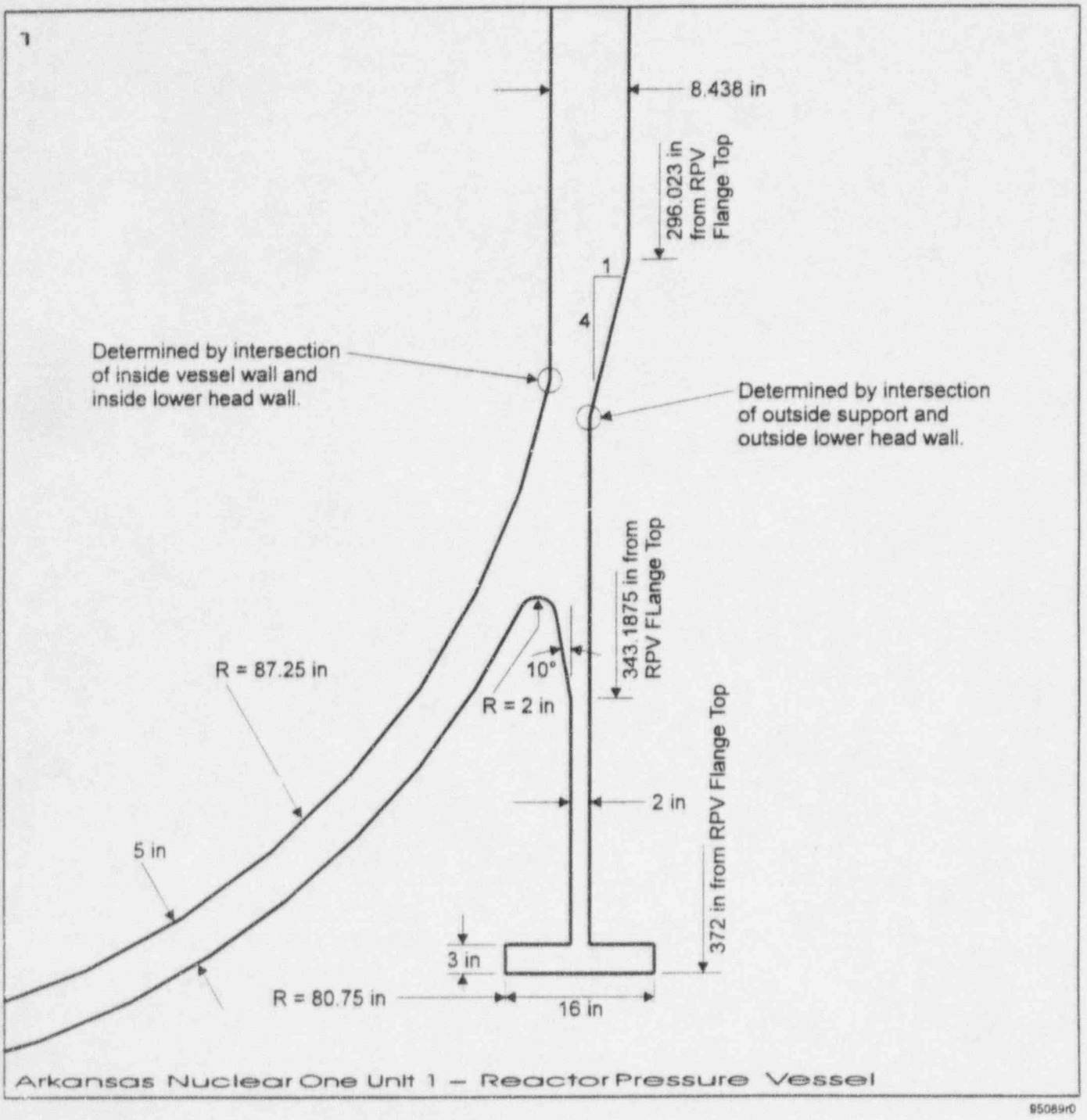

Figure 3-5. Vessel Geometry at ANO-1 - Details of Bottom Head Region

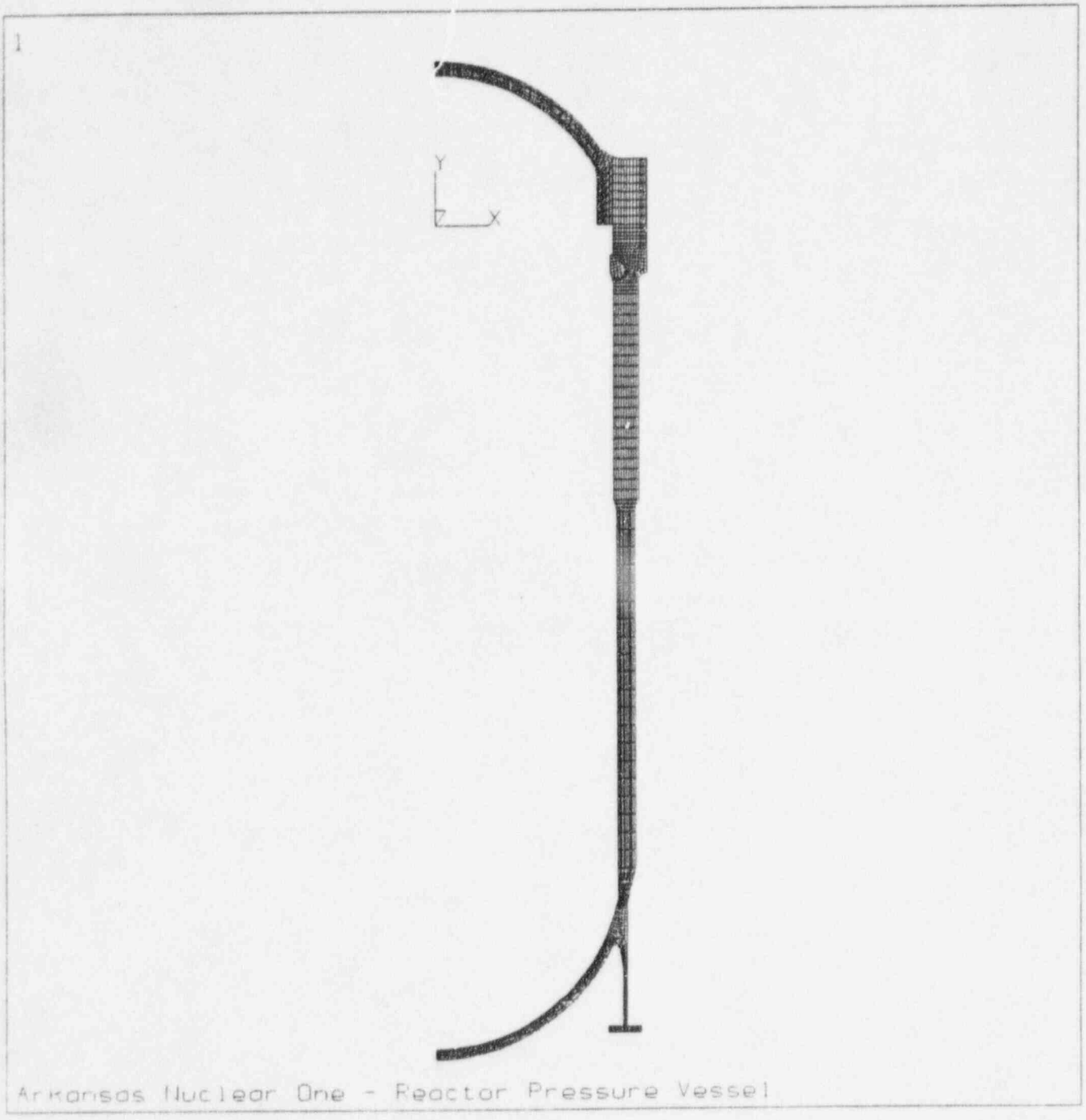

Figure 3-6. Axisymmetric Finite Element Model of ANO-1 Vessel

4.0 RESULTS

Graphs which define acceptable flaw sizes are included in Appendices A through I of this report for the corresponding vessel material groups shown in Table 3-1. For each material group, five graphs are presented for inside surface, outside surface and three subsurface flaws (eccentricity ratio, e/t = 0.35, 0, and -0.35) for axial and circumferential flaws. Results for five other subsurface flaw eccentricity ratios (-0.4, -0.25, -0.1, 0.2 and 0.45) are provided on a QUATTRO-PRO (Lotus 1-2-3 compatible) spreadsheet with accompanying APPENDA output ".SUM" files on the accompanying diskette.

4.1 IWB-3500 Evaluation Standards

For completeness, each of the evaluations also considered the IWB-3500 evaluation standards from Table IWB-3500-1. For subsurface flaws, the limitations of proximity to the surface of the base metal are shown for rapid evaluation. Linear interpolation may be used for intermediate flaw eccentricities.

The evaluation standards of IWB-3500 are also included for reference as the lower bound in the location-specific flaw acceptance graphs in Appendices A to I. In these sets of curves, the acceptable inside surface flaw is the depth of the cladding plus the acceptance standards. In all graphs, it has been assumed that the cladding thickness is 3/16 inch.

4.2 IWB-3600 Evaluations

The graphs of Appendices A to I show the acceptable flaw sizes based on this evaluation. The minimum allowable flaw size for all cases evaluated is shown and considers the effects of crack growth to end-of-life (32 EFPY). Each Appendix has two evaluations, one for axially-oriented flaws and the other for circumferentially-oriented flaws. The general scheme is to show the allowables for inside surface flaws, outside surface flaws and a range of subsurface flaws for various values of flaw eccentricity. Results for subsurface

flaws with five other eccentricity ratios are available on site for review as an electronic file. For subsurface flaws with intermediate values of flaw eccentricity, linear interpolation can be used.

For all the graphs presented in Appendices A through I, a default maximum flaw size was determined such that the nominal stress would increase to approximately 1.5 times the nominal stress if a long flaw existed at the location. This was done because IWB-3610(d)(1) requires that the primary stress limits of NB-3000 (of ASME Section III) be satisfied for the size of the evaluated flaw. For actual flaws found in a reactor pressure vessel, this should never become limiting because NB-3000 allows local primary membrane stresses to approach 1.5 S_m provided that the extent of the region with stress exceeding 1.1 S_m does not exceed $\sqrt{Rt}$ (where R is the mean vessel radius and t is the thickness). This compares to the requirement for the design equations for pressure sizing where the stress must be maintained below S_m. Based on this ratio, the additional primary stress criterion might become governing for axial flaws with depths approaching one-third of the wall thickness that have any significant extent, provided that the pressure stress is near the allowable stress. Since the stresses acting on circumferential flaws are about one half of that for axial flaws, greater flaw depths would be allowed for flaws with a circumferential orientation.

It should be noted that most of the allowable flaw sizes for near-surface subsurface flaws are governed by proximity requirements at the surface and not by crack tip stress intensity factor. In these cases, the flaws may be acceptable when evaluated as surface flaws. More details of the fracture mechanics evaluations to establish the flaw acceptance diagrams are presented in Reference 17.

5.0 CONCLUSIONS AND DISCUSSION

A comprehensive evaluation of potential flaws in the ANO-1 RPV shell welds and plate material has been completed. To limit the number of evaluations (and pages of this report) to a manageable size, a limiting set of locations was determined (welds) and flaw acceptance diagrams were developed for these locations. As in all engineering evaluations, a number of assumptions were built into these evaluations, including:

- A conservative assessment of cladding stresses was included.

- The effects of both deepest point and surface stress intensity factors were included.

- The largest acceptable flaw size was determined. There may be smaller flaw sizes (mainly for surface flaws) that would be unacceptable if evaluated without consideration of larger acceptable sizes.

- The assessments were computed for hydrotest and heatup/cooldown pressures and temperatures consistent with the vessel pressure/temperature limits for the current technical specifications [13]. Boltup at ambient temperature was considered for the upper flange weld.

- A conservative assessment of cyclic crack growth was included for all plant transients that can affect overall vessel heatup and cooldown to end of life.

- The analyses were conducted both with and without the effects of weld residual stresses.

- For the beltline region, the maximum effects of shift in the reference temperature were considered.

The results of the current evaluation show significantly smaller flaws for the inside surface than that presented in Reference 1. Several reasons are as follows:

- For the irradiated beltline regions, end-of-life fluence was considered.
- The effects of cladding were included. Reference 1 did not include cladding effects as required by Section XI, Appendix A.
- Weld residual stresses were considered, since recent publications [15] show that these are not reduced to zero by service or post weld heat treatment.
- A broad range of heatup and cooldown conditions were evaluated. In many cases, these were more limiting than the cases considered in Reference 1.
- The complete stress distribution through the wall was determined for all loading conditions, whereas Reference 1 appeared to work with linearized inside to outside stresses.

On the other hand, the current report performs specific analysis for subsurface and outside surface flaws. In some cases, these allow for larger flaws than Reference 1.

Based on the above, it is believed that the results of the evaluations are correct and conservative. However, because of the number of evaluations, every one could not be studied in detail to quantify and understand the conservatisms. Thus, these results by themselves should not serve as the sole basis for accepting flaws that significantly exceed the acceptance standards of IWB-3500. On the other hand, alternate analysis can probably be conducted, removing some of the conservatisms to show acceptability of larger flaws, by using tools like SI's fracture mechanics computer program pc-**CRACK** [18]. In addition, the requirements of NB-3000 for primary stress limits must be checked.

The information presented in the Appendices of this report should allow Entergy engineers to perform rapid assessment of any indications reported during RPV inservice examinations.

6.0 REFERENCES

1. B&W Document No. 77-1139631-00, ANO-1 Inservice Inspection Allowable Flaw Indications", December 1982.

2. "Rules for In-service Inspection of Nuclear Power Plant Components," Section XI of the ASME Boiler and Pressure Vessel Code, 1989 Edition, American Society of Mechanical Engineers, New York, July 1, 1989.

3. Raju, I. S., and Newman, J. C., "Stress-Intensity Factors for Internal and External Surface Cracks in Cylindrical Vessels," Journal of Pressure Vessel Technology, 104/298, November, 1982.

4. Tada, Paris and Irwin, "Stress Analysis of Cracks," Del Research Corporation, 1973.

5. Kuo, A.Y., Deardorff, A.F., & Riccardella, P.C., "Thermal Stress Intensity Factor of an Axial Crack in a Cladded Cylinder," presented at 1993 ASME Pressure Vessel & Piping Conference.

6. U.S. Nuclear Regulatory Commission, Regulatory Guide 1.99, Revision 2, May 1988.

7. APPENDA and MAPPA, "Computer Programs for Performing Flaw Tolerance Analysis of Reactor Vessel Shells," Structural Integrity Associates (QA-1800), June 1994.

8. SI Calculation ANO-10Q-301, "ANO-1 Vessel Materials Evaluation", Revision 0.

9. B&W Drawing 6600-MIB-1-7, "Arrgt. Reactor Vessel, Long. Sec.", Revision 7, dated 11/1/94, SI File ANO-10Q-208.

10. B&W Drawing MIB-223, "Upper Shell Assembly", Revision 0, dated 8/2/91, SI File ANO-10Q-208.

11. B&W Drawing MIB-230, "Vessel HD & Suppt Assy & Det.", Revision 0, dated 8/2/91, SI File ANO-10Q-208.

12. "Design Report - Arkansas Power & Light Company, Arkansas Power #1, Reactor Vessel and Closure Head", Including Stress Analysis Reports Numbers 1 through 11, Customer Order No. M-1-6600, B&W Contract No. 620-0008-51/52, March 1974, SI File Numbers ANO-10Q-209 through ANO-10Q-216.

13. Excerpts from ANO-1 Technical Specifications, Section 3.1.2, SI File ANO-10Q-302.

14. SI Calculation ANO-10Q-302, "ANO-1 Reactor Vessel Stress Analysis", Revision 0.

15. EPRI-TR-100251, "White Paper on Reactor Vessel Integrity Requirements for Level A and B Conditions," Electric Power Research Institute, January 1993.

16. PIPE-TS2, "A Computer Program to Compute the Transient Thermal and Thermal Stress Response of an Axisymmetric Two-Material Cylinder," Structural Integrity Associates, Version 1.01, (QA-1260), April 1991.

17. SI Calculation ANO-10Q-303, "APPENDA/MAPPA Reactor Vessel Flaw Evaluation", Revision 0.

18. "**pc-CRACK** Fracture Mechanics Software" Version 2.1, Structural Integrity Associates, San Jose, 1991.

APPENDIX A

Flaw Acceptance Diagrams for Group A Materials

Items Covered

- Upper Head to Flange Weld
- Adjacent Head Plate (Mk #24)
- Adjacent Flange (Mk #7)

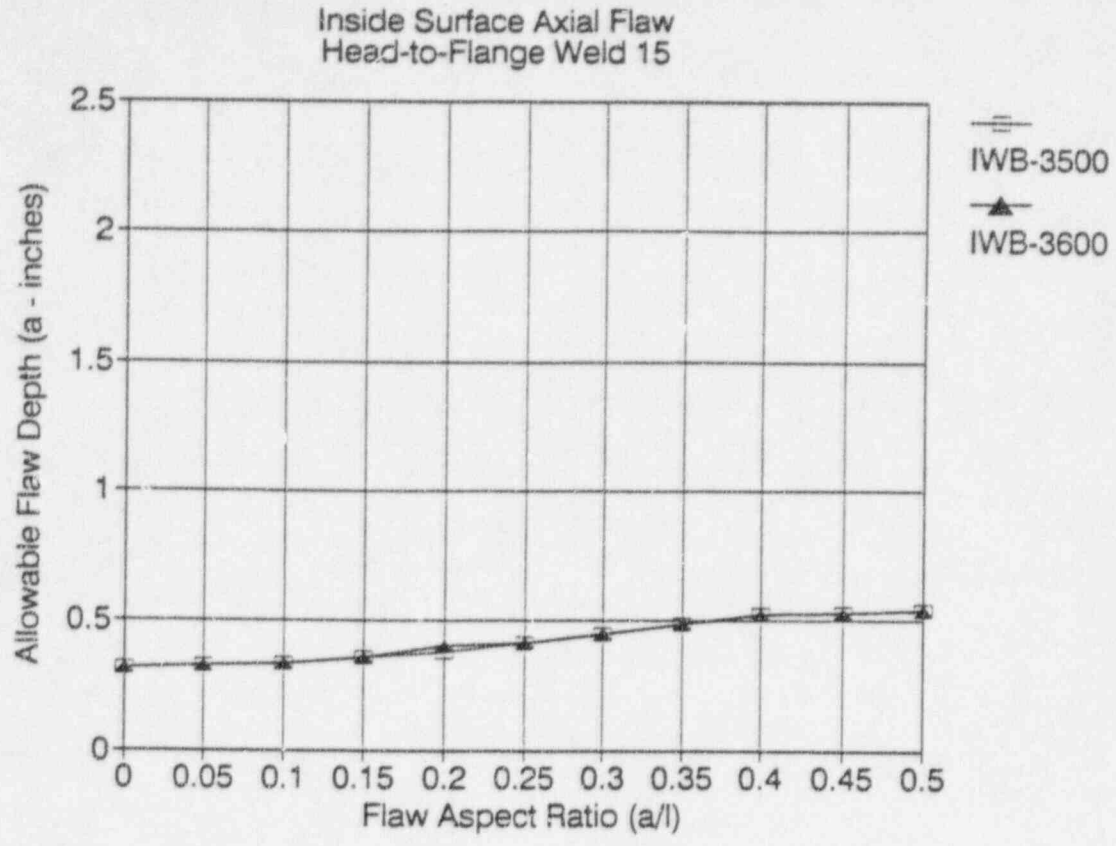

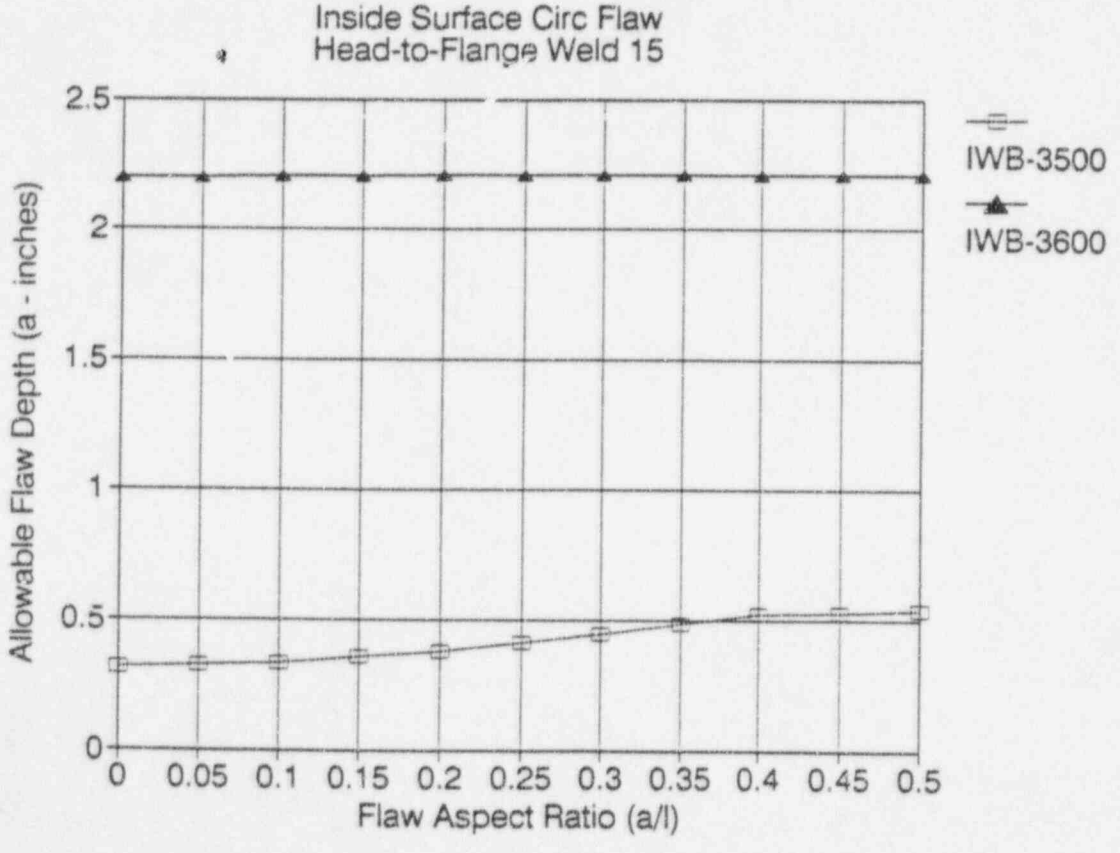

Figure A-1. Flaw Acceptance Diagram For Inside Surface Flaws (Group A)

Note: Flaw depth includes thickness of cladding.

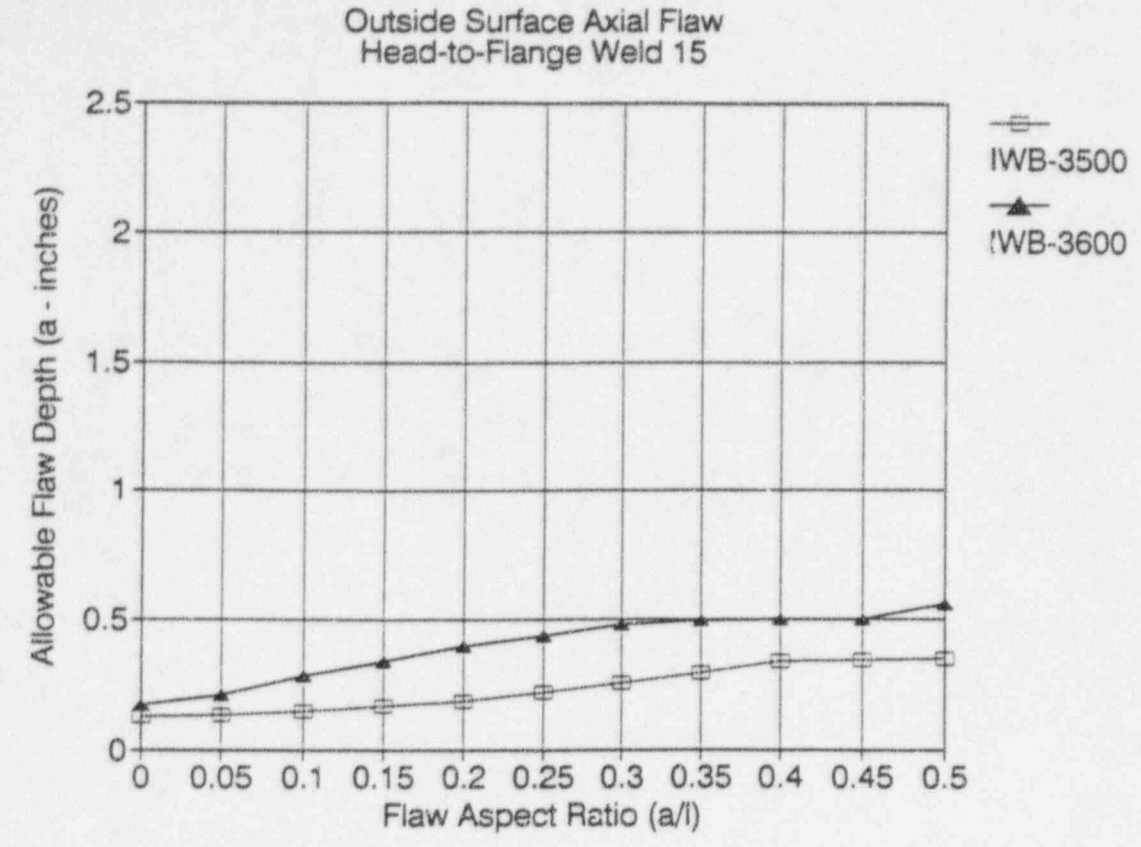

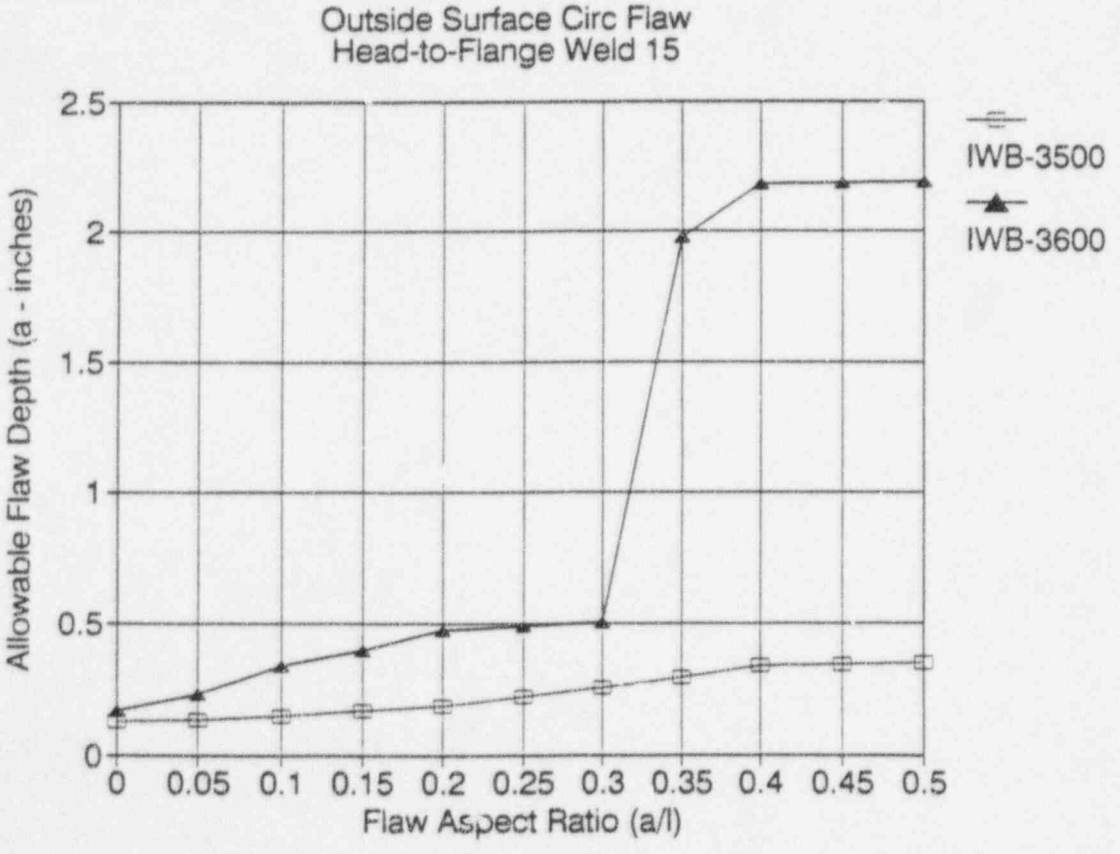

Figure A-2 Flaw Acceptance Diagram for Outside Surface Flaws (Group A)

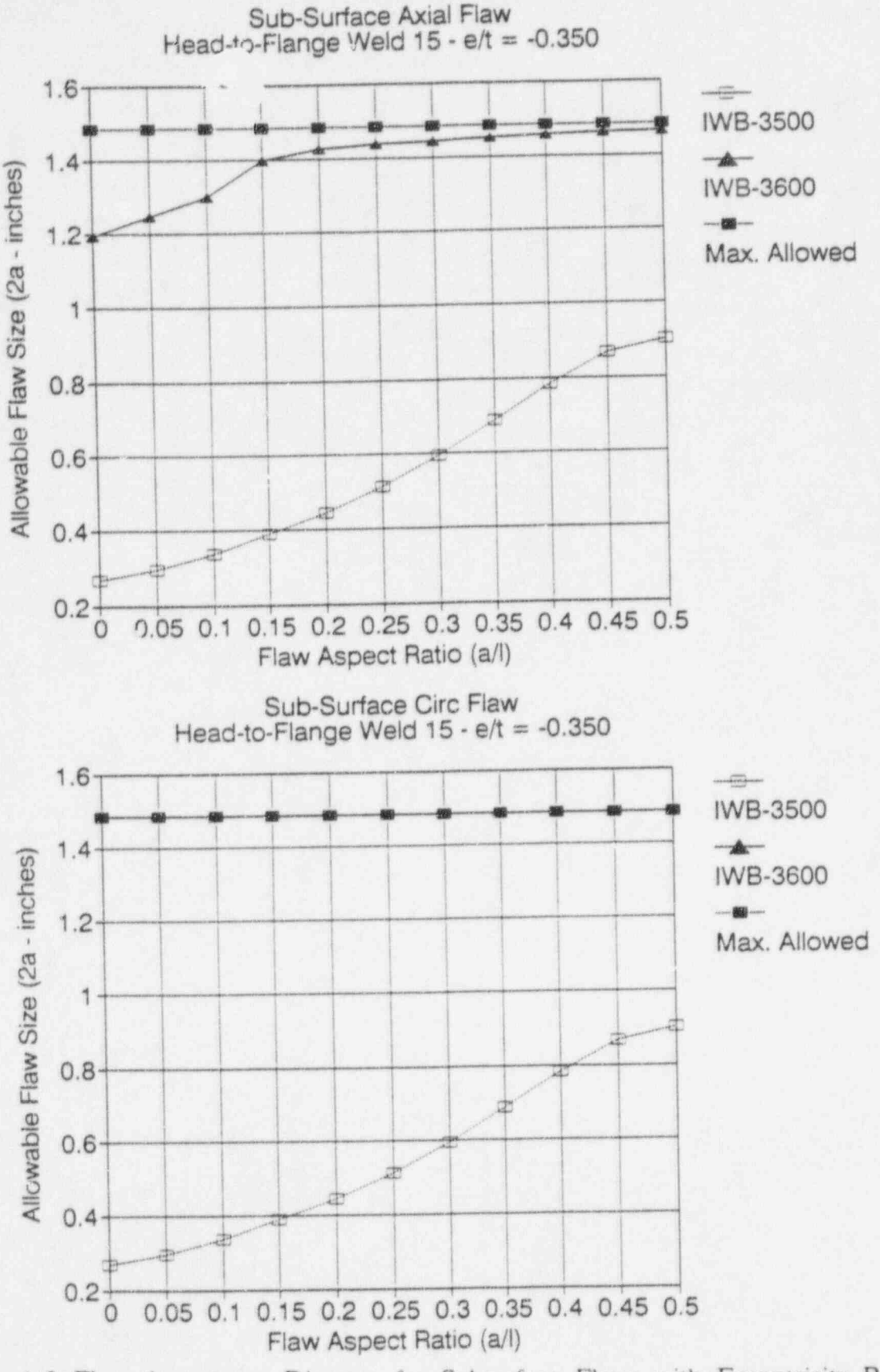

Figure A-3. Flaw Acceptance Diagram for Subsurface Flaws with Eccentricity Ratio of -0.35 (Group A)

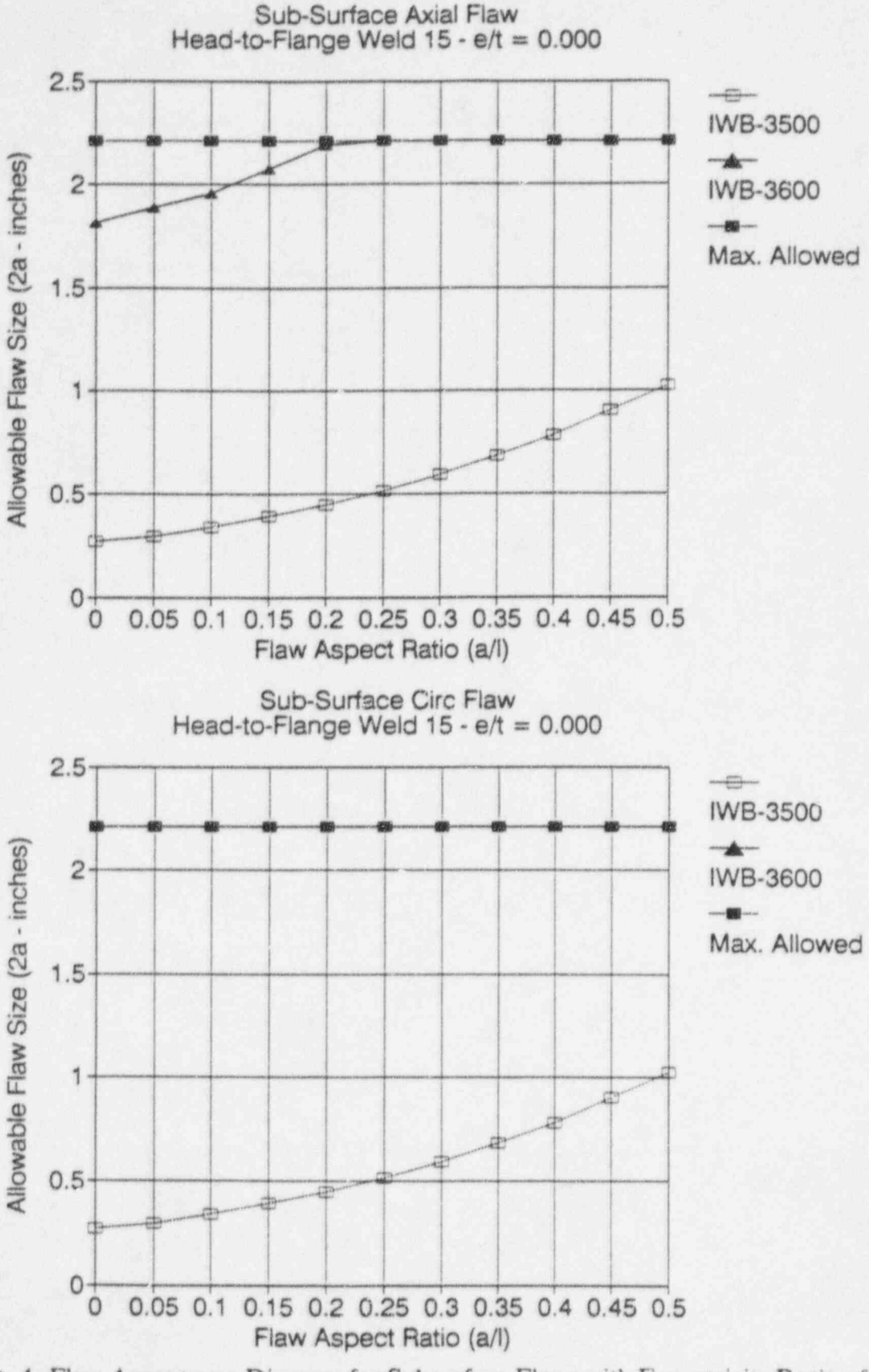

Figure A-4. Flaw Acceptance Diagram for Subsurface Flaws with Eccentricity Ratio of 0.0 (Group A)

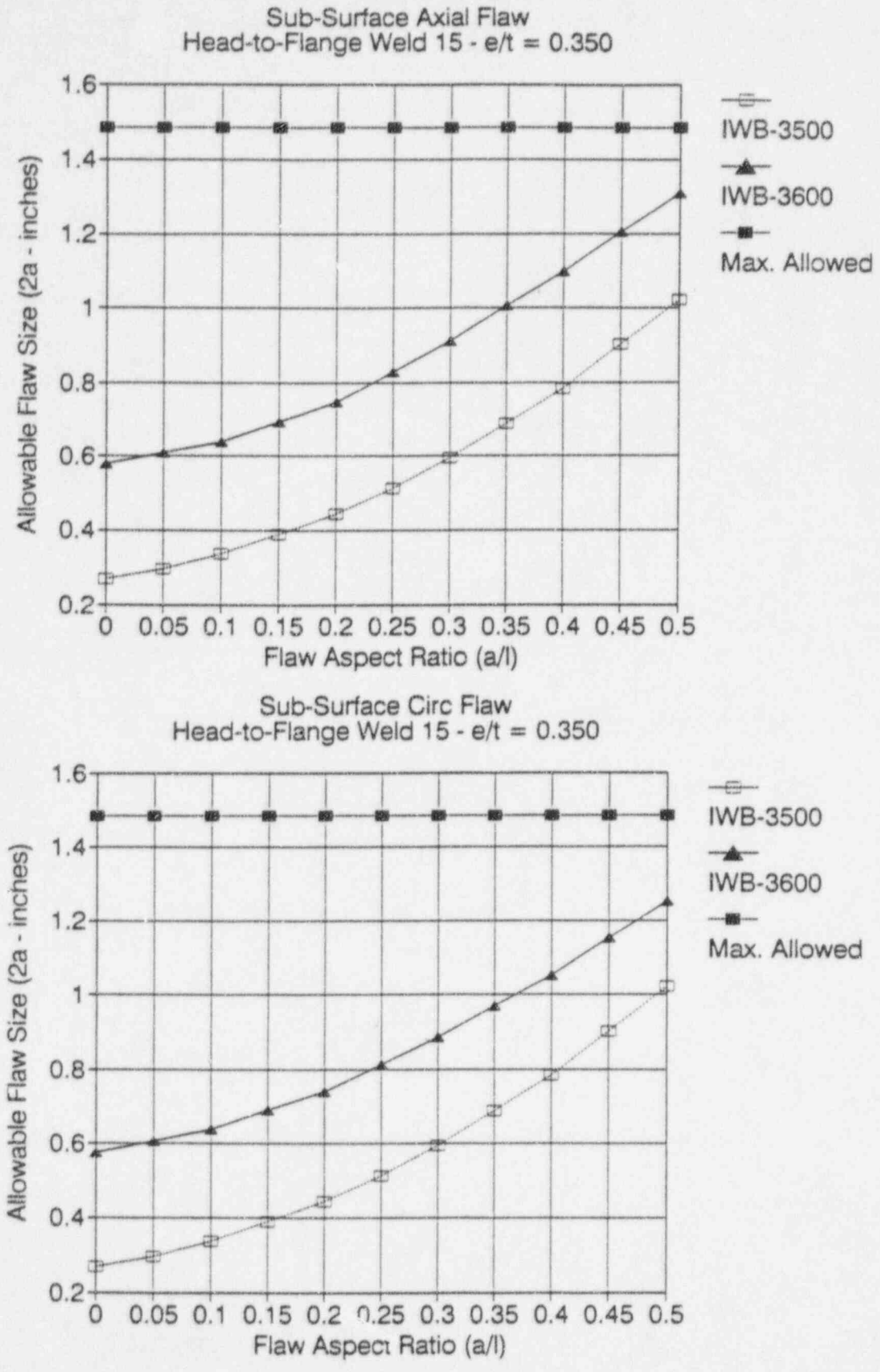

Figure A-5. Flaw Acceptance Diagram for Subsurface Flaws with Eccentricity Ratio of 0.35 (Group A)

APPENDIX B

Flaw Acceptance Diagrams for Group B Materials

Items Covered

- Vessel Flange to Nozzle Belt Weld (01-001)
- Adjacent Flange (Mk #7)
- Adjacent Upper Nozzle Belt (Mk #86)

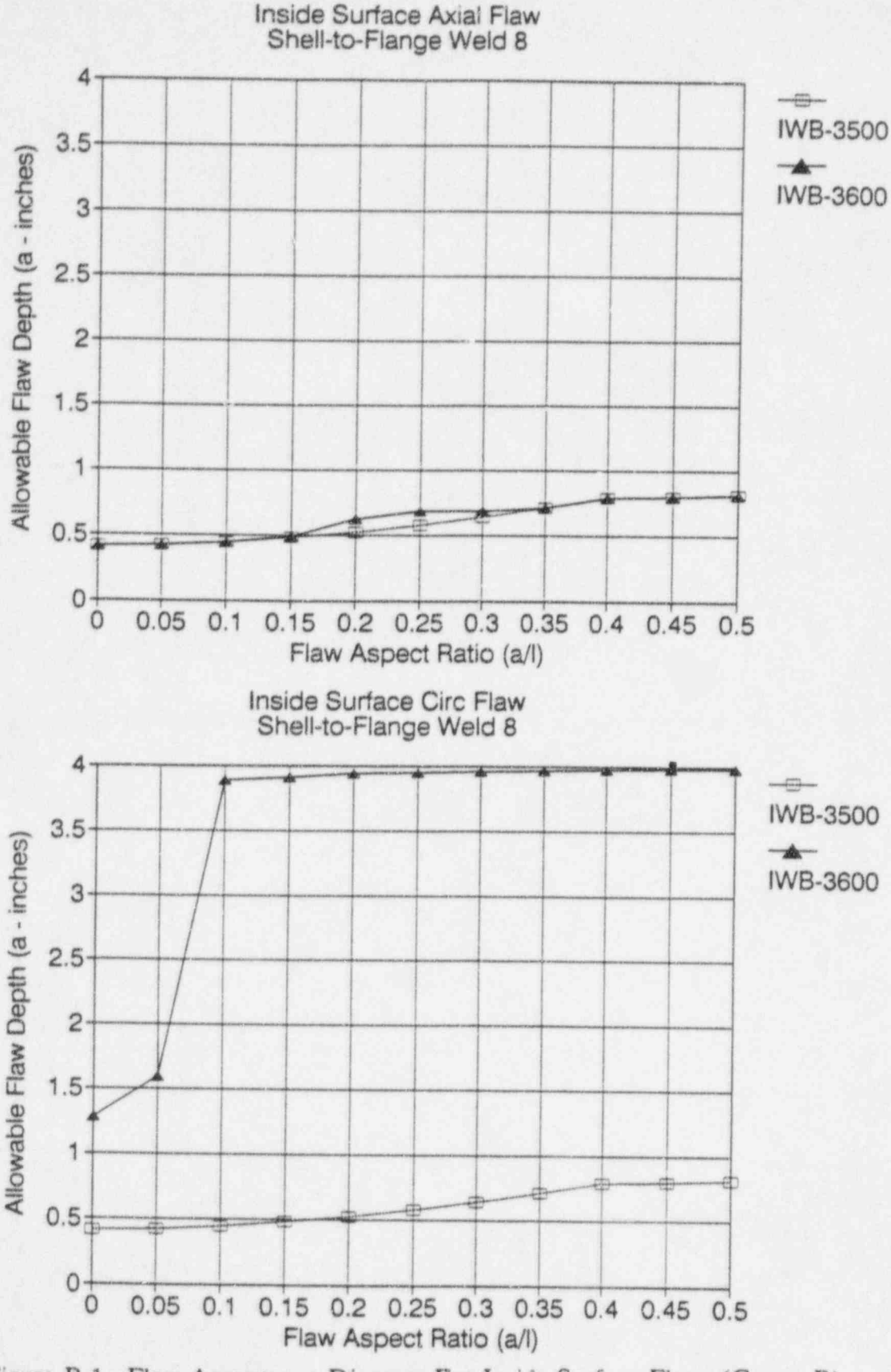

Figure B-1. Flaw Acceptance Diagram For Inside Surface Flaws (Group B)

Note: Flaw depth includes thickness of cladding.

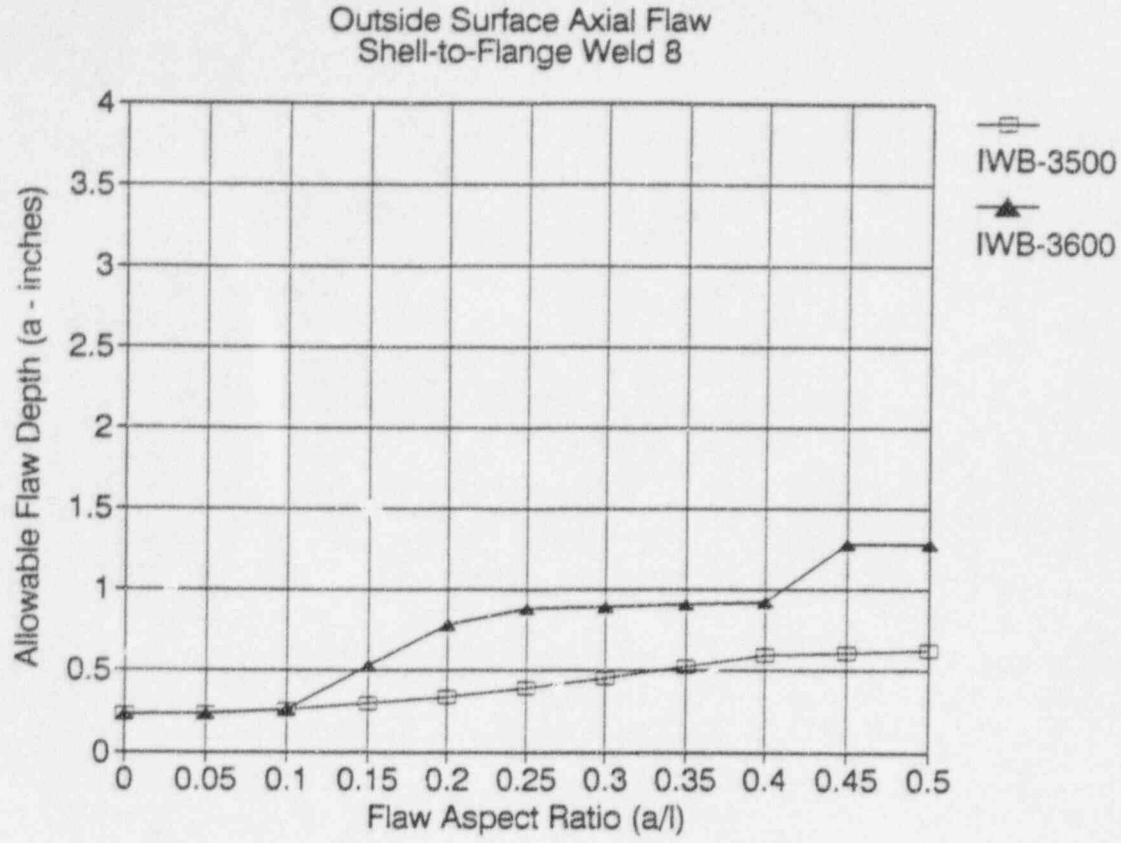

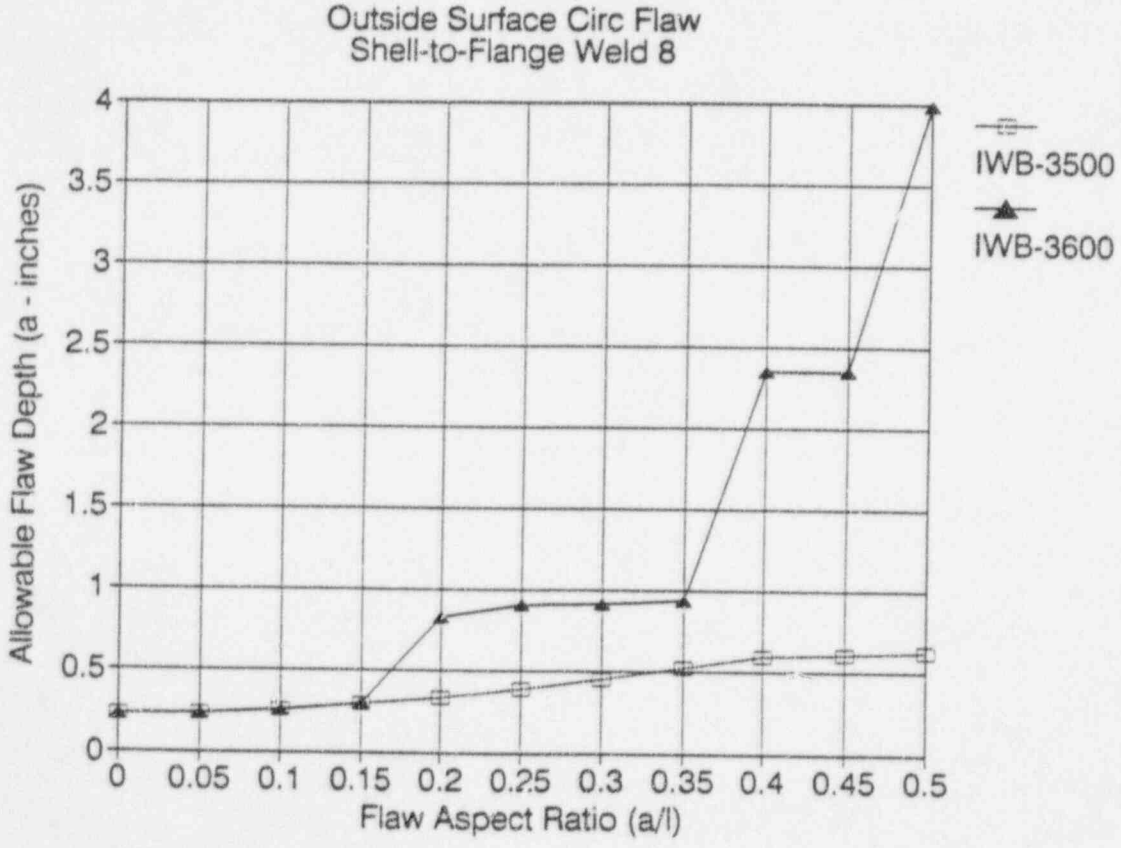

Figure B-2. Flaw Acceptance Diagram for Outside Surface Flaws (Group B)

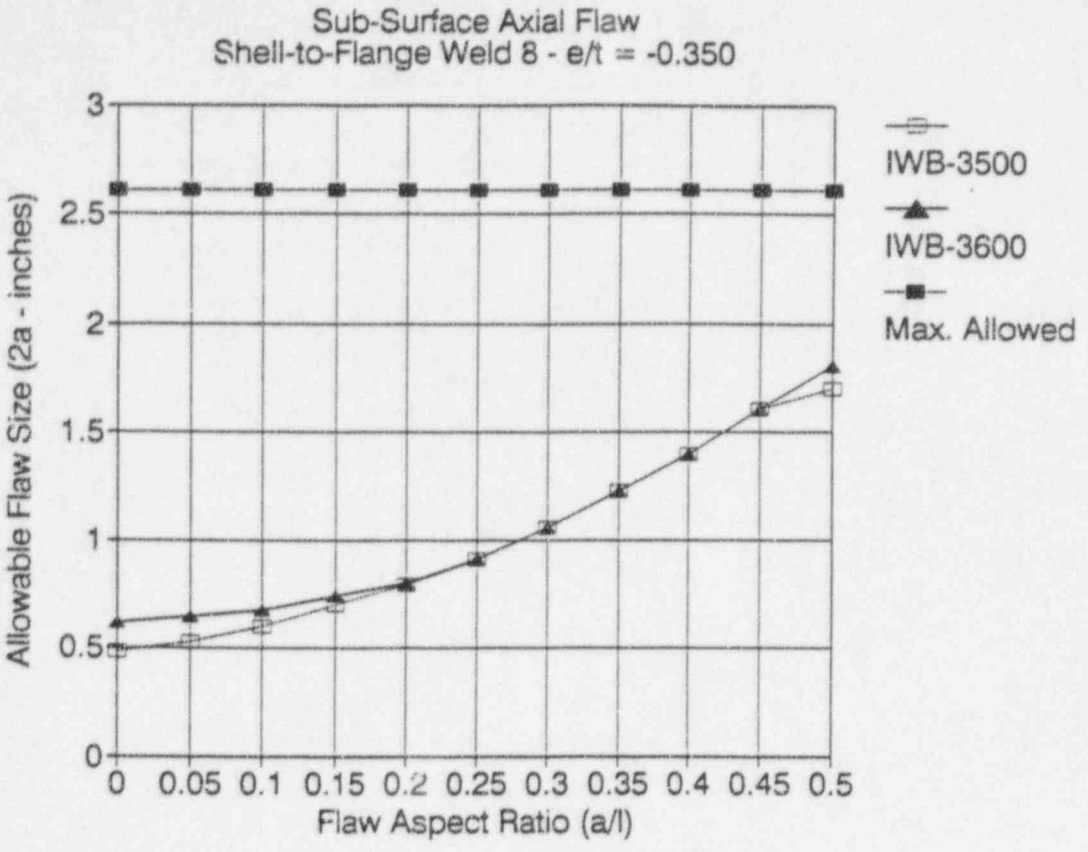

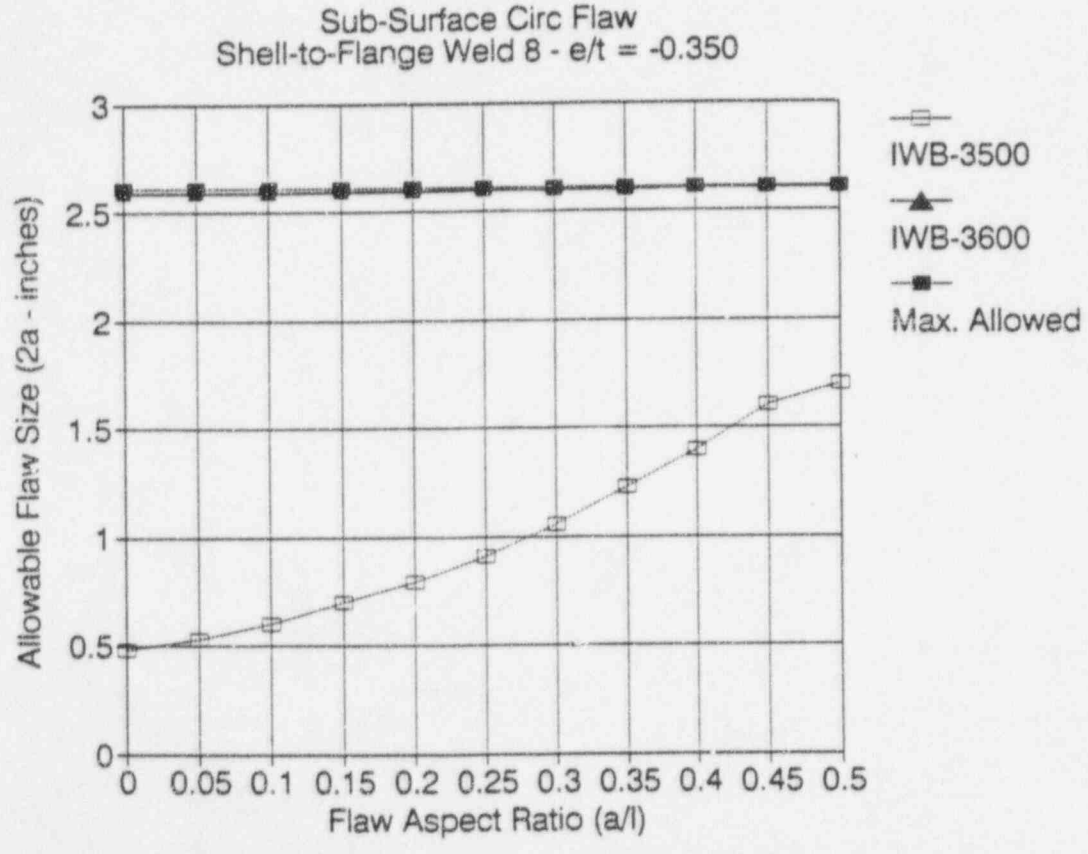

Figure B-3. Flaw Acceptance Diagram for Subsurface Flaws with Eccentricity Ratio of -0.35 (Group B)

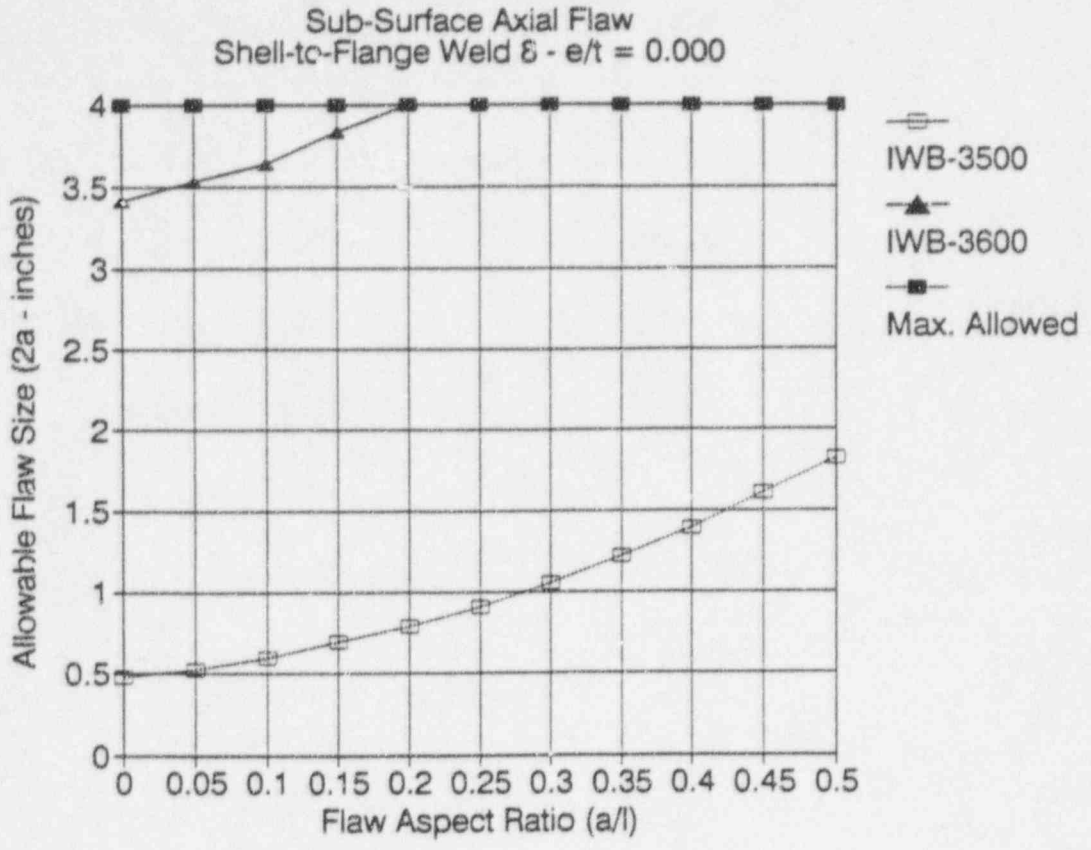

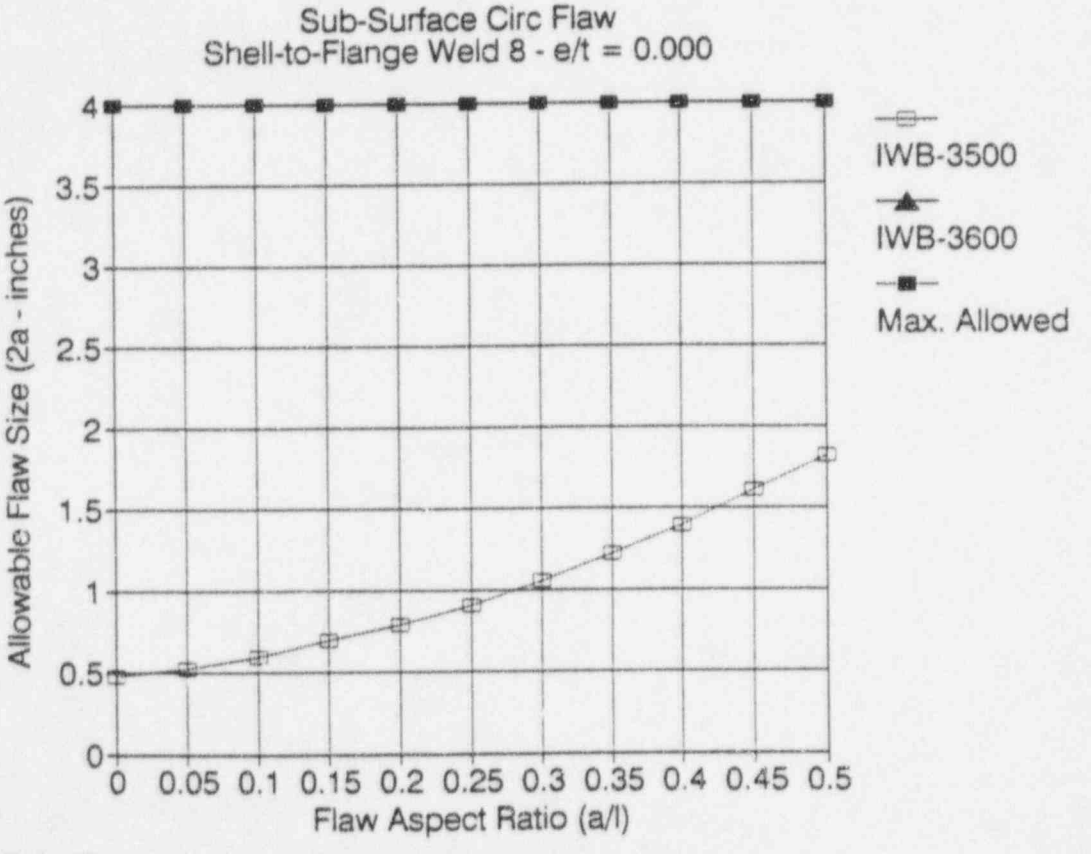

Figure B-4. Flaw Acceptance Diagram for Subsurface Flaws with Eccentricity Ratio of 0.0 (Group B)

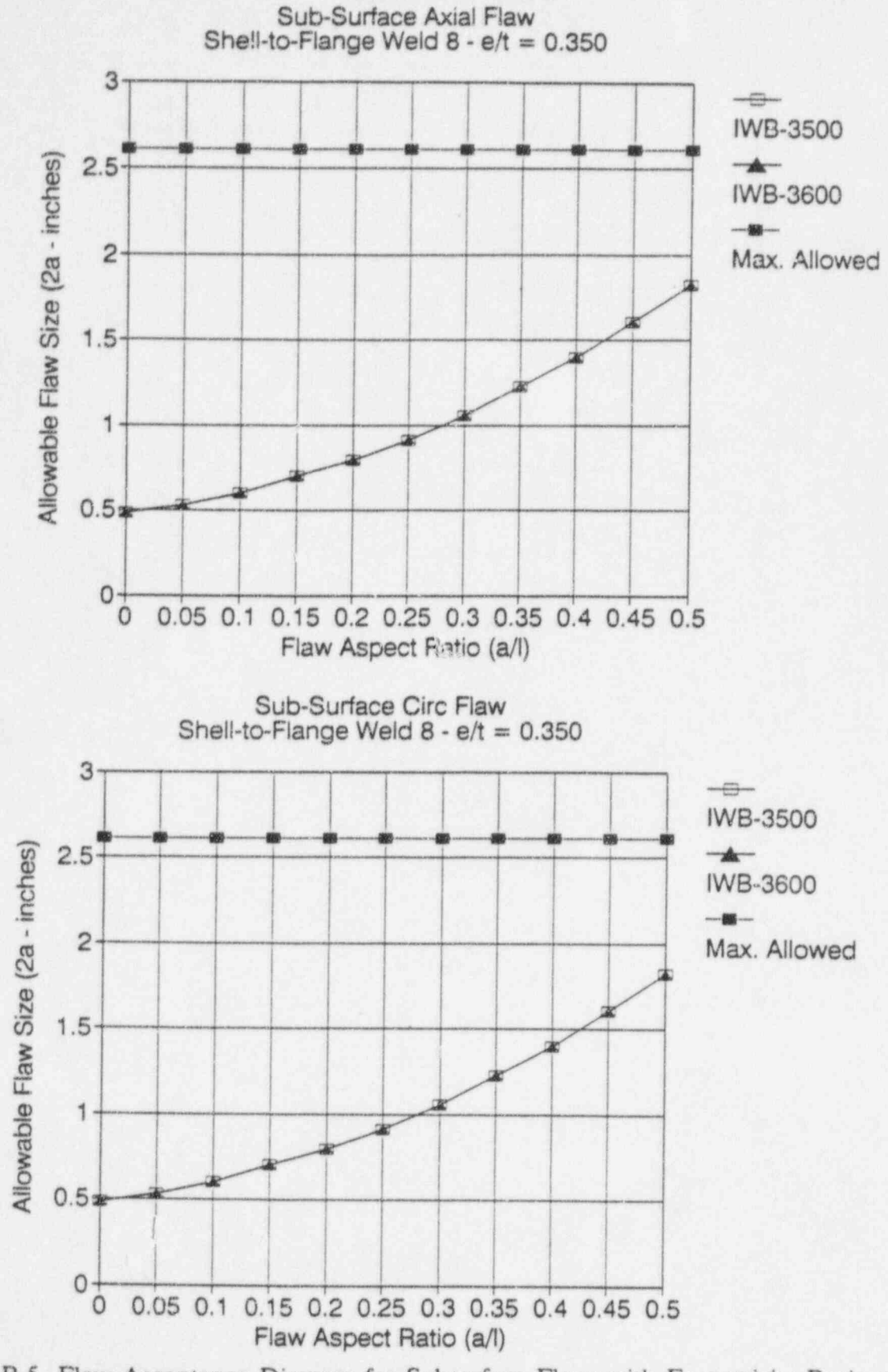

Figure B-5. Flaw Acceptance Diagram for Subsurface Flaws with Eccentricity Ratio of 0.35 (Group B)

APPENDIX C

Flaw Acceptance Diagrams for Group C Materials

Items Covered

- Nozzle Belt to Nozzle Belt Weld (01-002)
- Adjacent Nozzle Belts (Mk #86 and Mk #87)

Note:

For regions adjacent to the vessel inlet and outlet nozzles, special evaluations are required due to possible interaction effects

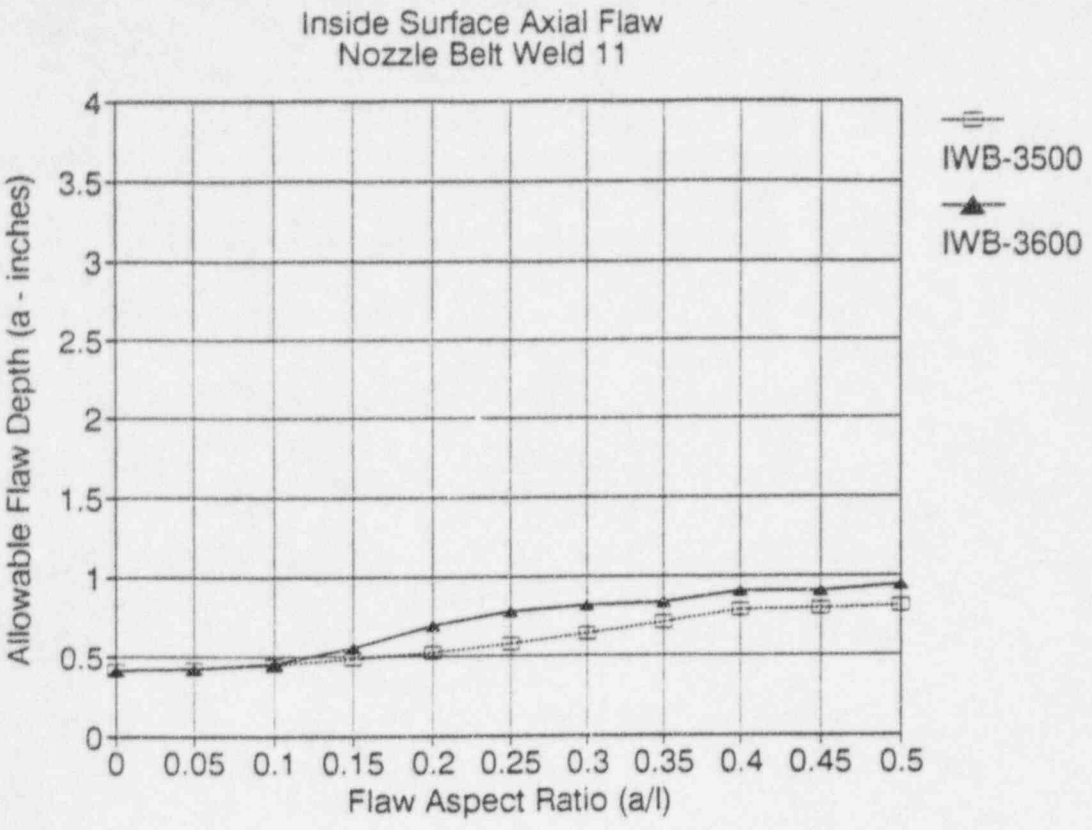

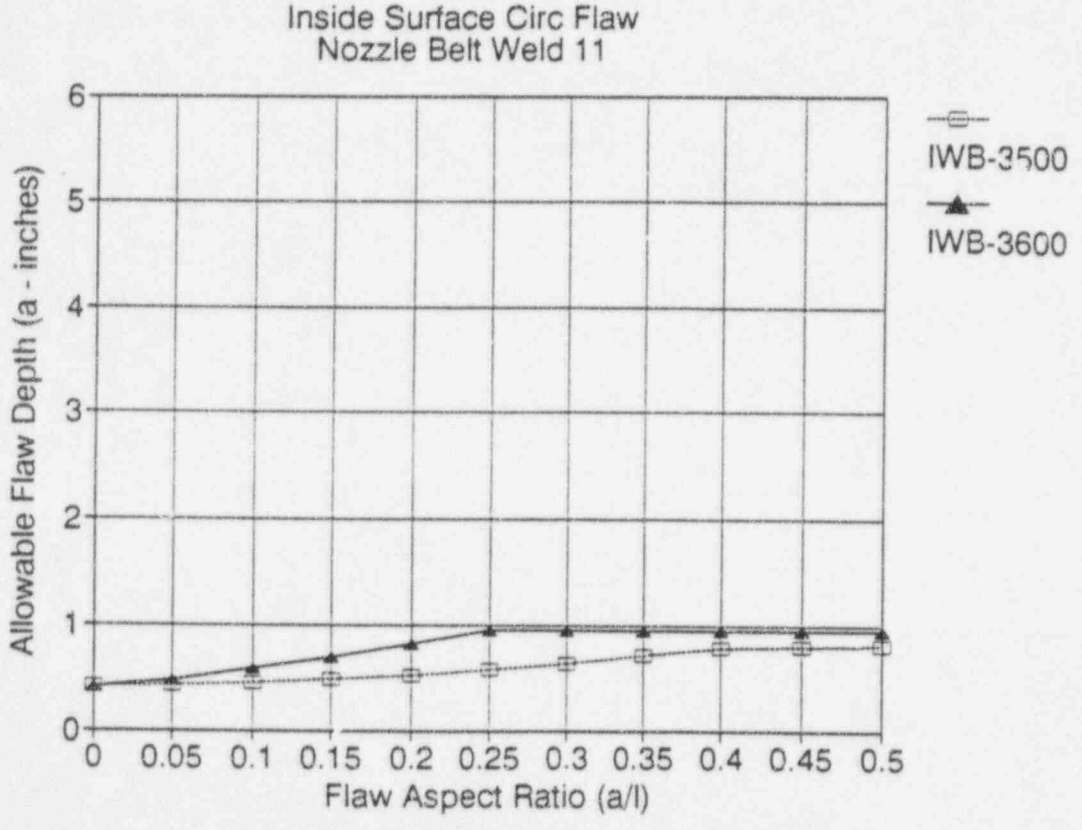

Figure C-1. Flaw Acceptance Diagram For Inside Surface Flaws (Group C)

Note: Flaw depth includes thickness of cladding.

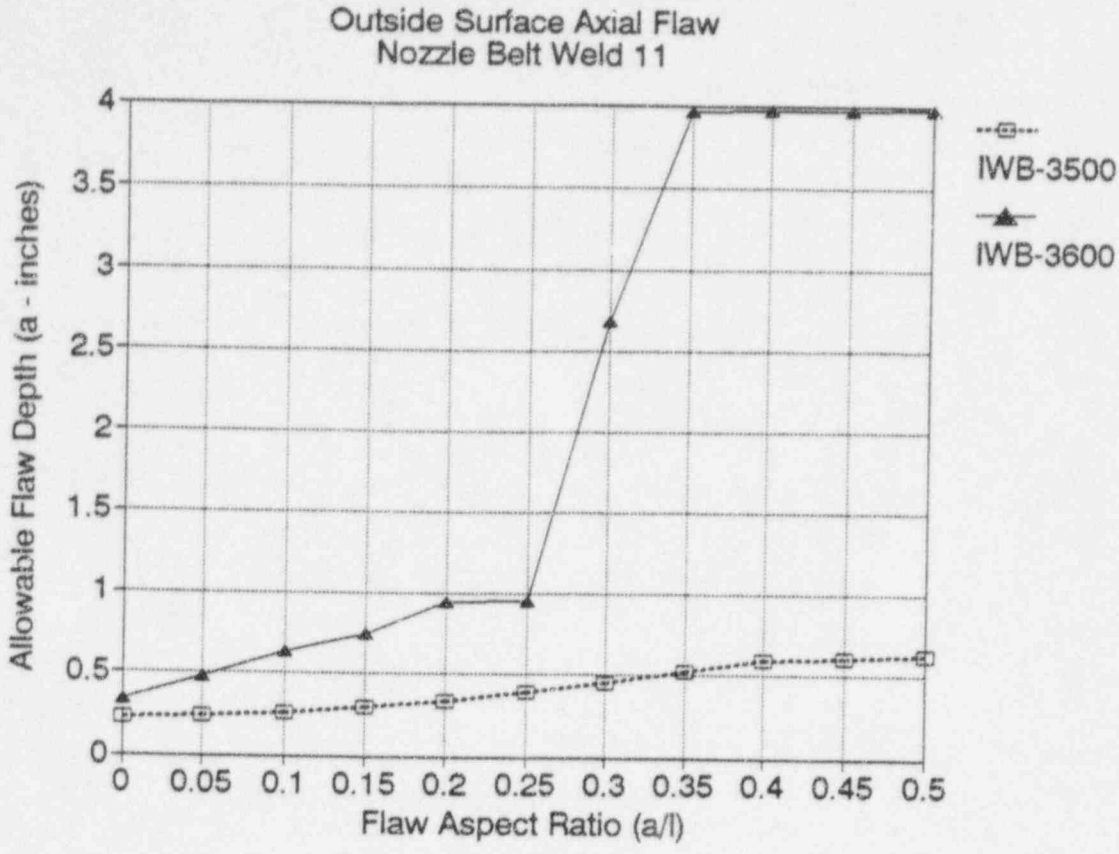

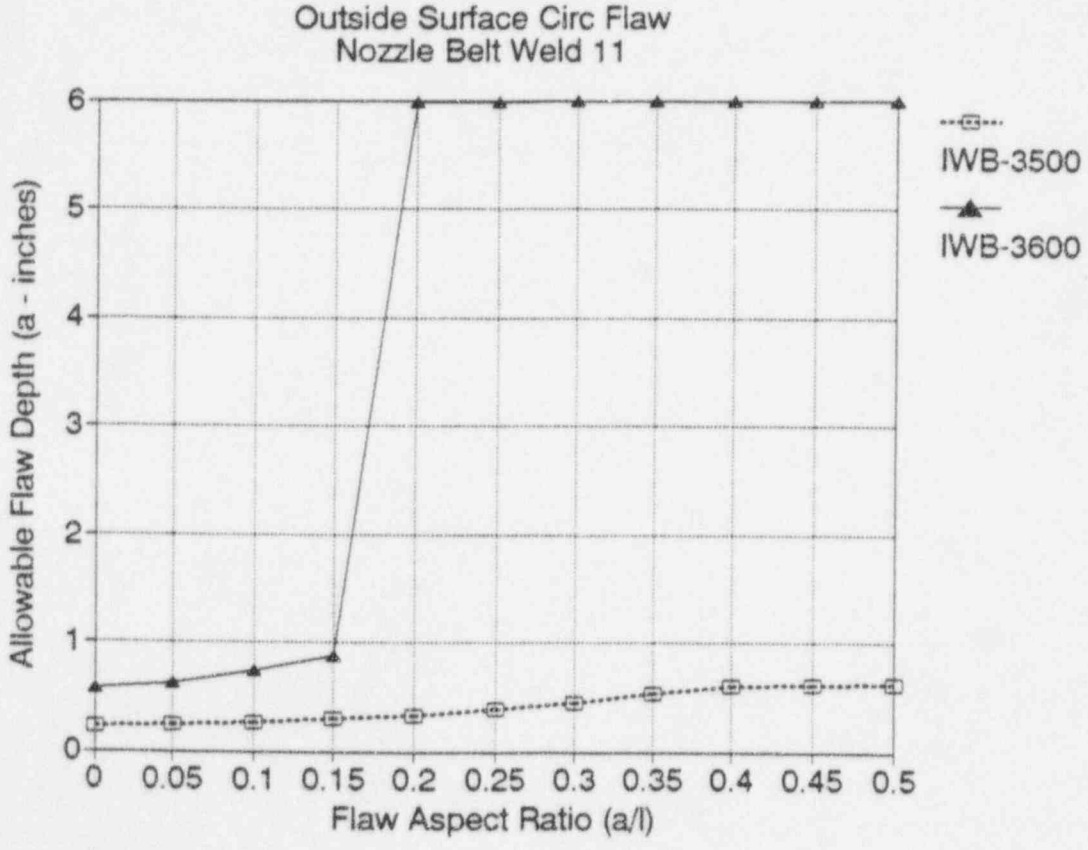

Figure C-2. Flaw Acceptance Diagram for Outside Surface Flaws (Group C)

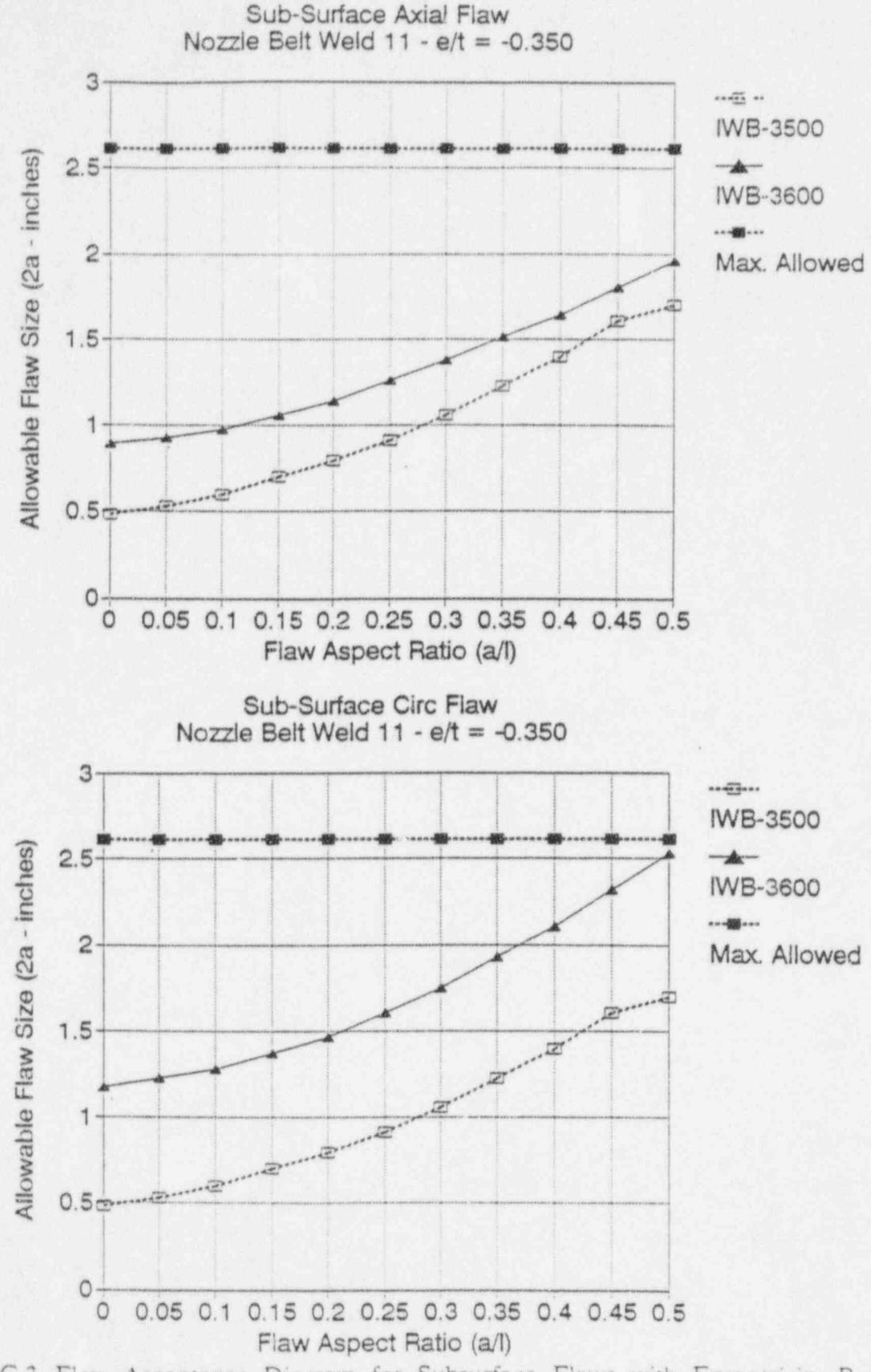

Figure C-3. Flaw Acceptance Diagram for Subsurface Flaws with Eccentricity Ratio of -0.35 (Group C)

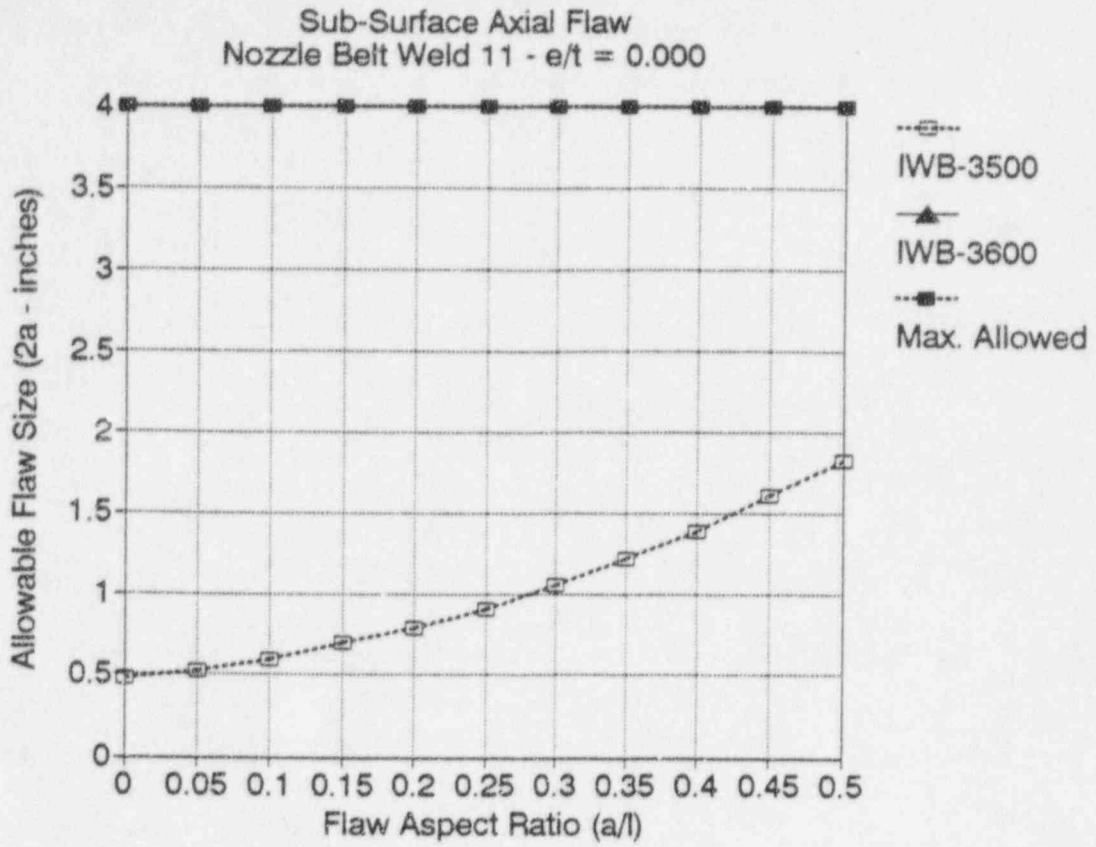

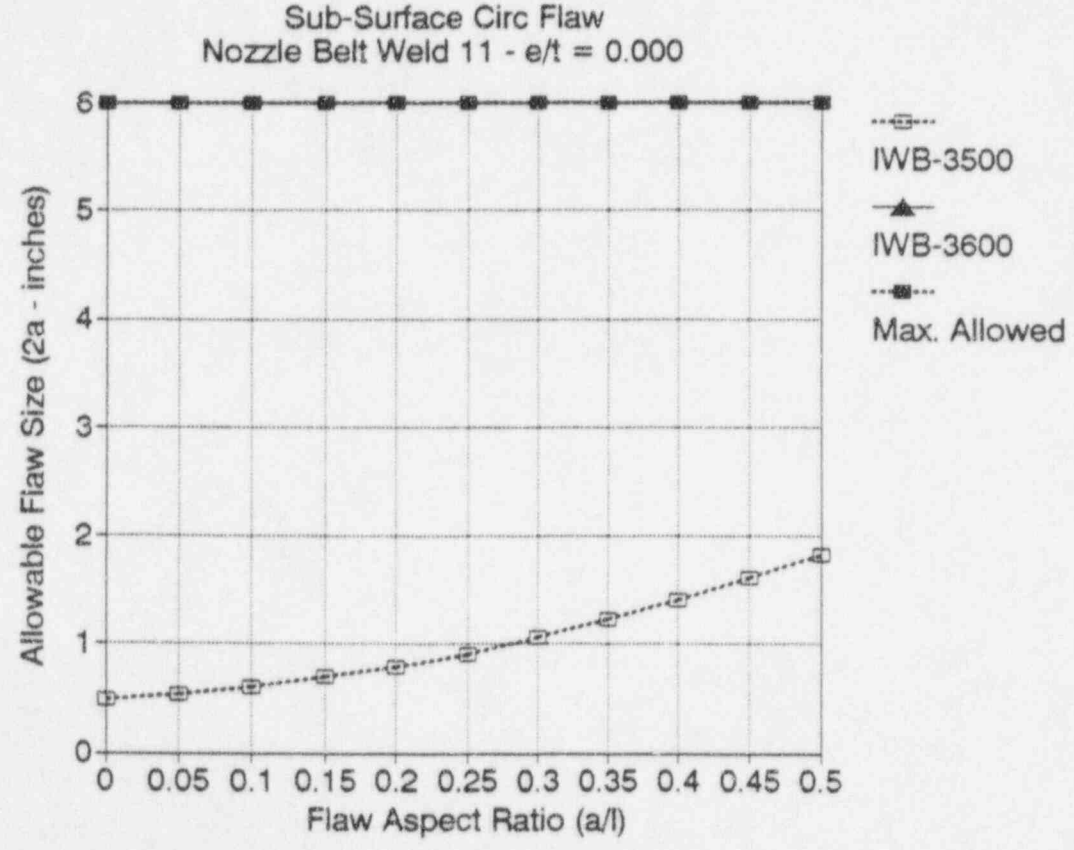

Figure C-4. Flaw Acceptance Diagram for Subsurface Flaws with Eccentricity Ratio of 0.0 (Group C)

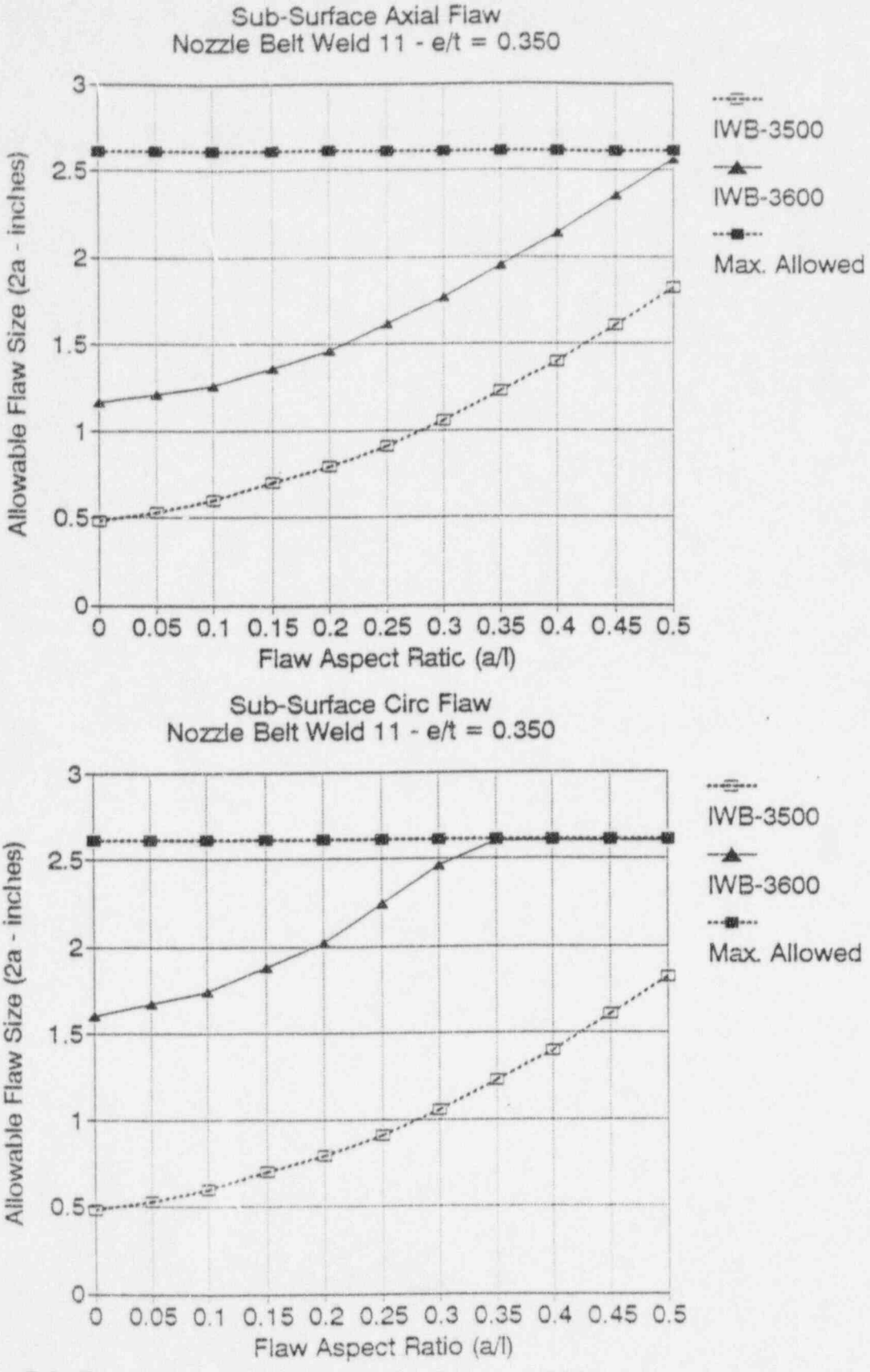

Figure C-5. Flaw Acceptance Diagram for Subsurface Flaws with Eccentricity Ratio of 0.35 (Group C)

APPENDIX D

Flaw Acceptance Diagrams for Group D Materials

Items Covered

- Lower Nozzle Belt Plate [1]
- Lower Shell Plate [2] (Mk #A2 - C5114)

[1] Adjacent to weld 01-003

[2] Portion above vessel thickness transition

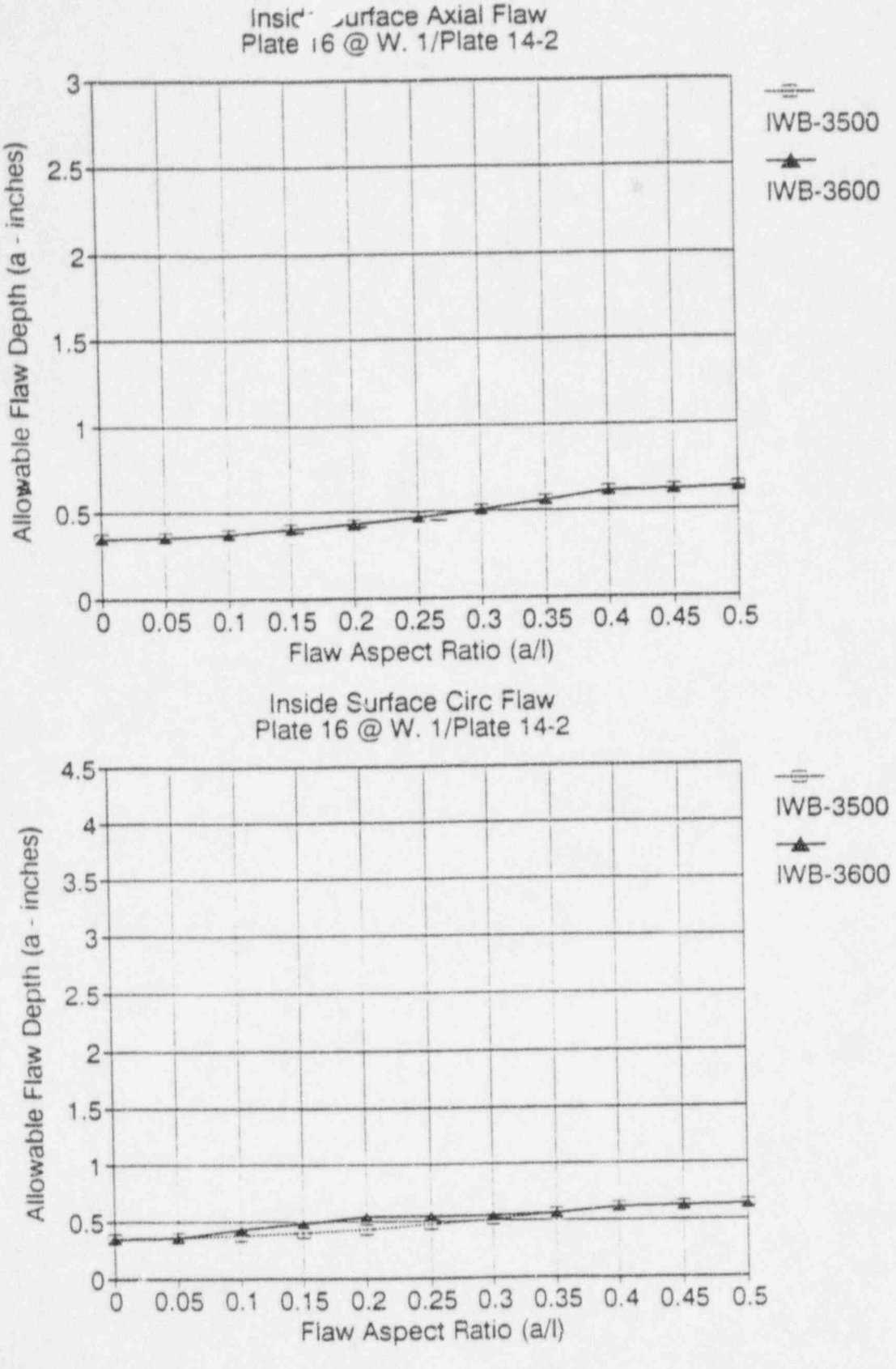

Figure D-1. Flaw Acceptance Diagram For Inside Surface Flaws (Group D)

Note: Flaw depth includes thickness of cladding.

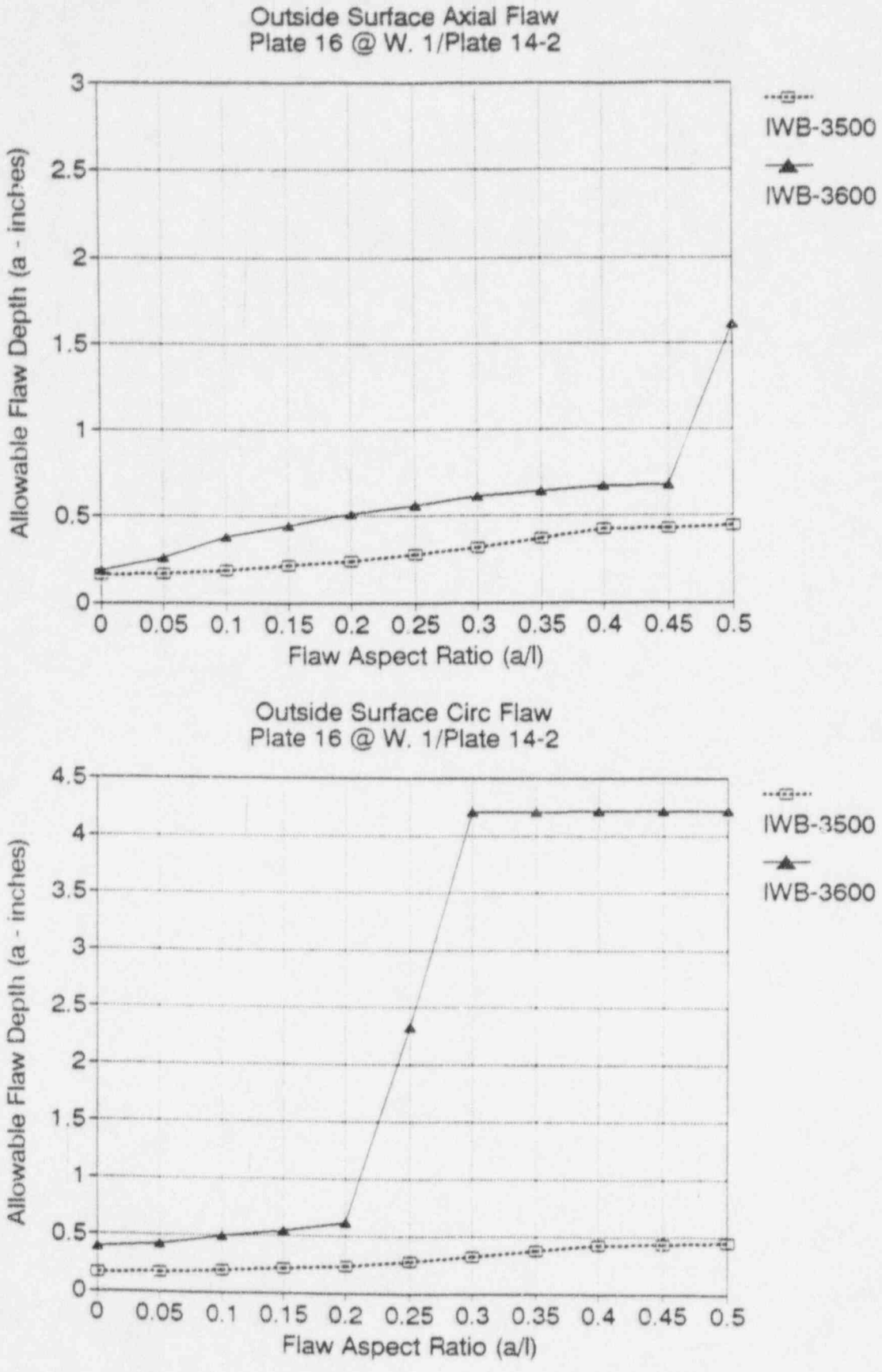

Figure D-2. Flaw Acceptance Diagram for Outside Surface Flaws (Group D)

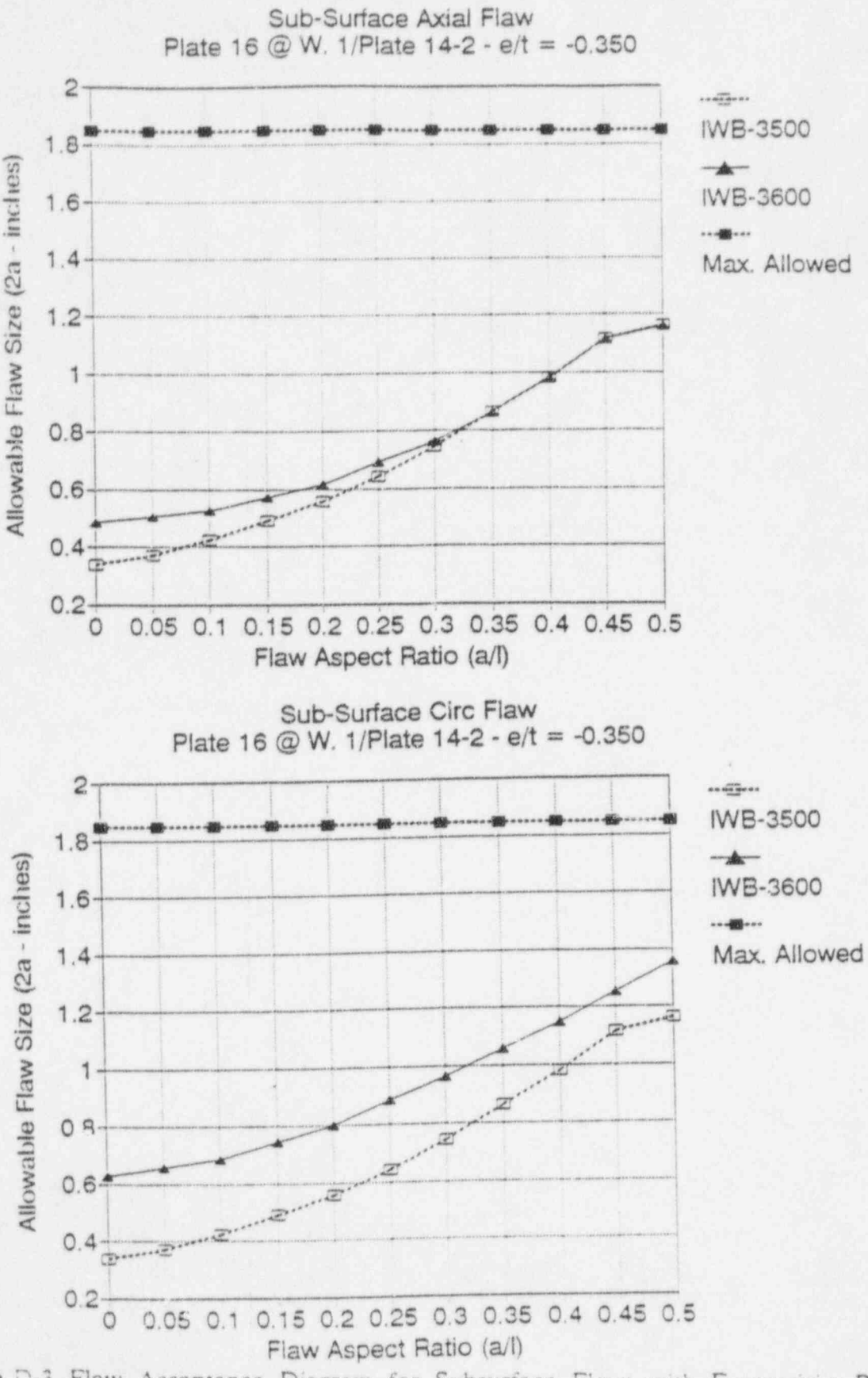

Figure D-3. Flaw Acceptance Diagram for Subsurface Flaws with Eccentricity Ratio of -0.35 (Group D)

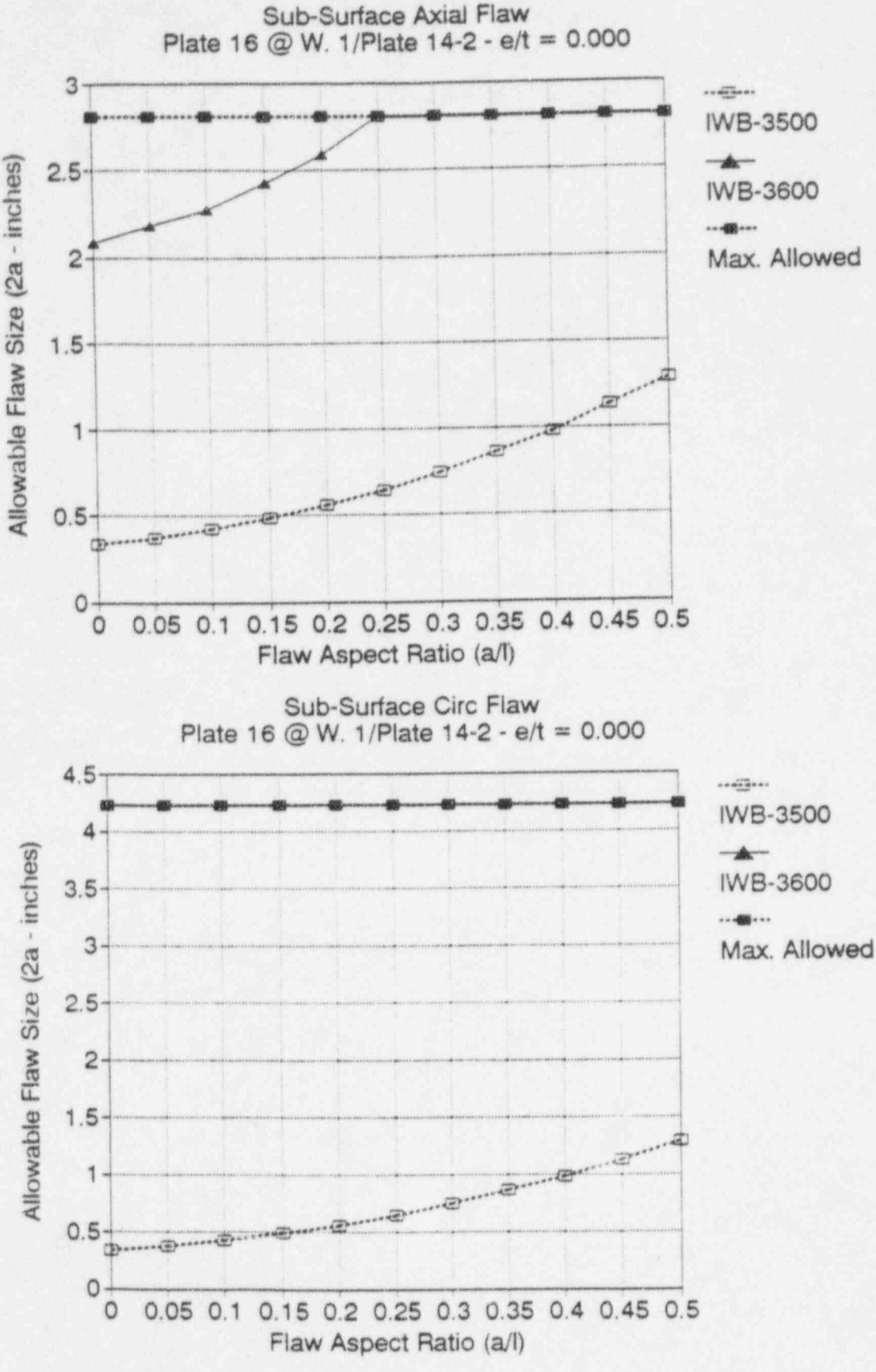

Figure D-4. Flaw Acceptance Diagram for Subsurface Flaws with Eccentricity Ratio of 0.0 (Group D)

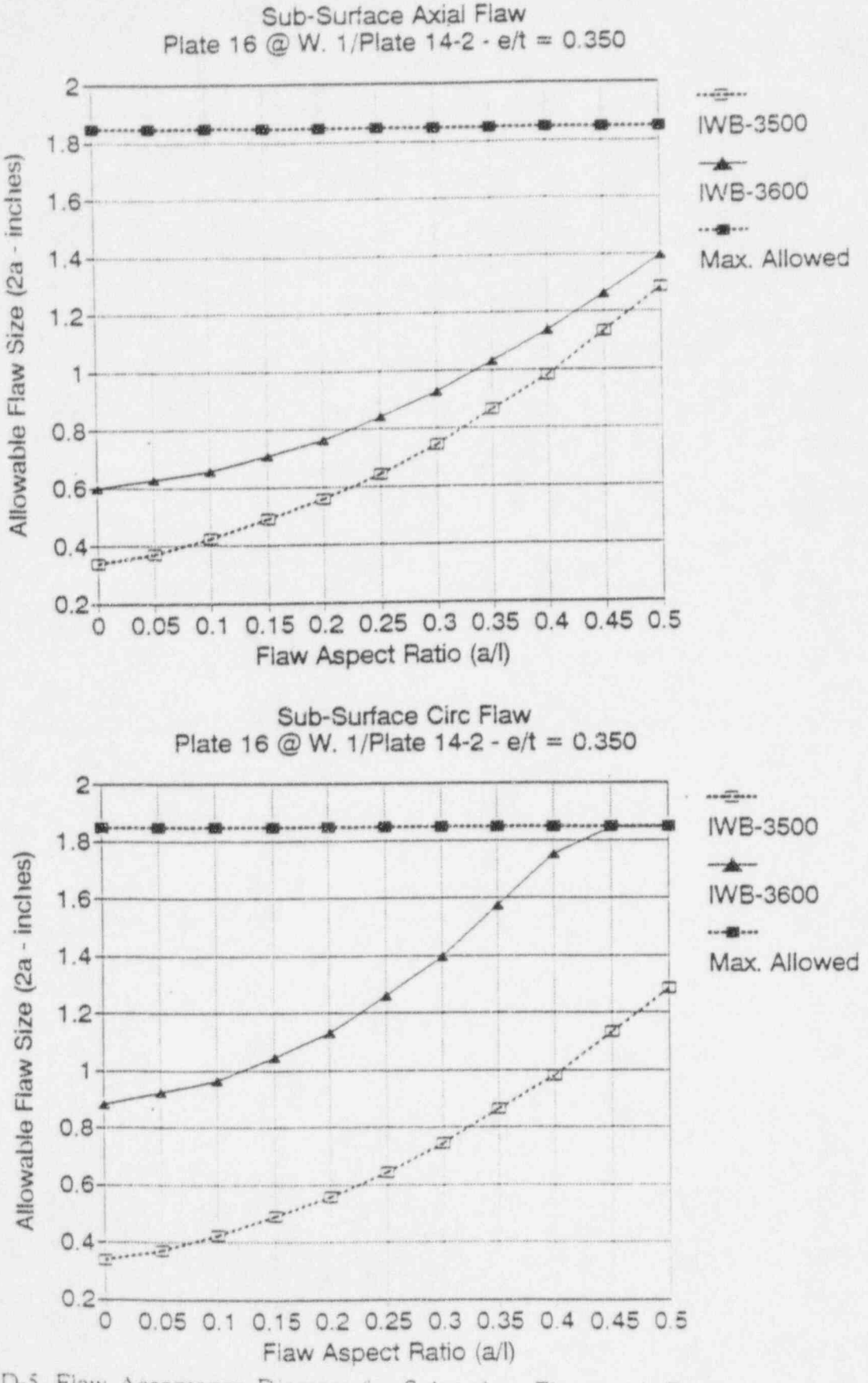

Figure D-5. Flaw Acceptance Diagram for Subsurface Flaws with Eccentricity Ratio of 0.35 (Group D)

APPENDIX E

Flaw Acceptance Diagrams for Group E Materials

Items Covered

- Upper Shell Plates (Mk #A1-C5120, Mk #A1-C5114)
- Lower Shell Plate [1] (Mk #A2-C5120)

[1] Applicable to portions of plate above the thickness transition. Special evaluation required for plate on transition. See Group H for plate adjacent to weld 01-005.

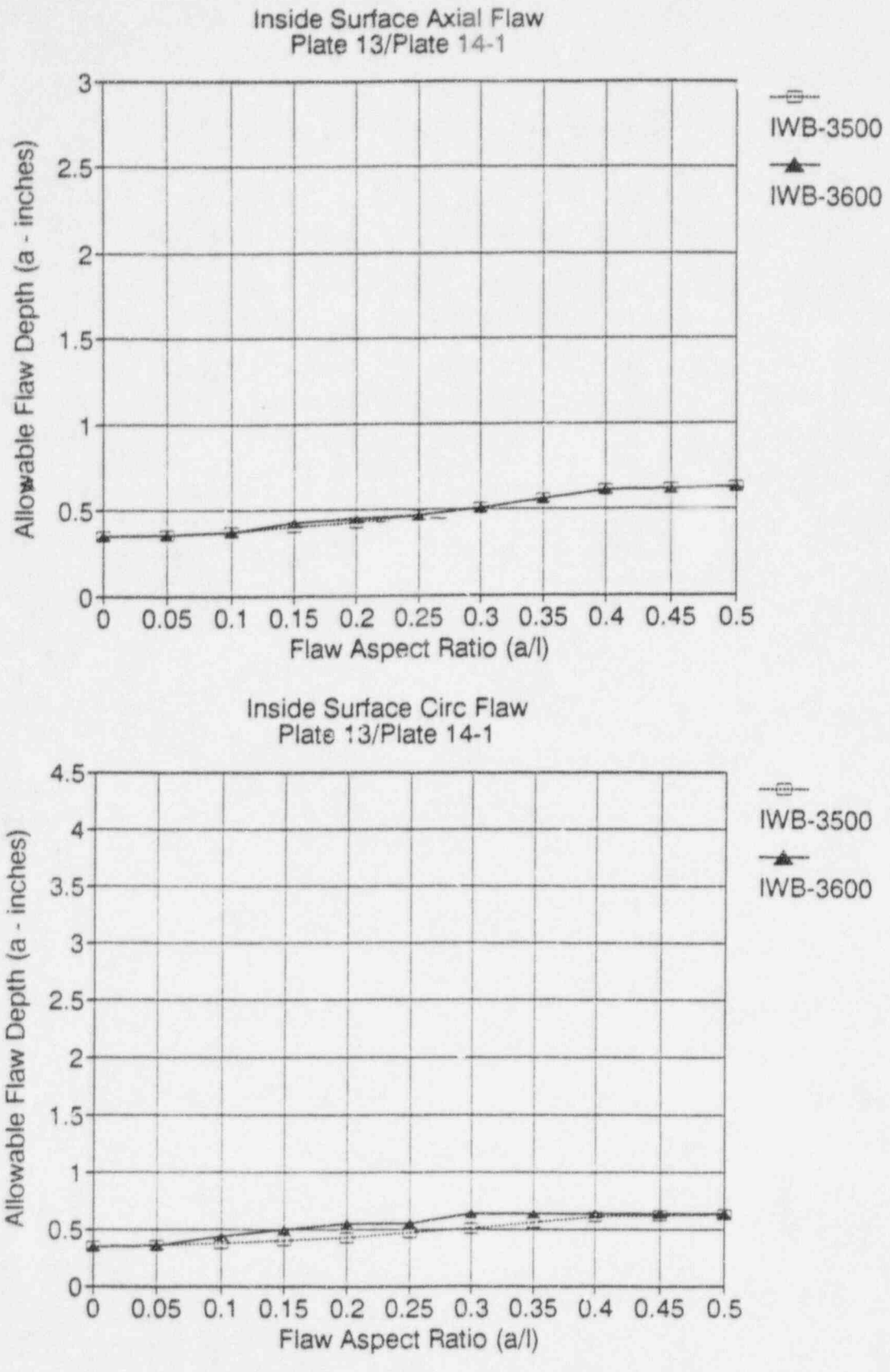

Figure E-1. Flaw Acceptance Diagram For Inside Surface Flaws (Group E)

Note: Flaw depth includes thickness of cladding.

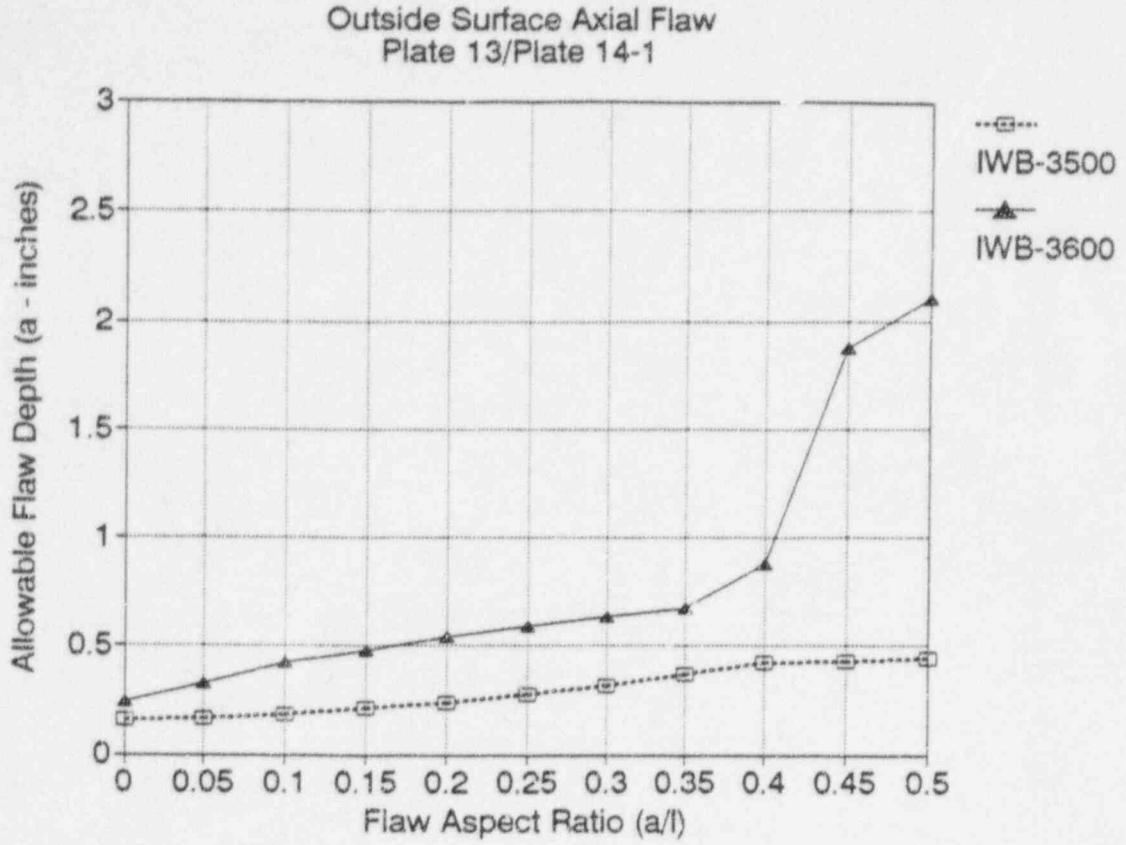

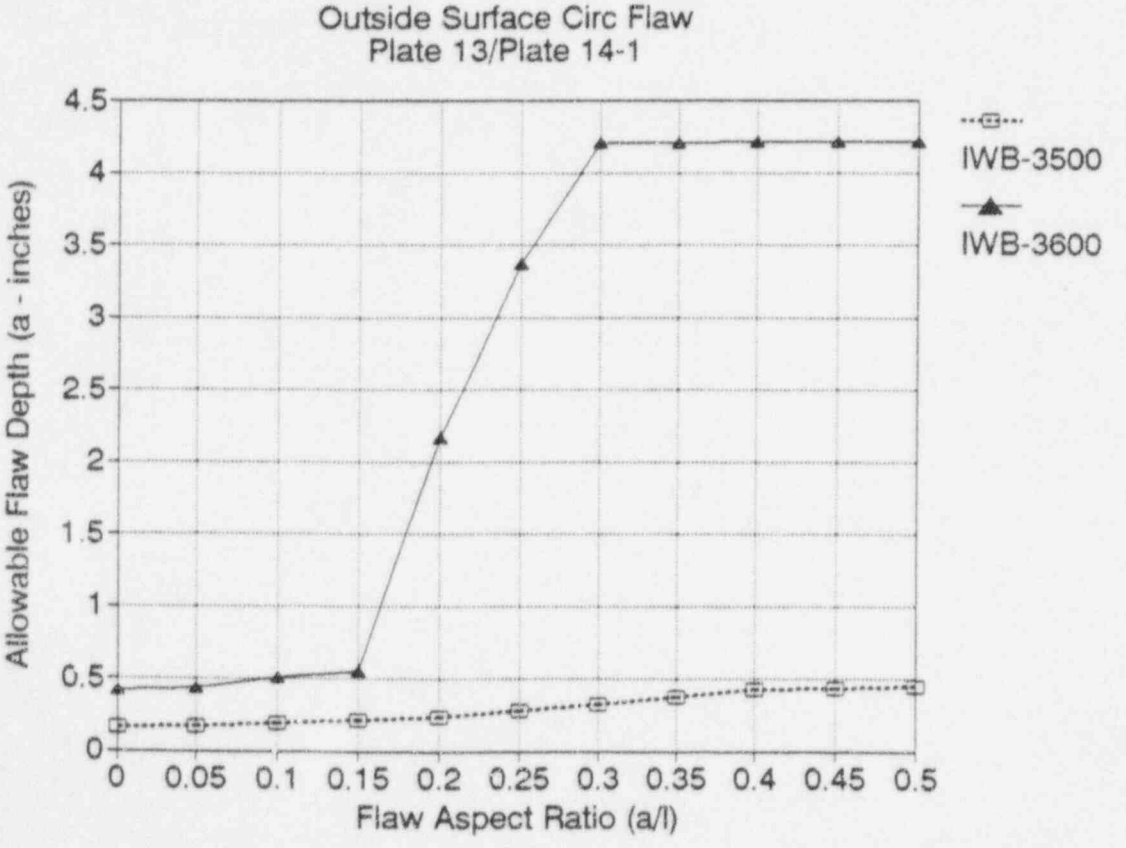

Figure E-2. Flaw Acceptance Diagram for Outside Surface Flaws (Group E)

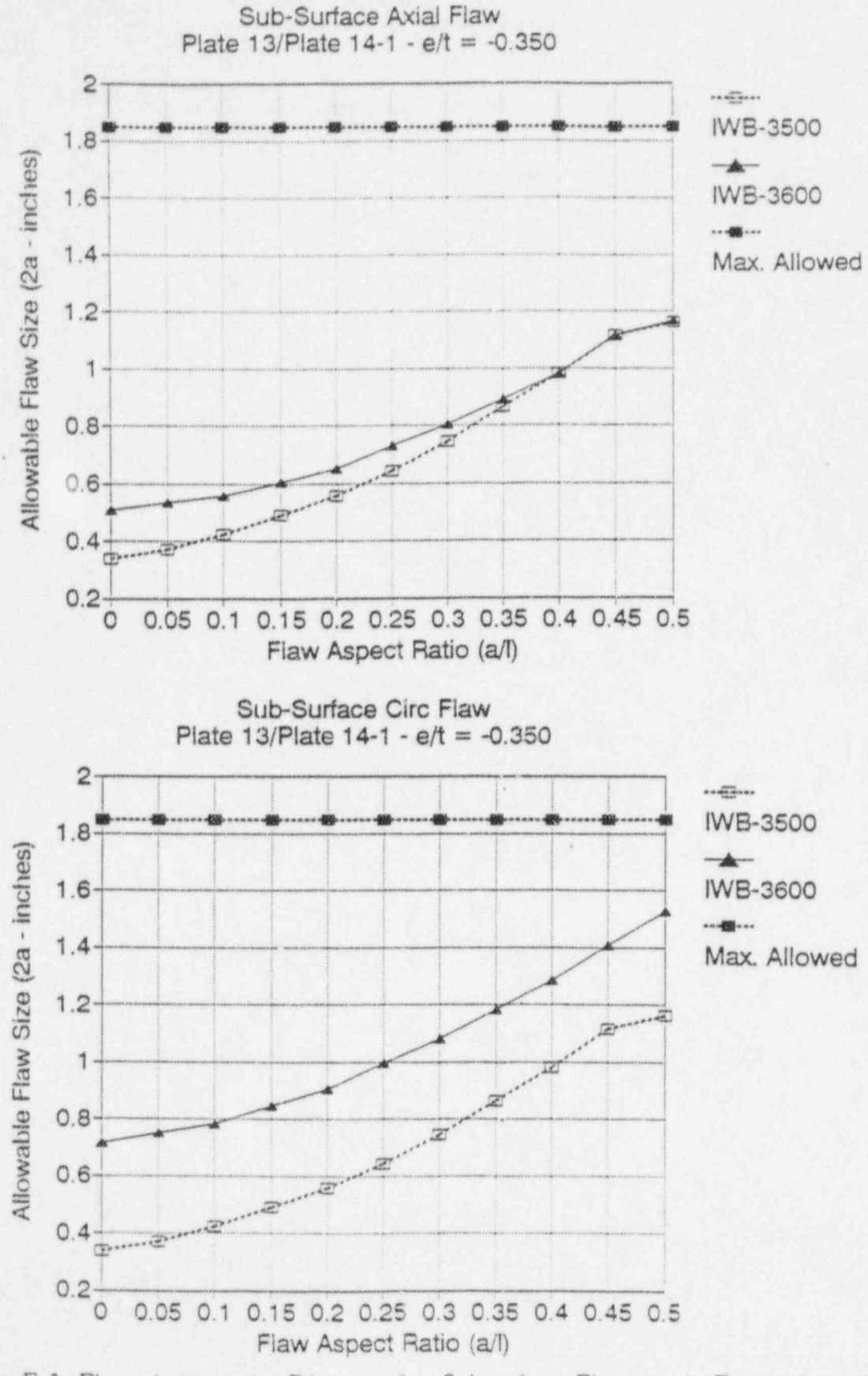

Figure E-3. Flaw Acceptance Diagram for Subsurface Flaws with Eccentricity Ratio of -0.35 (Group E)

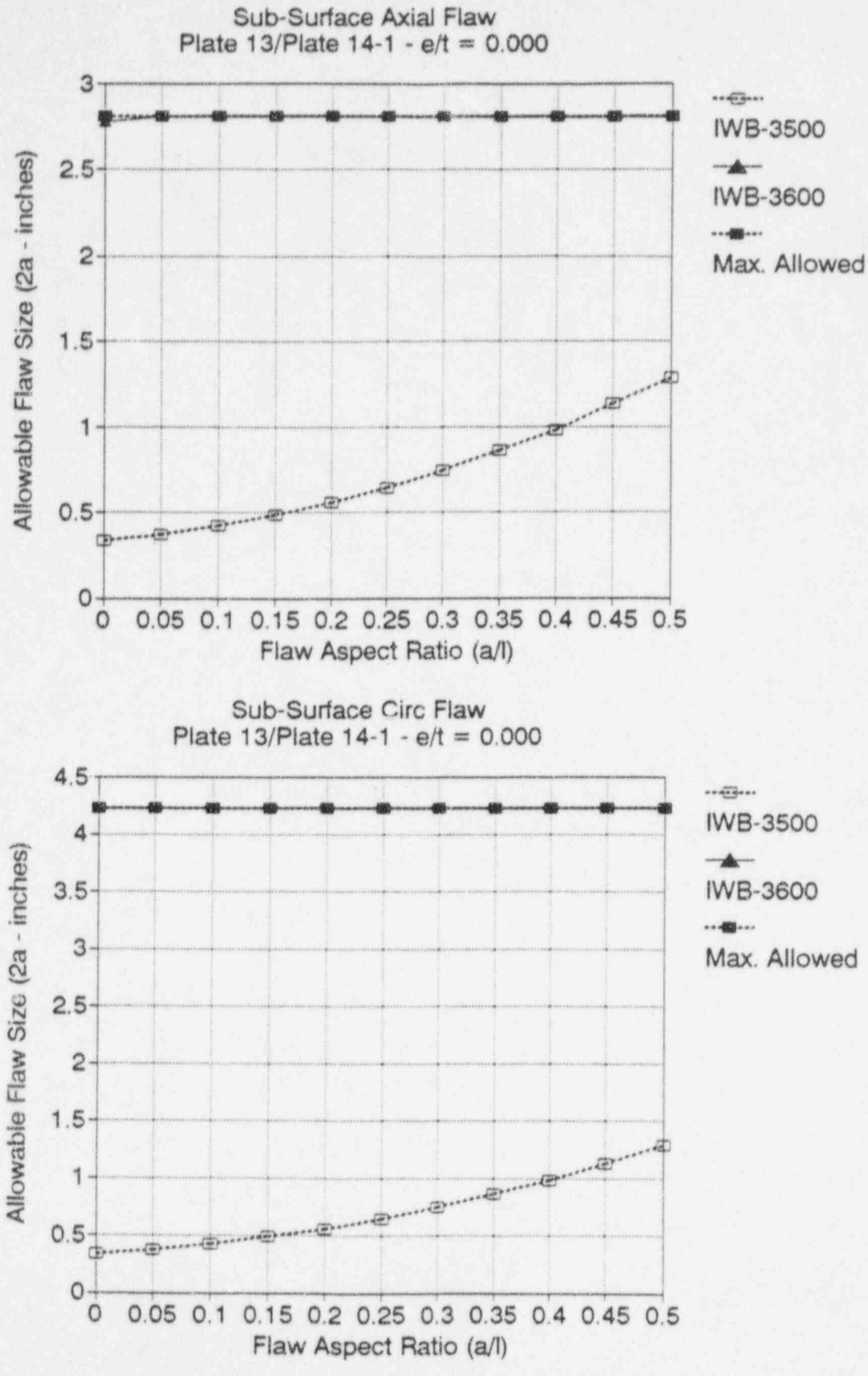

Figure E-4. Flaw Acceptance Diagram for Subsurface Flaws with Eccentricity Ratio of 0.0 (Group E)

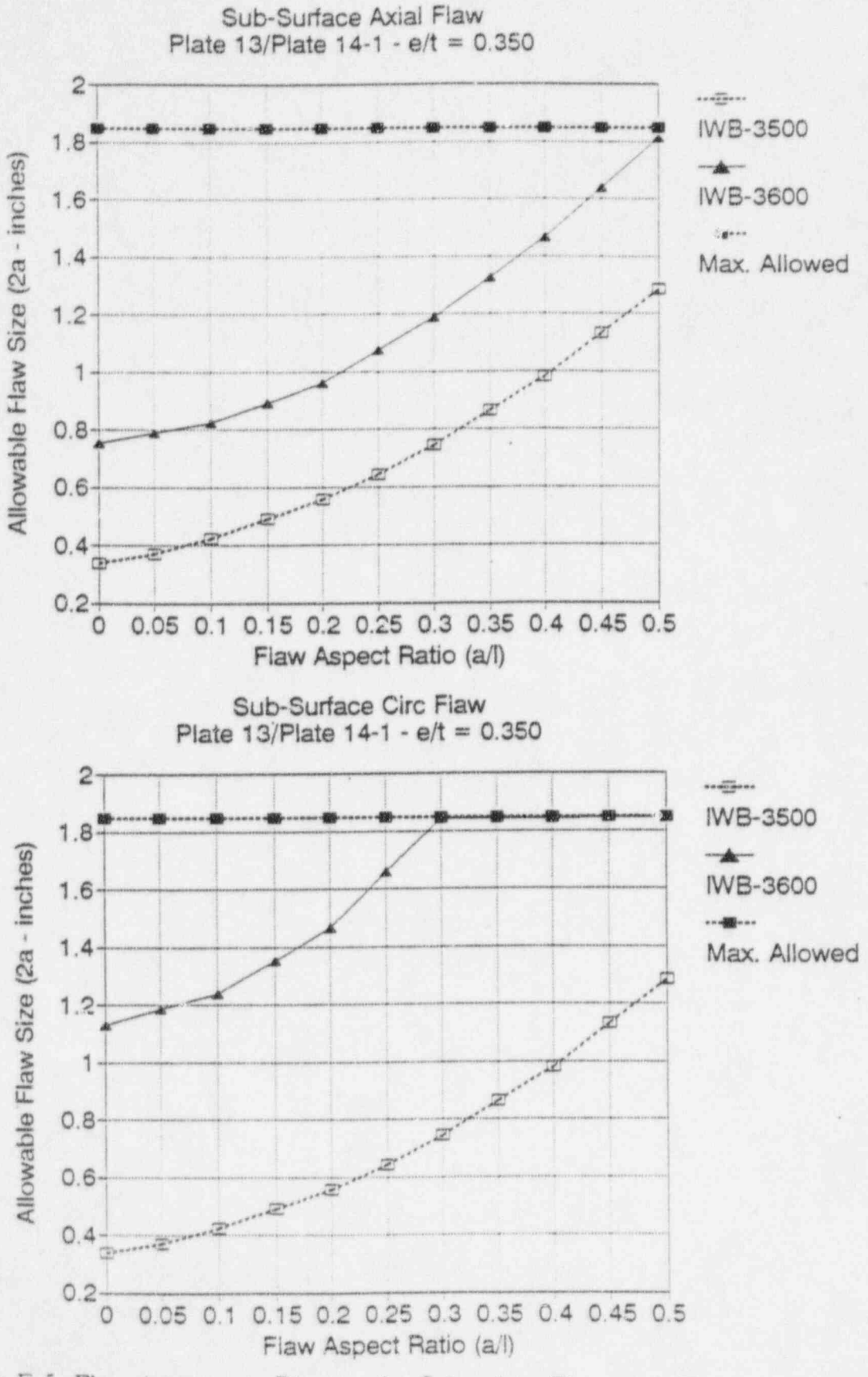

Figure E-5. Flaw Acceptance Diagram for Subsurface Flaws with Eccentricity Ratio of 0.35 (Group E)

APPENDIX F

Flaw Acceptance Diagrams for Group F Materials

Items Covered

- Upper Shell to Lower Shell Weld (01-004)

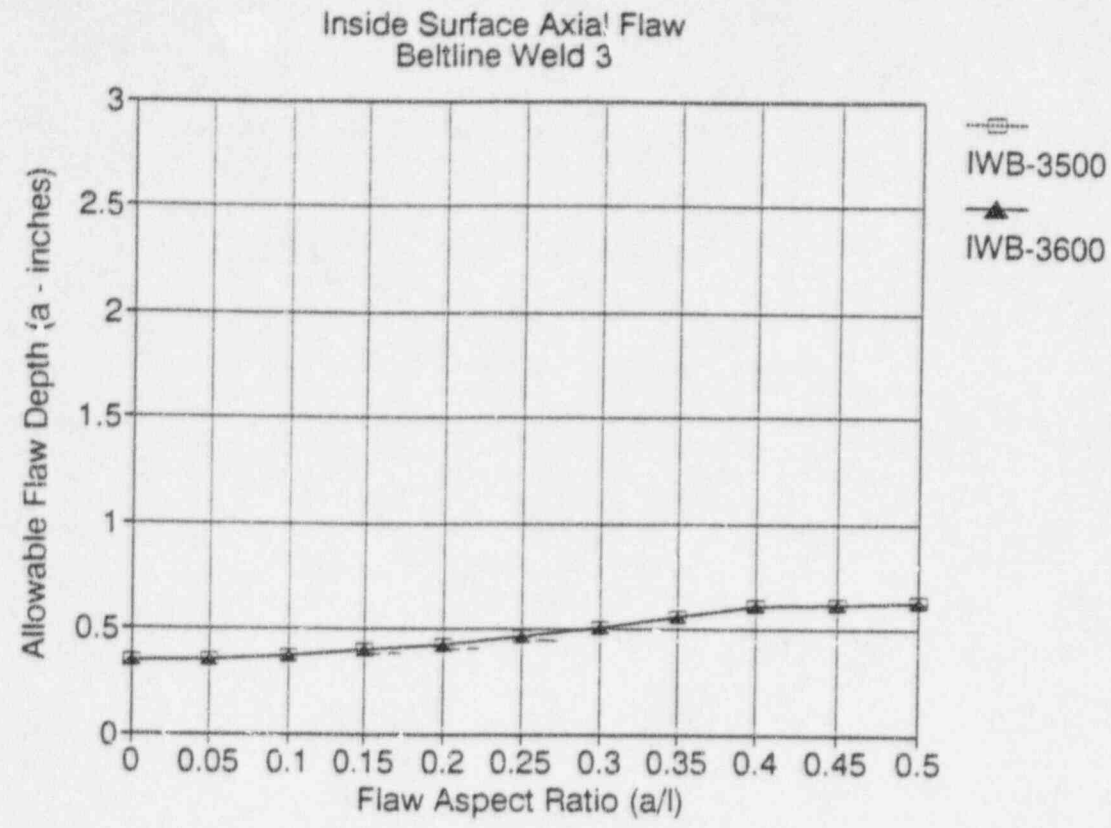

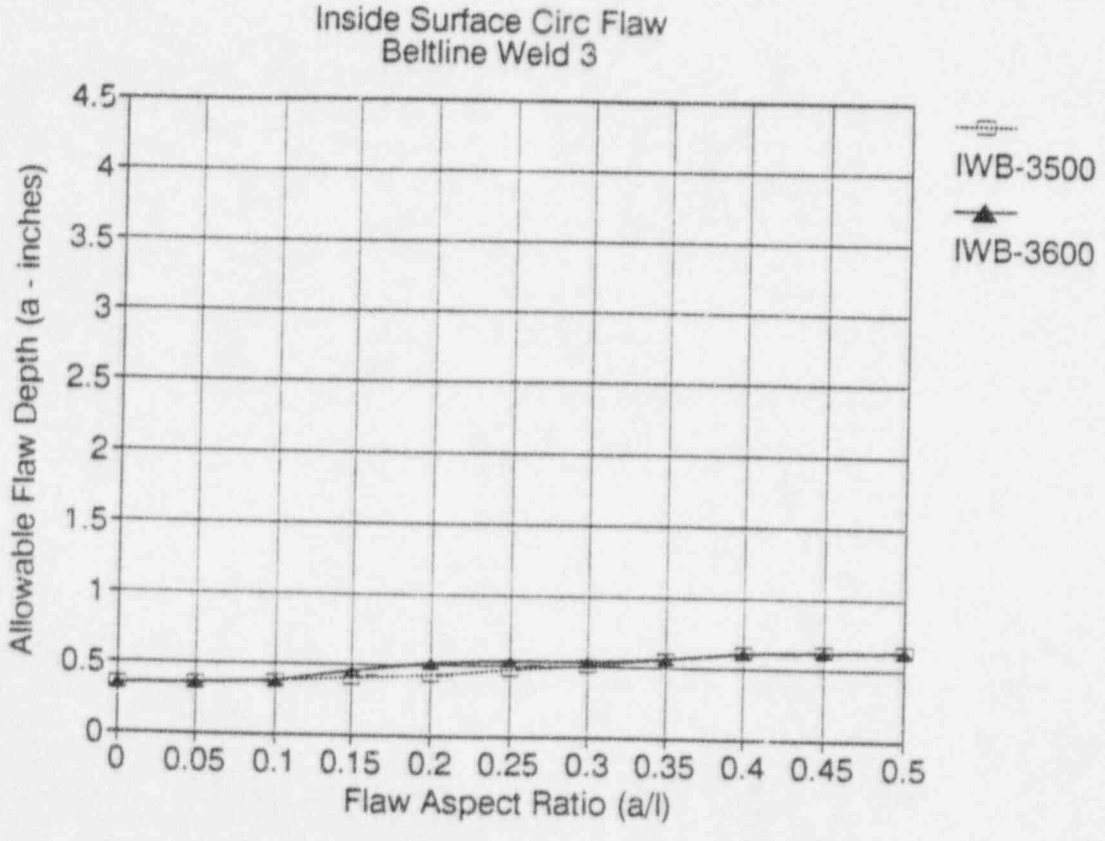

Figure F-1. Flaw Acceptance Diagram For Inside Surface Flaws (Group F)

Note: Flaw depth includes thickness of cladding.

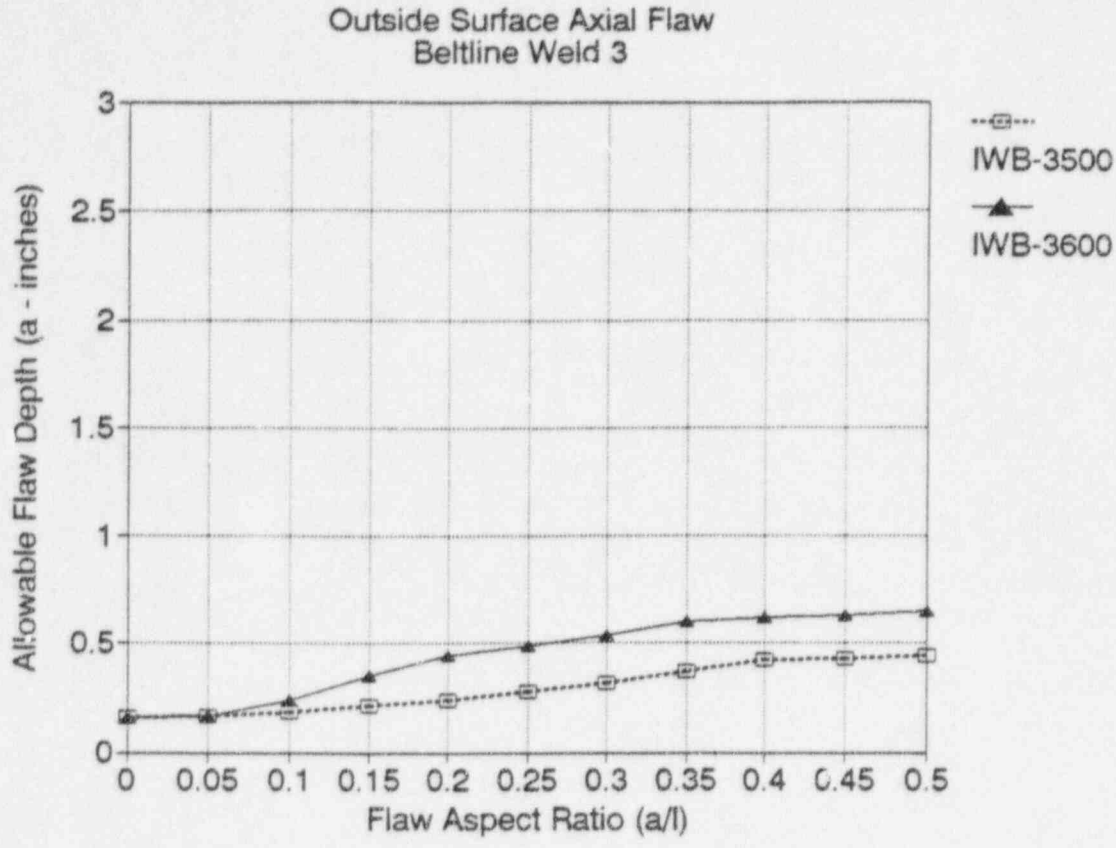

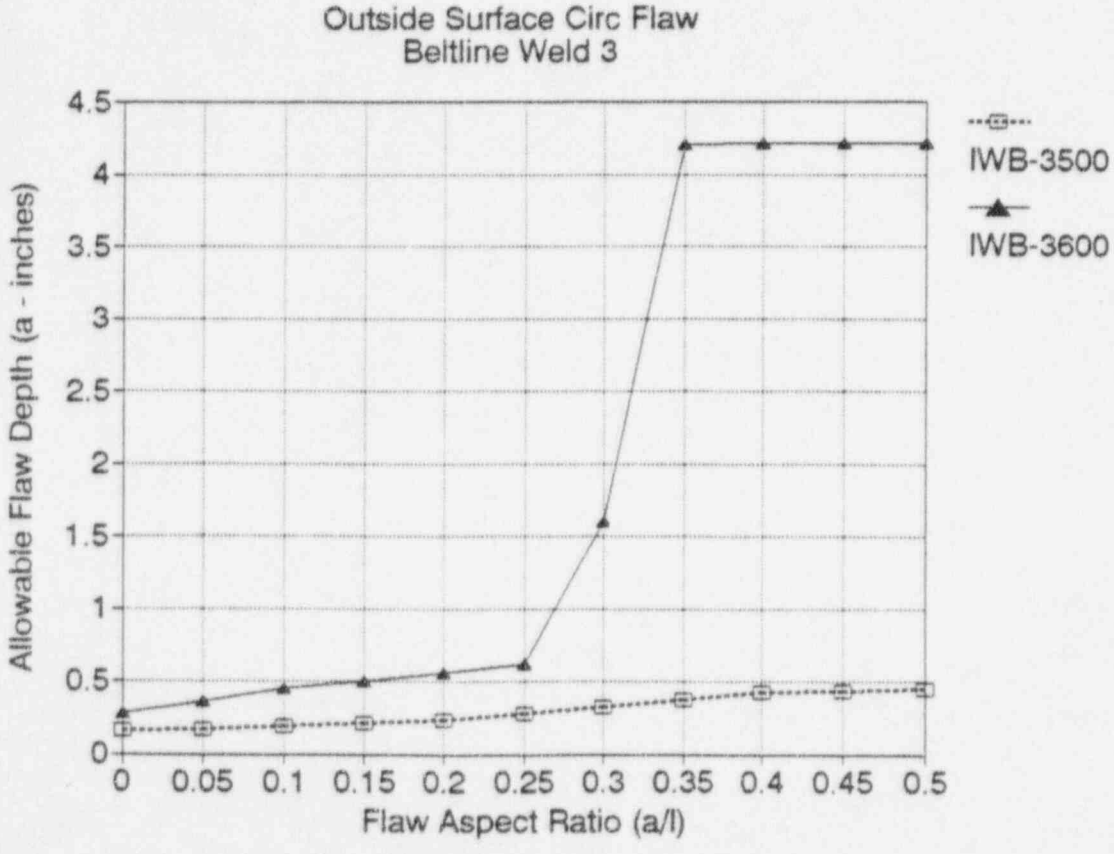

Figure F-2. Flaw Acceptance Diagram for Outside Surface Flaws (Group F)

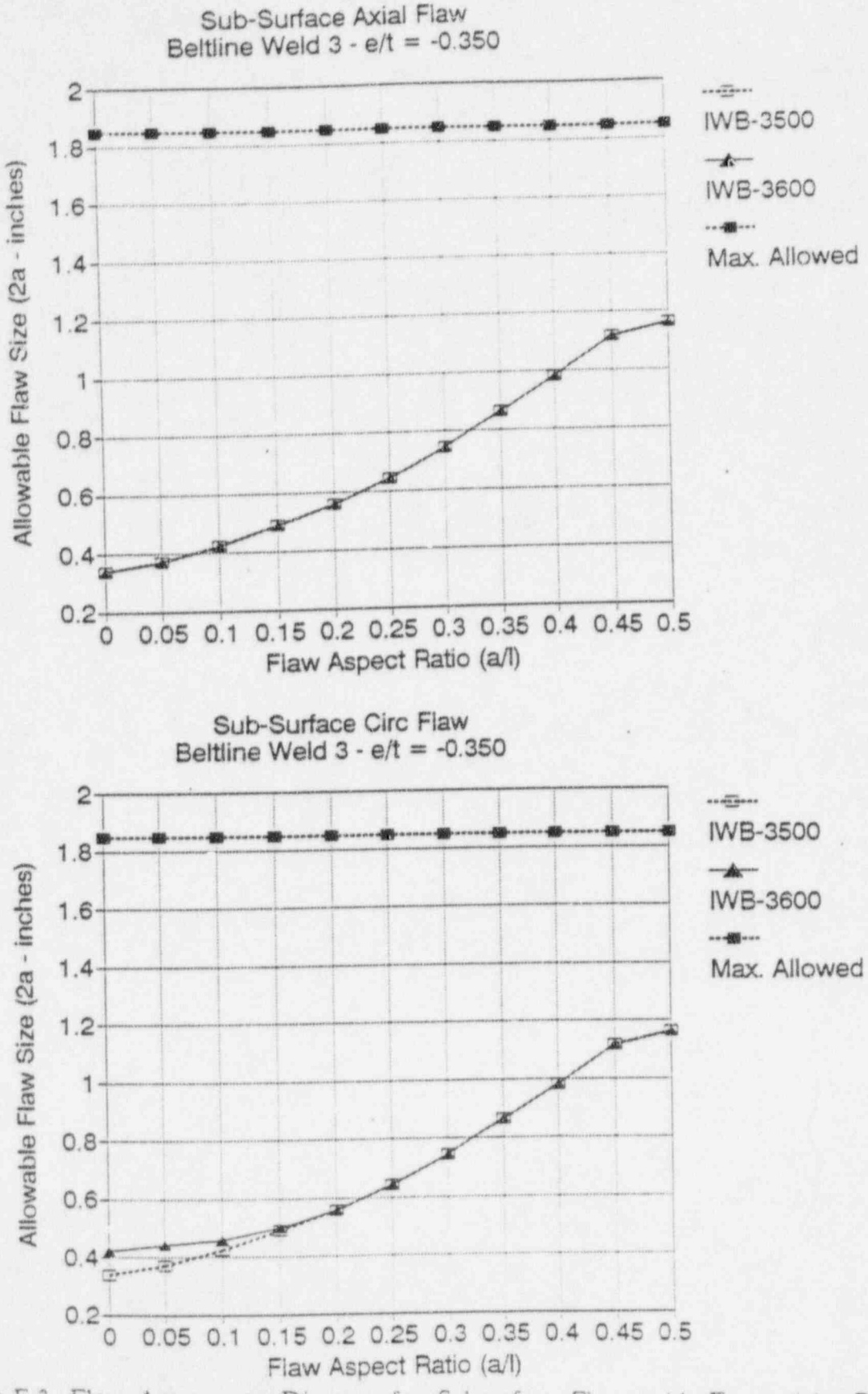

Figure F-3. Flaw Acceptance Diagram for Subsurface Flaws with Eccentricity Ratio of -0.35 (Group F)

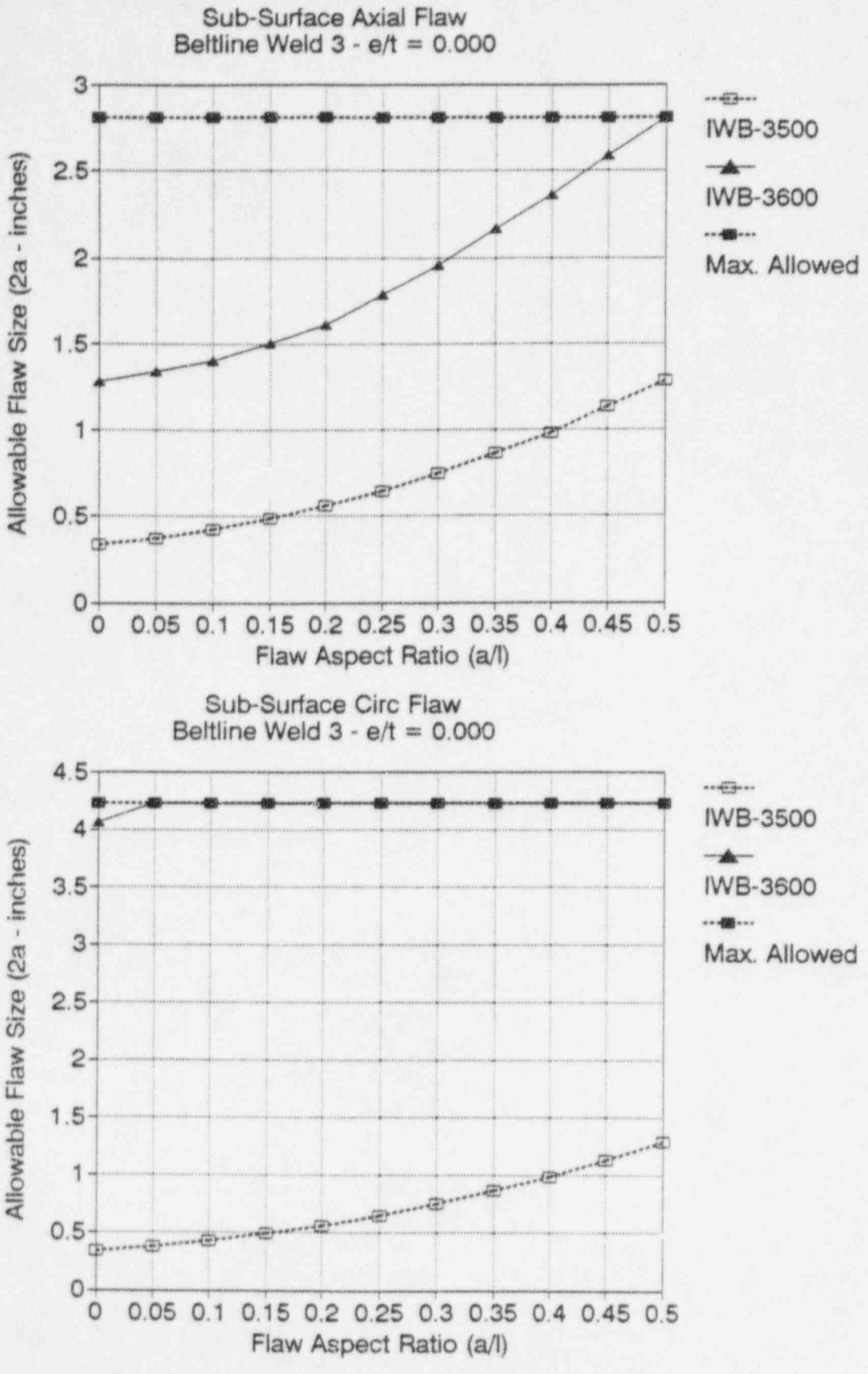

Figure F-4. Flaw Acceptance Diagram for Subsurface Flaws with Eccentricity Ratio of 0.0 (Group F)

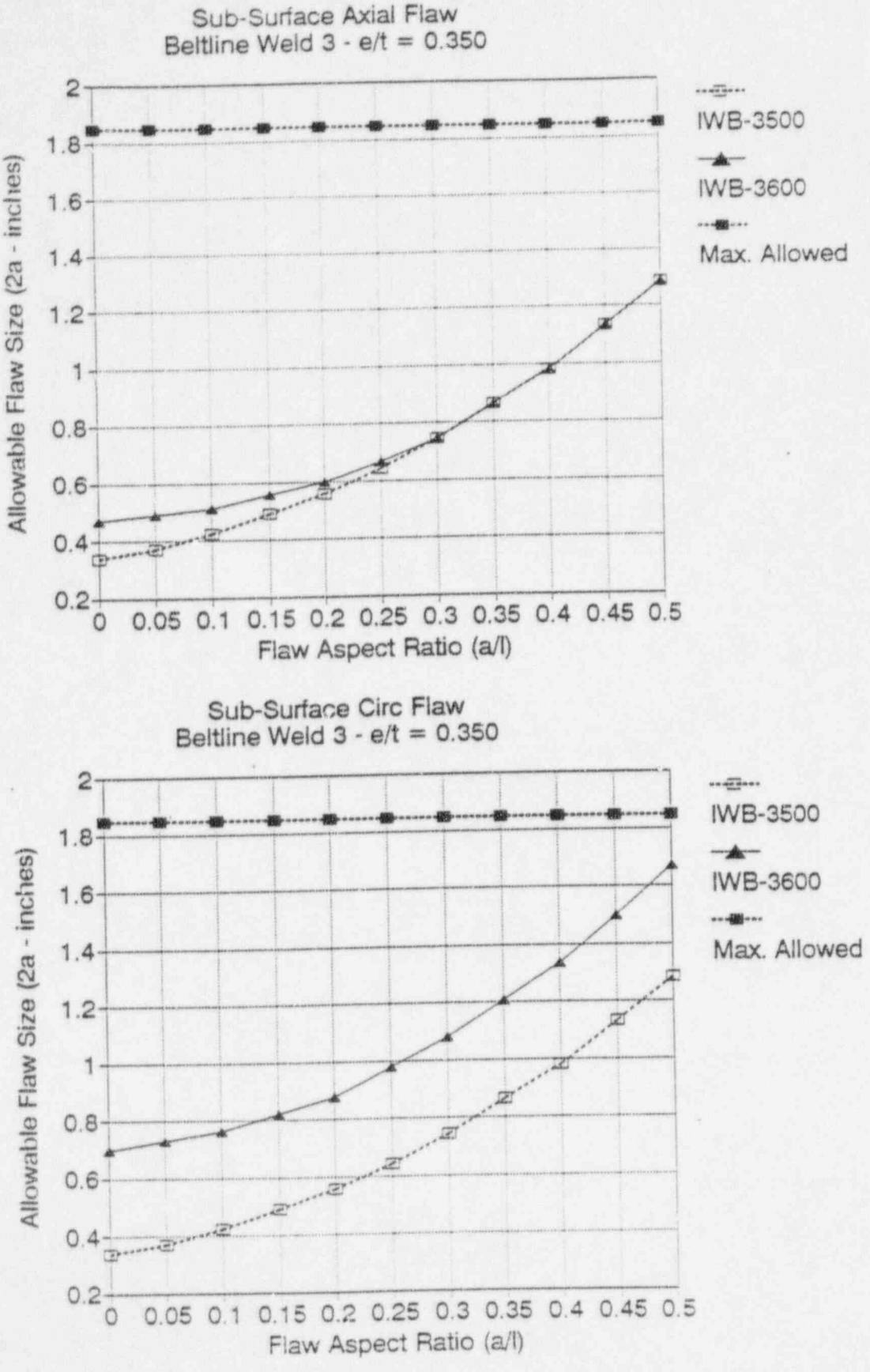

Figure F-5. Flaw Acceptance Diagram for Subsurface Flaws with Eccentricity Ratio of 0.35 (Group F)

APPENDIX G

Flaw Acceptance Diagrams for Group G Materials

Items Covered

- Beltline Nozzle Belt-to-Upper Shell Welds (01-003)
- Beltline Longitudinal Welds [1] (01-007 to 01-010)

[1] Applicable to portions of welds above thickness transition. Special evaluation required for welds located on transition.

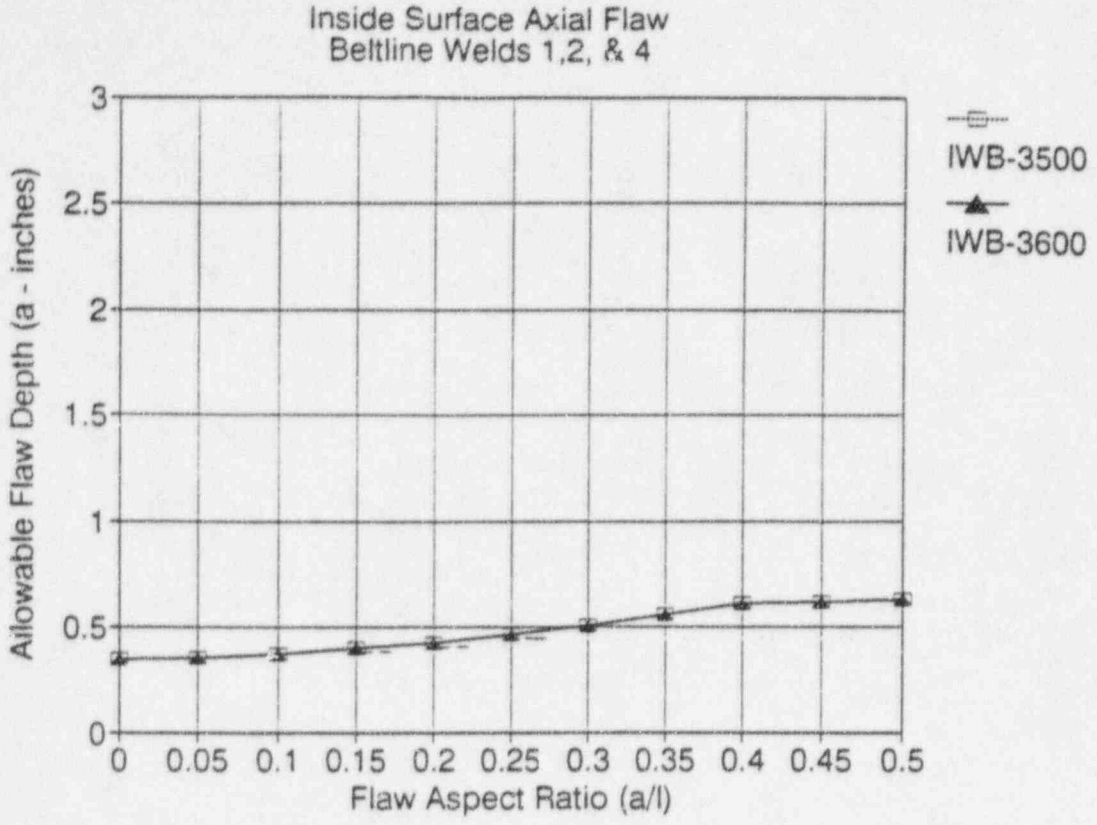

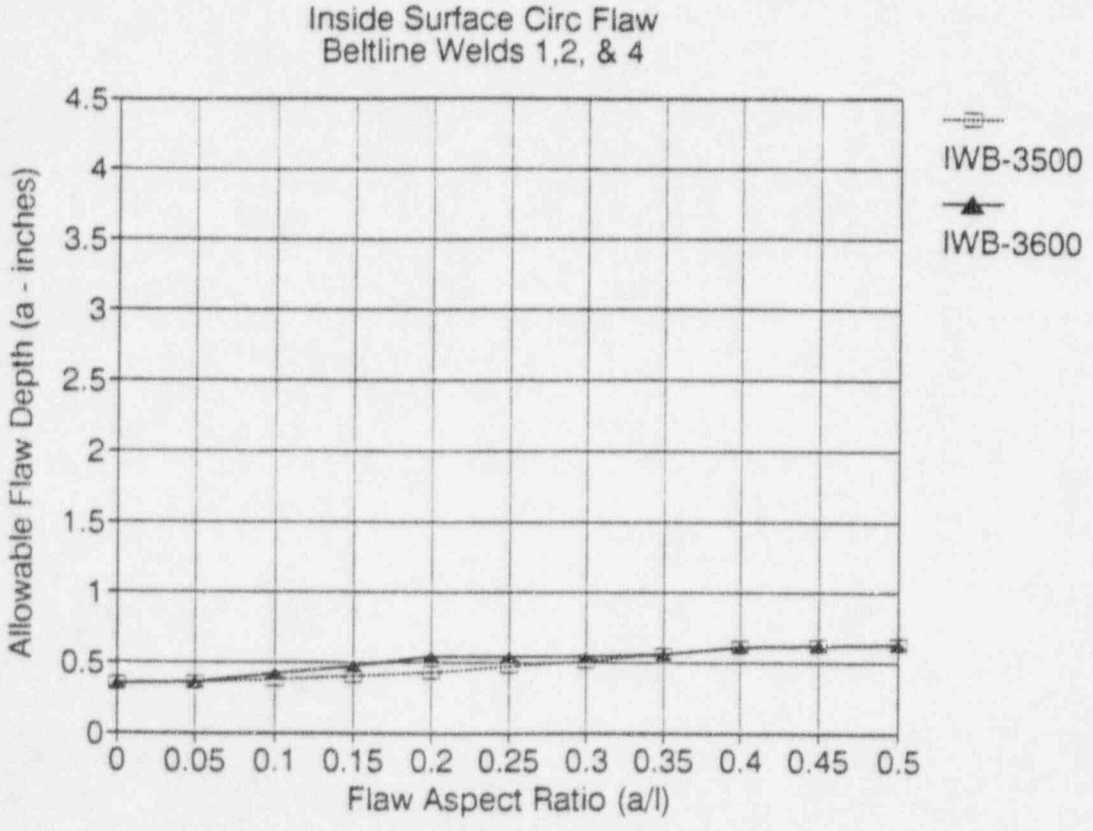

Figure G-1. Flaw Acceptance Diagram For Inside Surface Flaws (Group G)

Note: Flaw depth includes thickness of cladding.

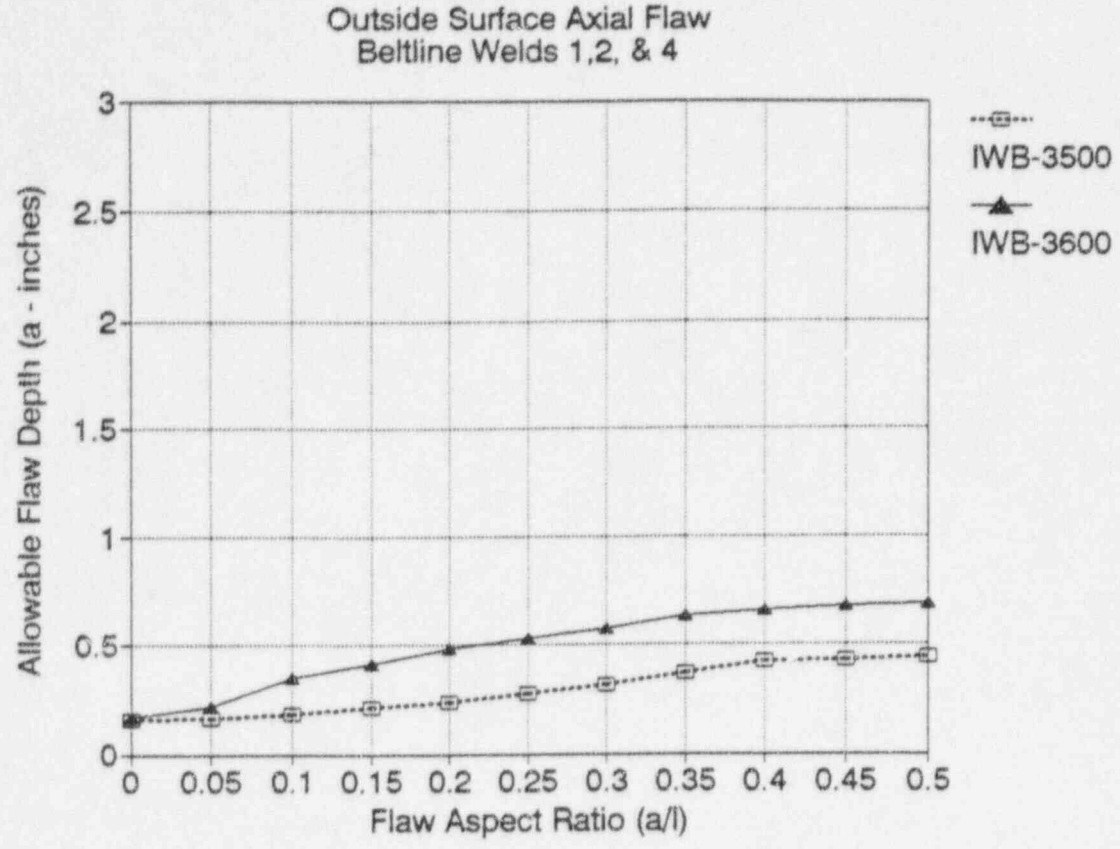

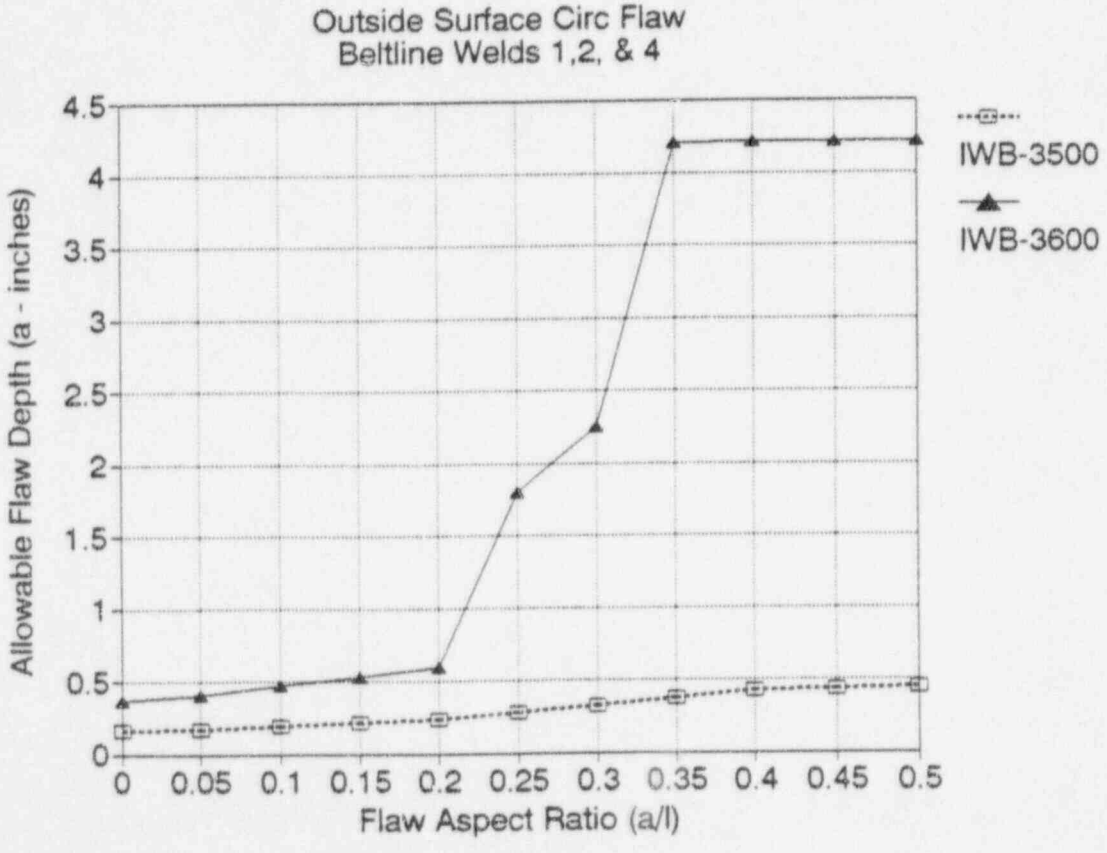

Figure G-2. Flaw Acceptance Diagram for Outside Surface Flaws (Group G)

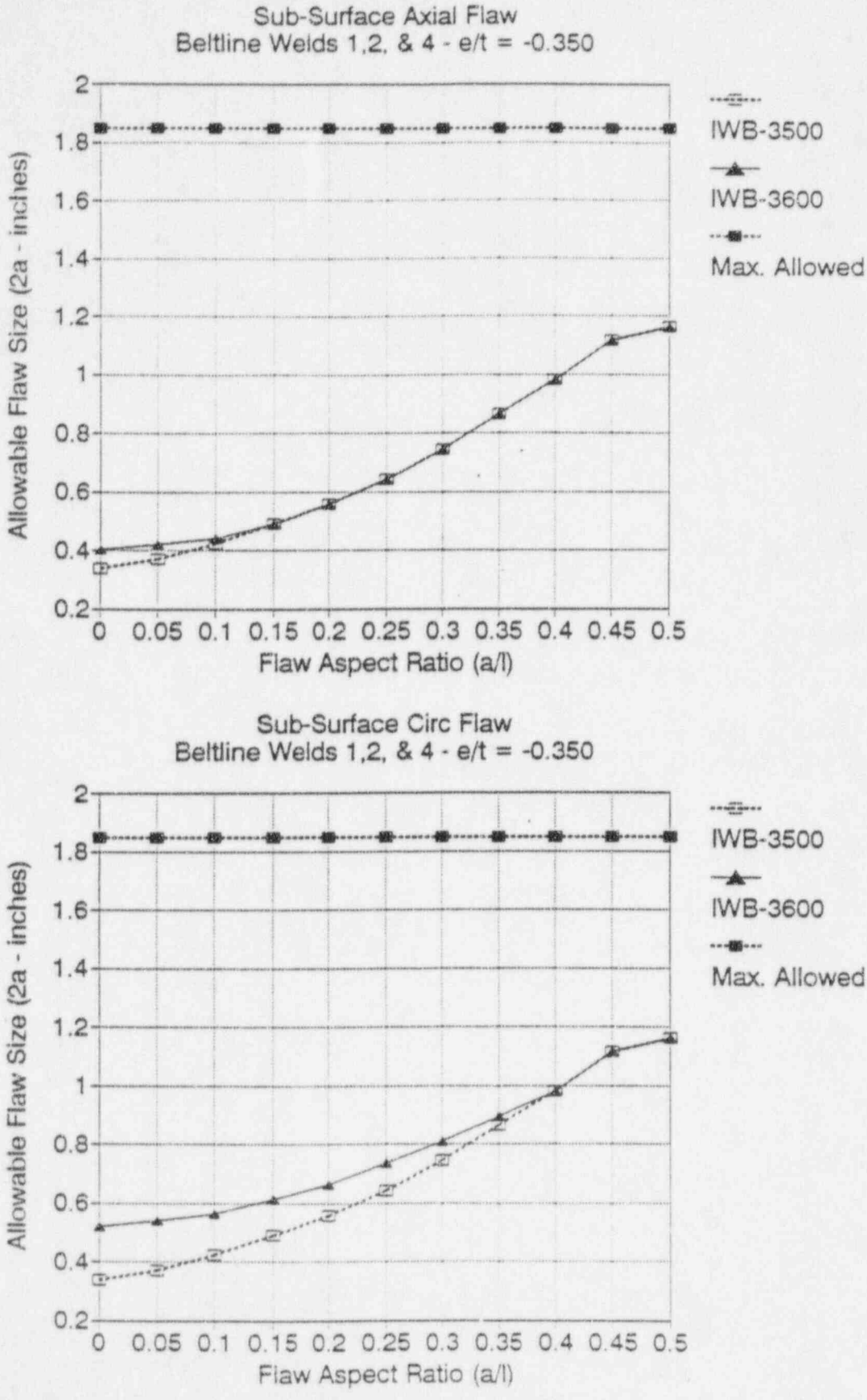

Figure G-3. Flaw Acceptance Diagram for Subsurface Flaws with Eccentricity Ratio of -0.35 (Group G)

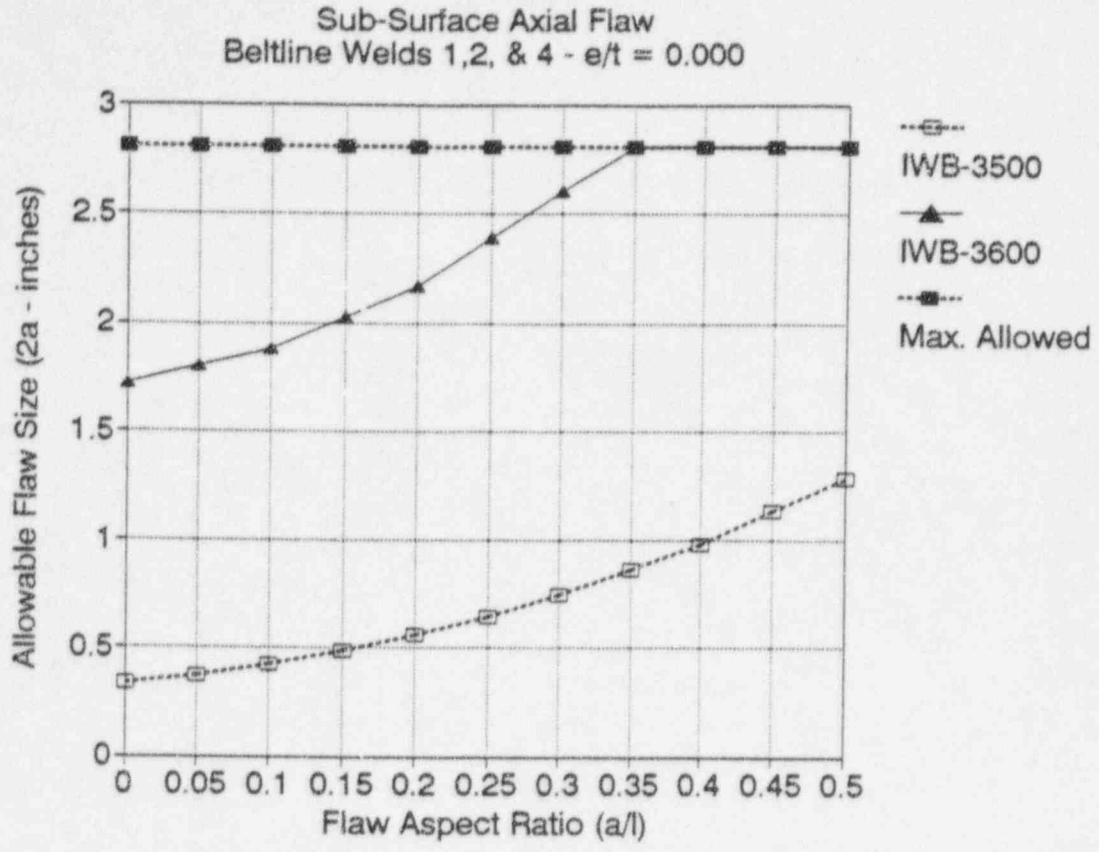

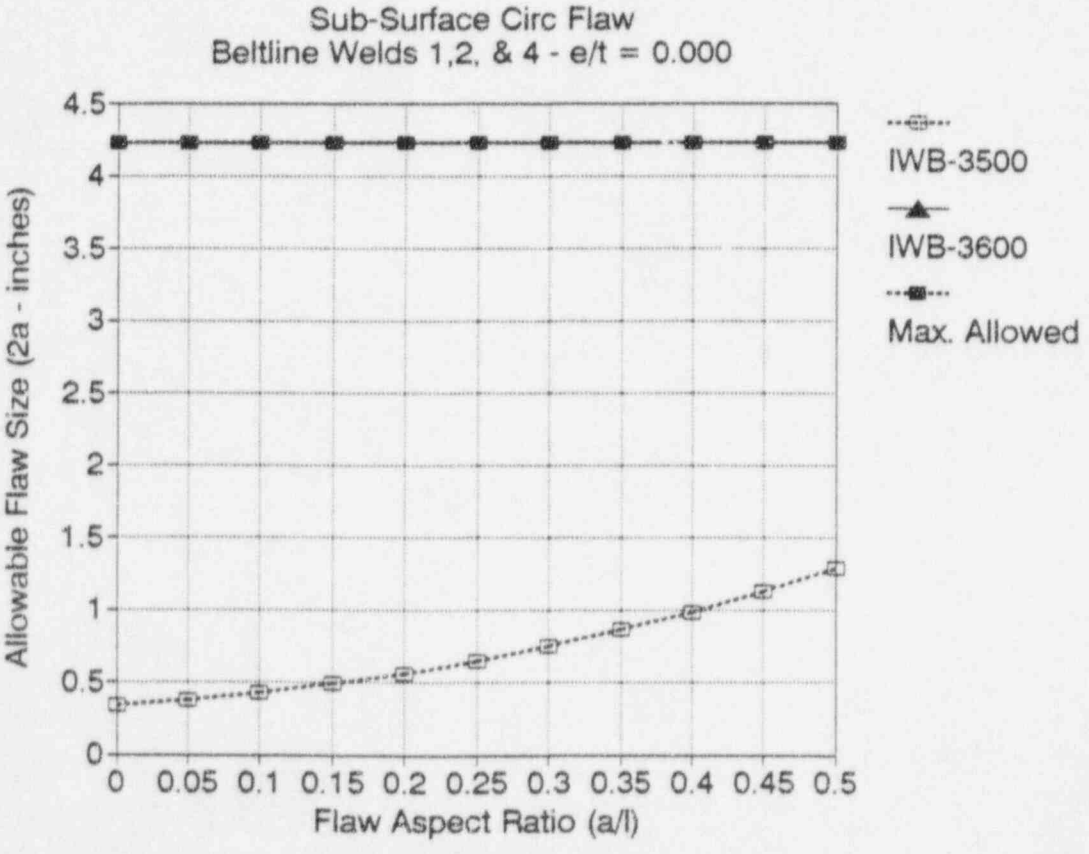

Figure G-4. Flaw Acceptance Diagram for Subsurface Flaws with Eccentricity Ratio of 0.0 (Group G)

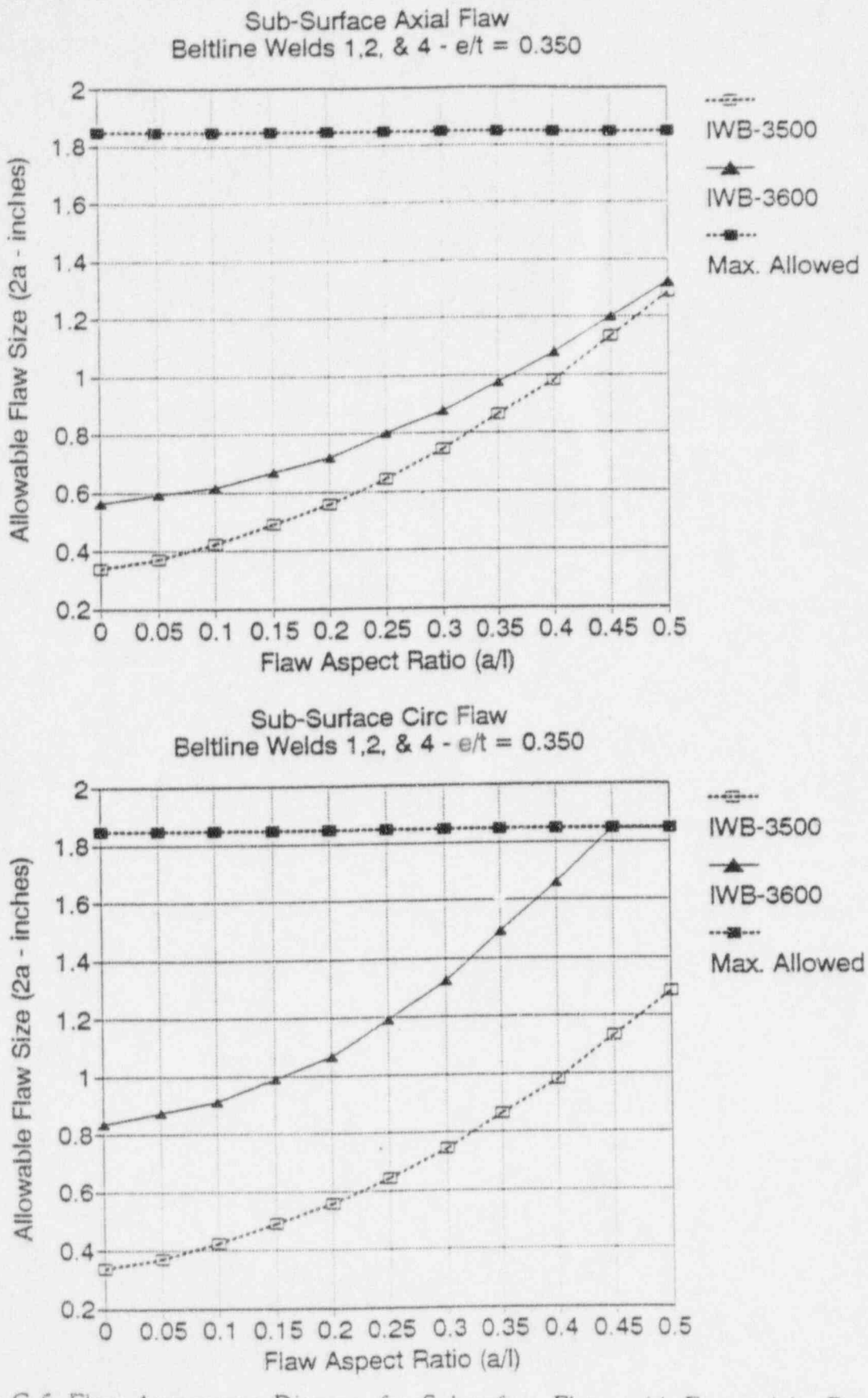

Figure G-5. Flaw Acceptance Diagram for Subsurface Flaws with Eccentricity Ratio of 0.35 (Group G)

APPENDIX H

Flaw Acceptance Diagrams for Group H Materials

Items Covered

- Lower Shell to Transition Forging Weld (01-005)
- Adjacent Lower Shell Plates (Mk #A2 - C5120 and C5114)
- Adjacent Transition Forging (Mk #36)

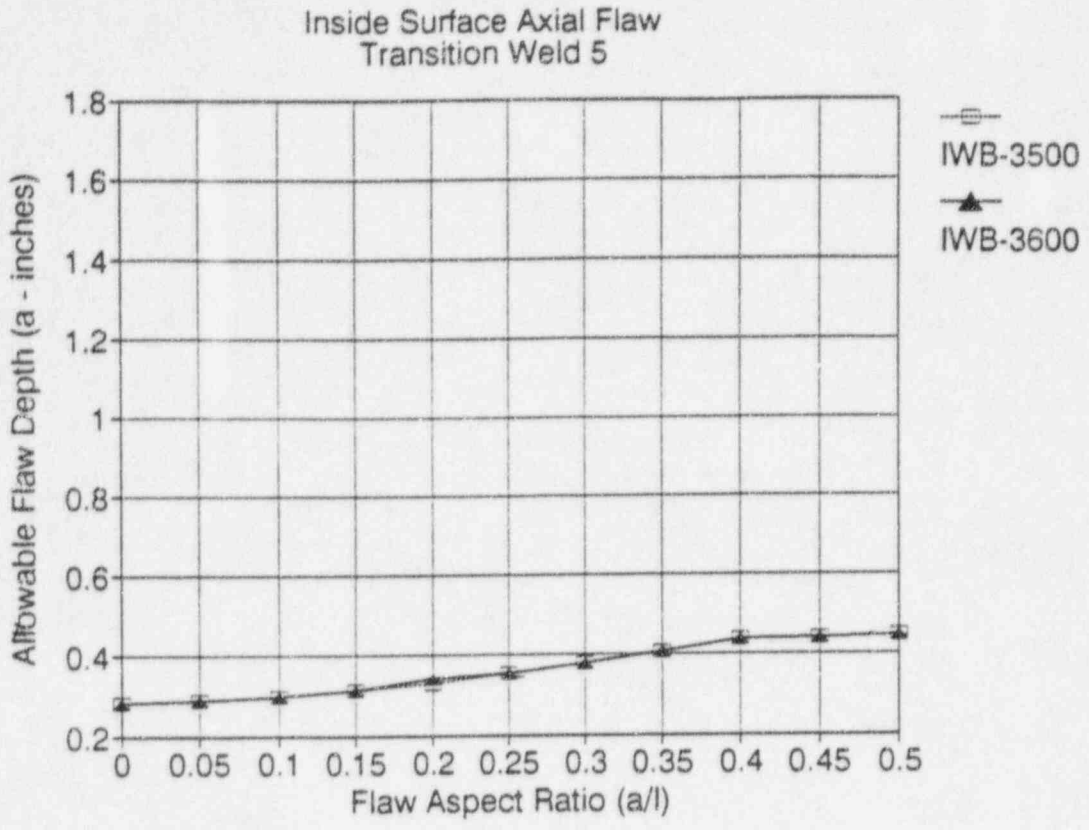

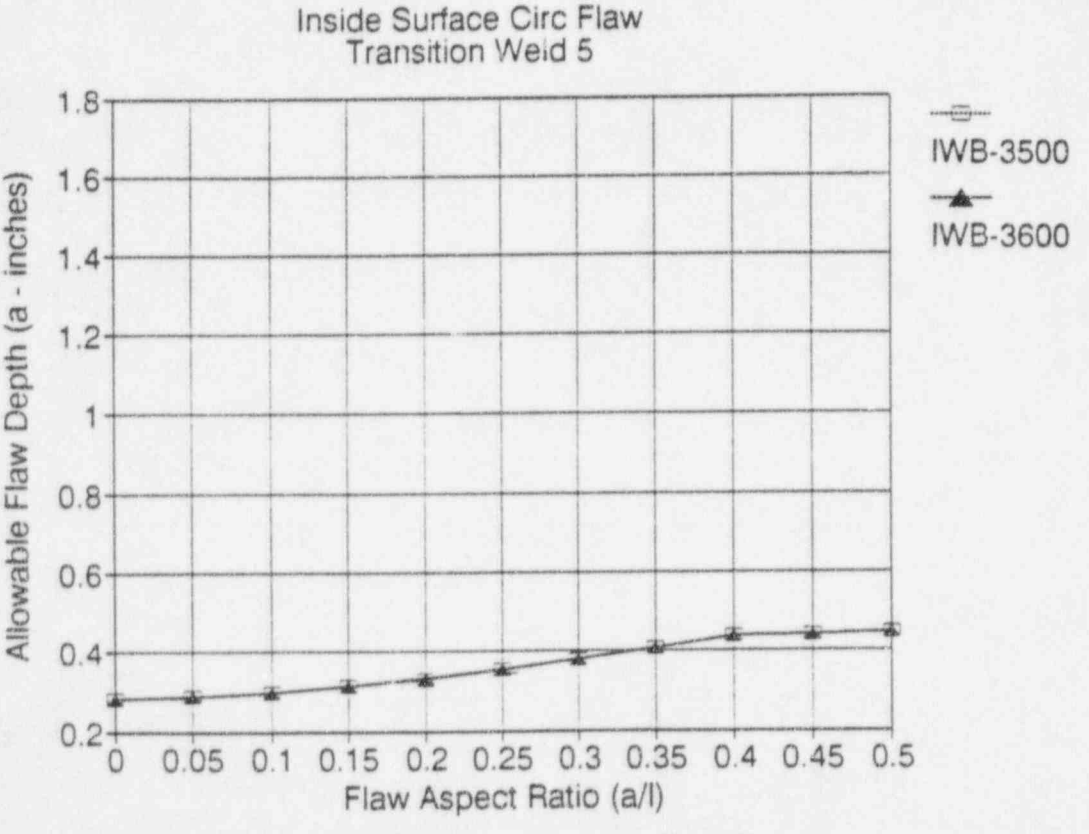

Figure H-1. Flaw Acceptance Diagram For Inside Surface Flaws (Group H)

Note: Flaw depth includes thickness of cladding.

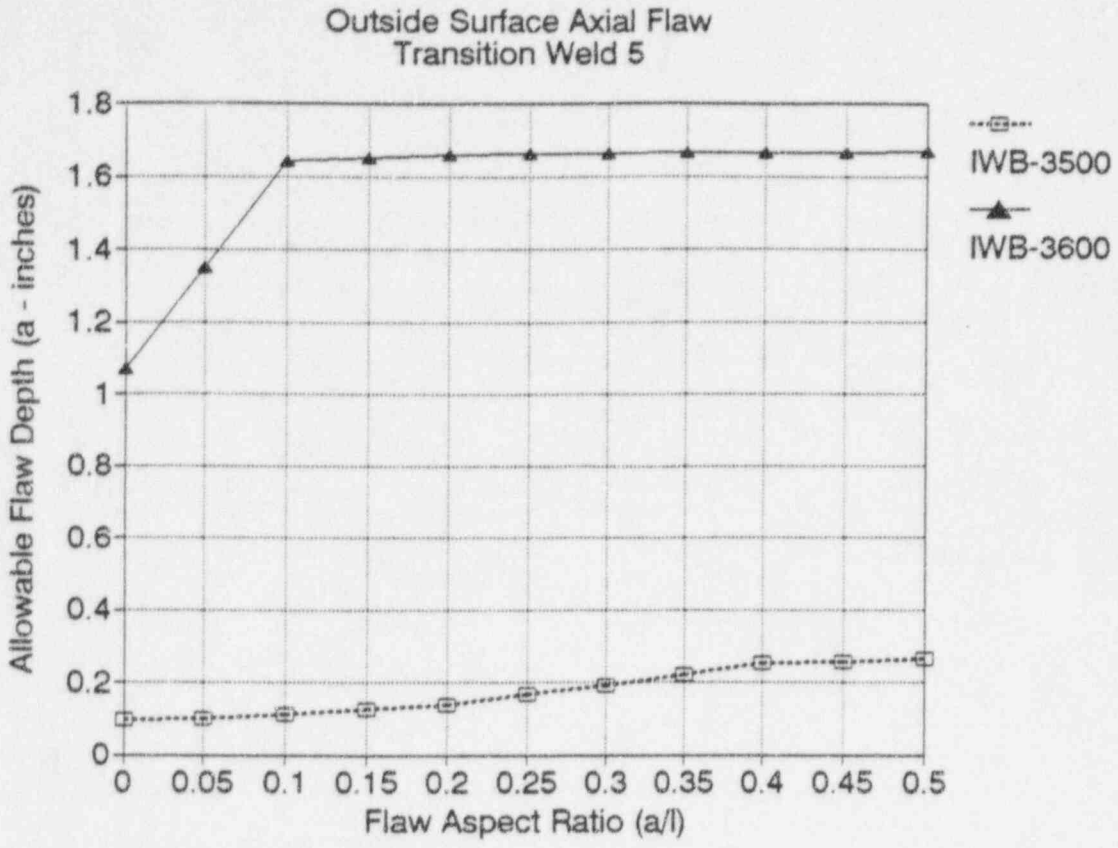

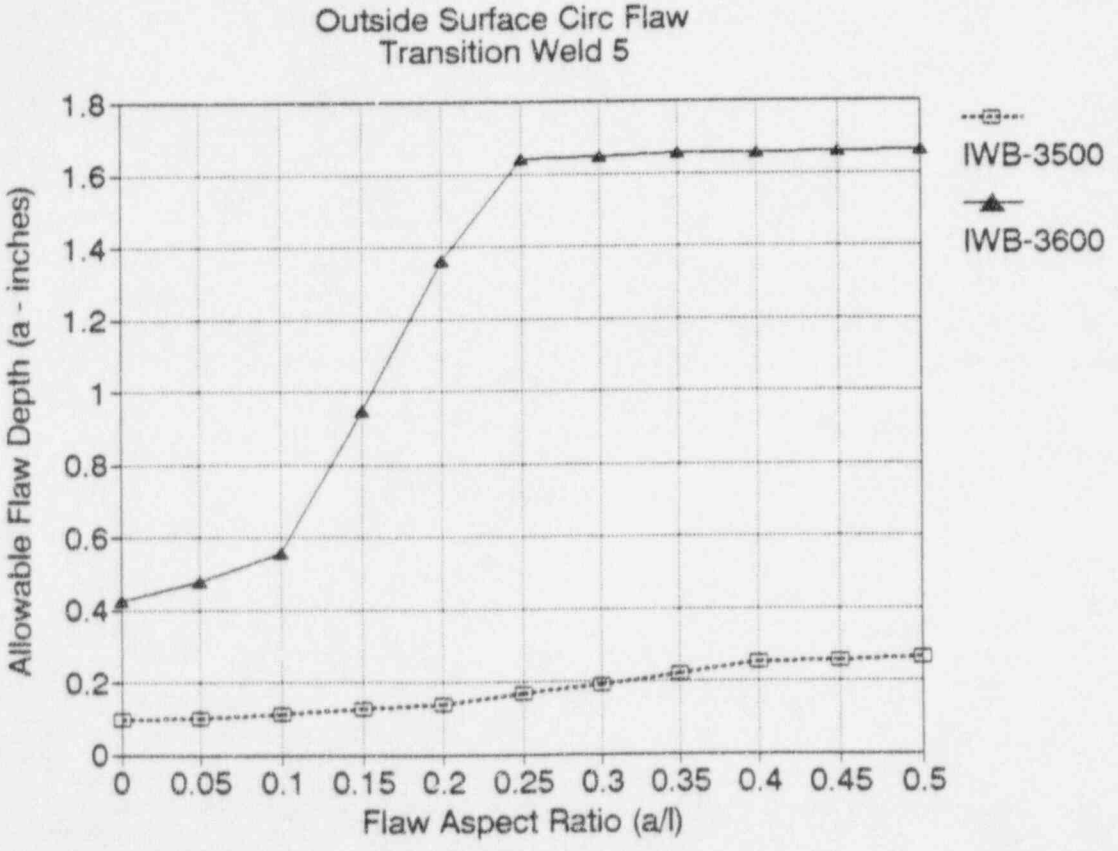

Figure H-2. Flaw Acceptance Diagram for Outside Surface Flaws (Group H)

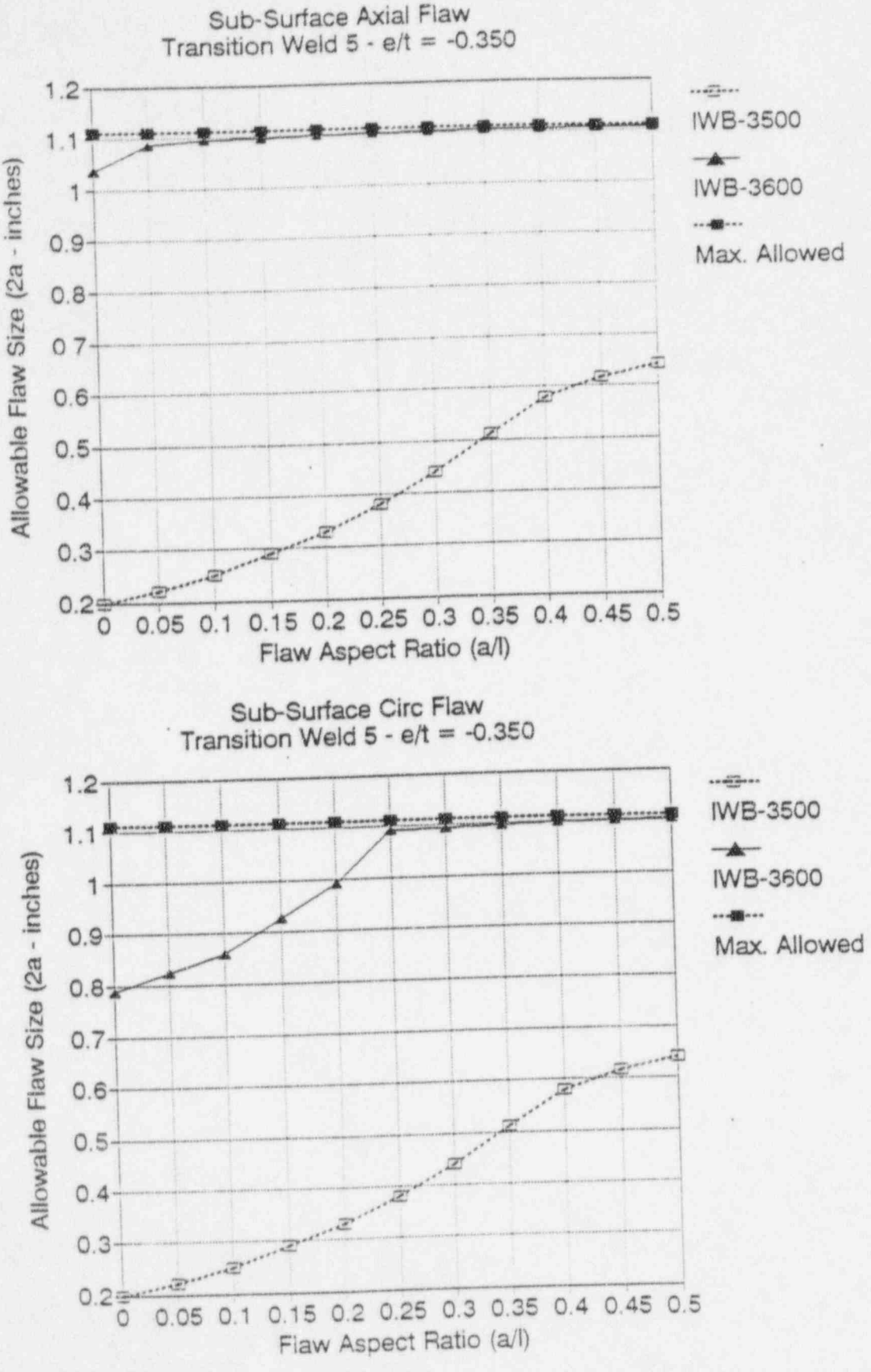

Figure H-3. Flaw Acceptance Diagram for Subsurface Flaws with Eccentricity Ratio of -0.35 (Group H)

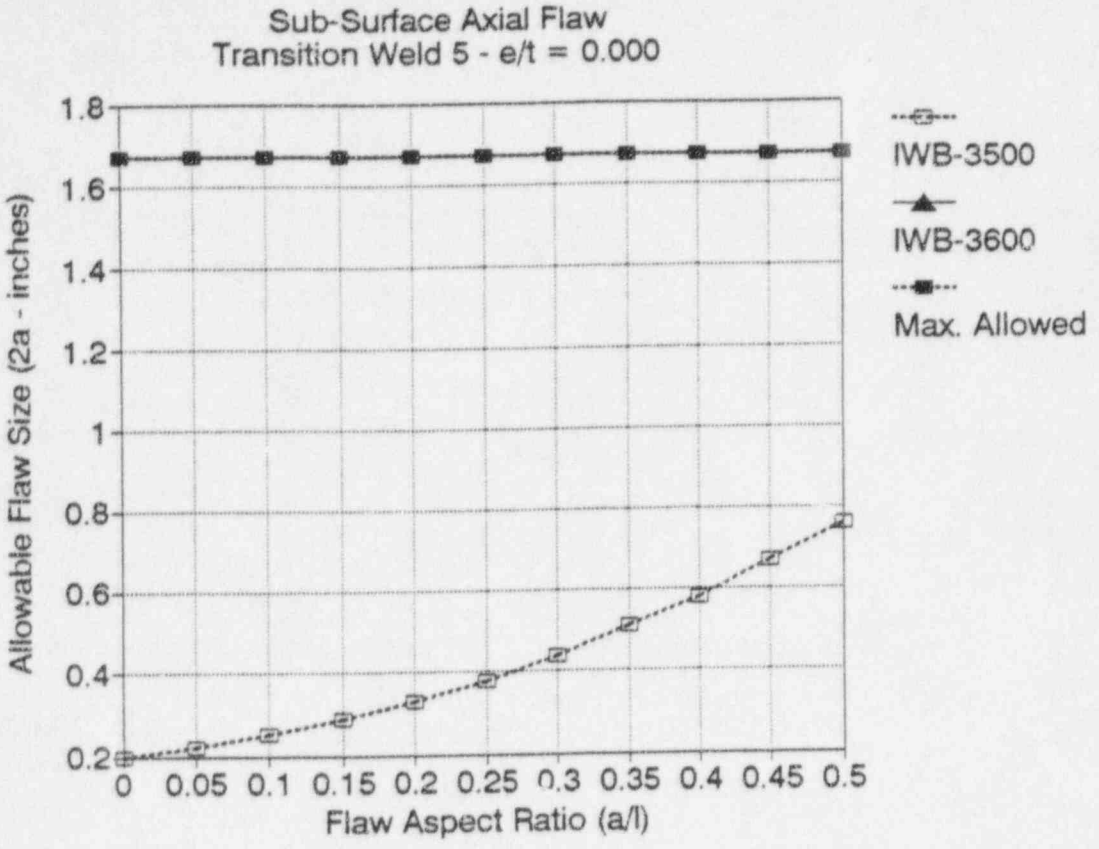

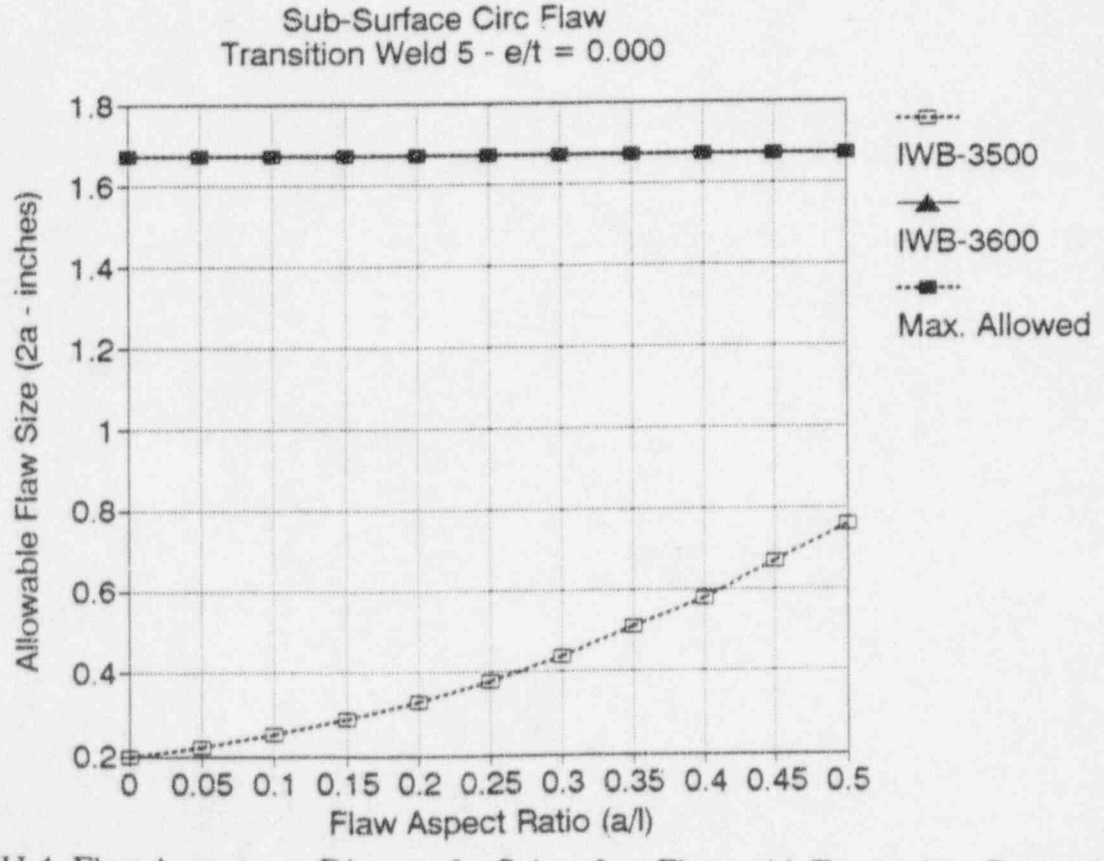

Figure H-4. Flaw Acceptance Diagram for Subsurface Flaws with Eccentricity Ratio of 0.0 (Group H)

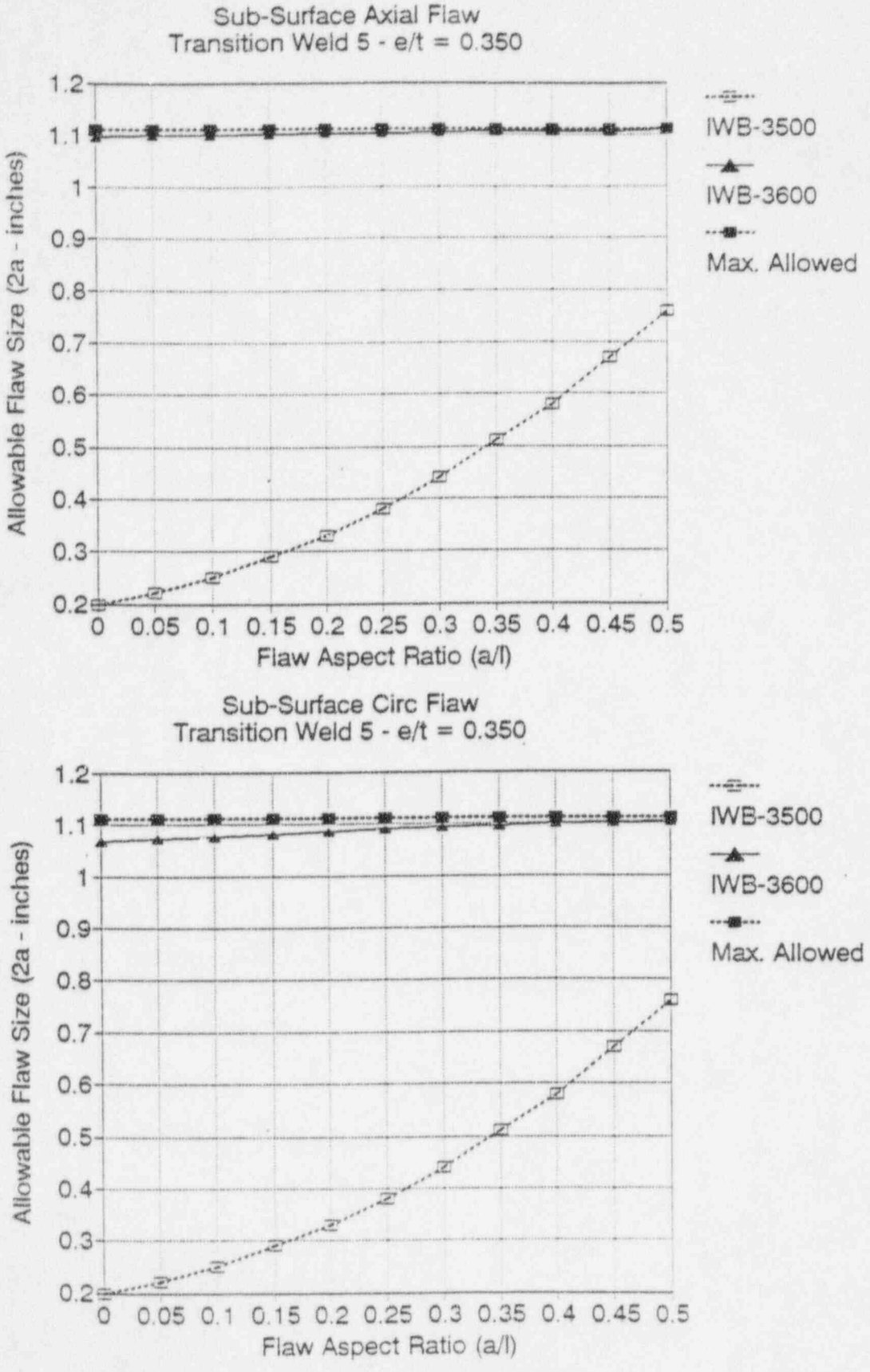

Figure H-5. Flaw Acceptance Diagram for Subsurface Flaws with Eccentricity Ratio of 0.35 (Group H)

APPENDIX I

Flaw Acceptance Diagrams for Group I Materials

Items Covered

- Weld to Lower Head (01-006)
- Adjacent Forging and Lower Head (Mk #36 and Mk #6)

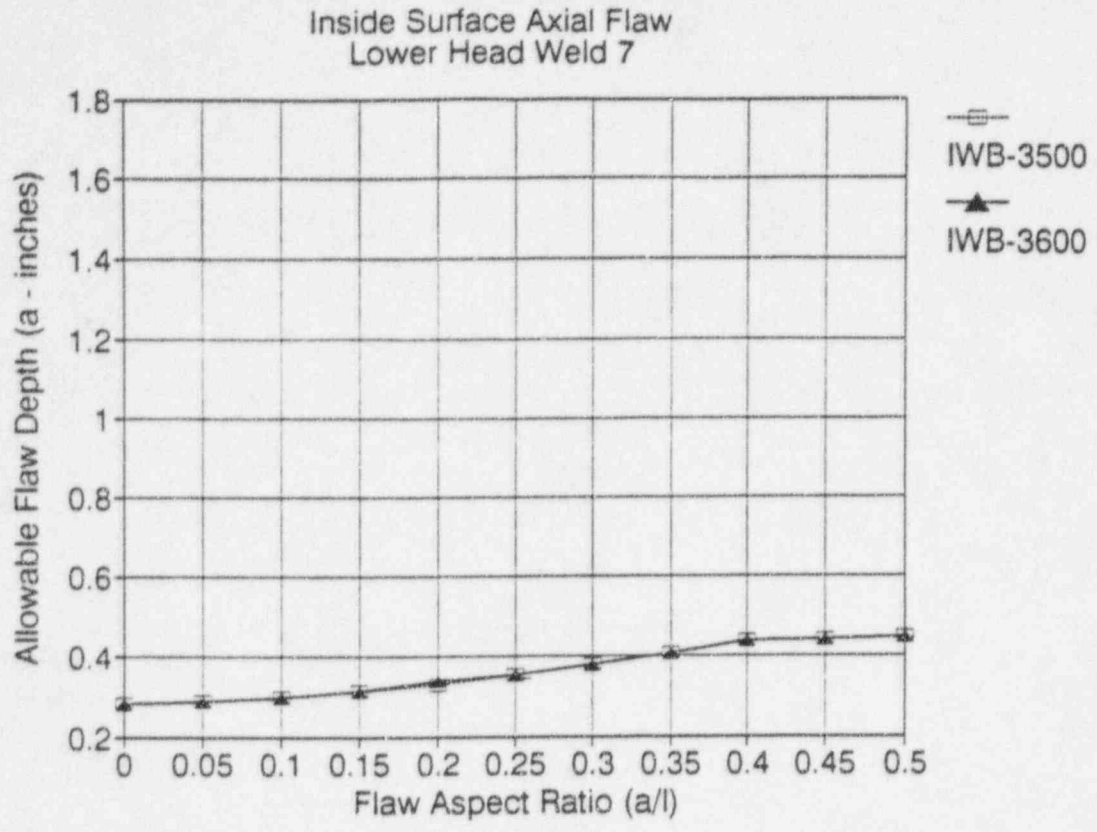

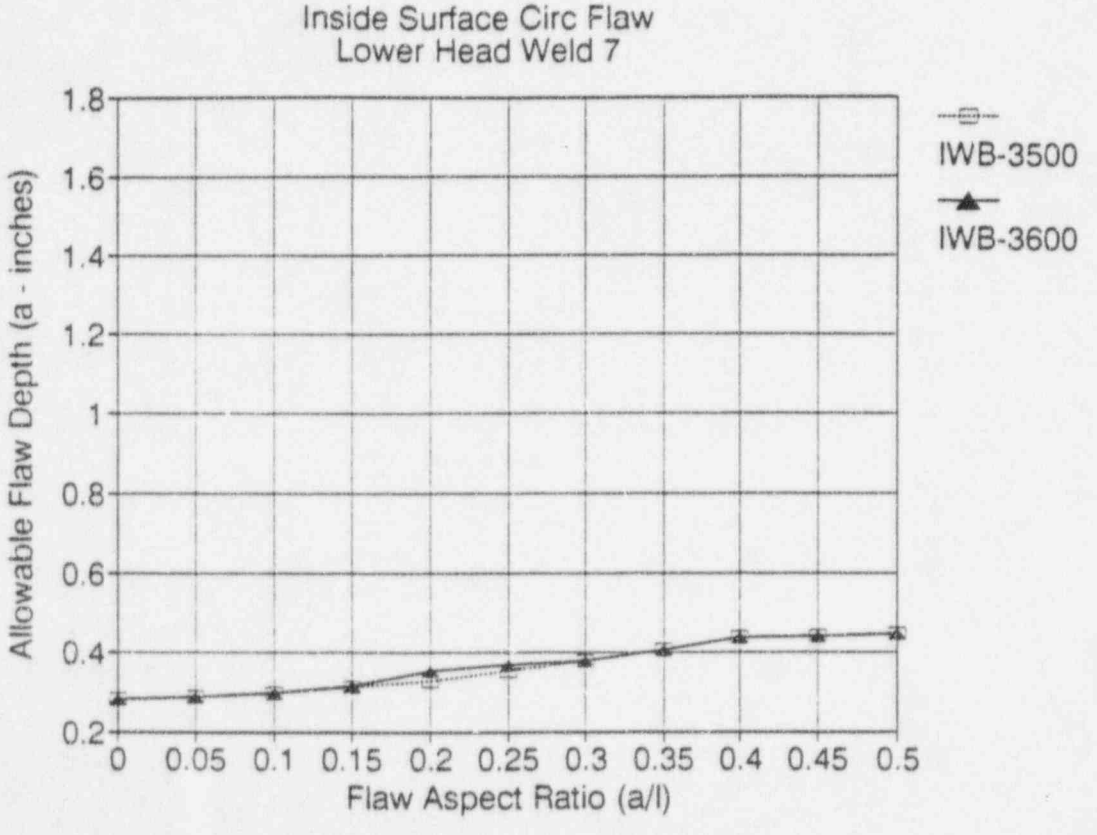

Figure I-1. Flaw Acceptance Diagram For Inside Surface Flaws (Group I)

Note: Flaw depth includes thickness of cladding.

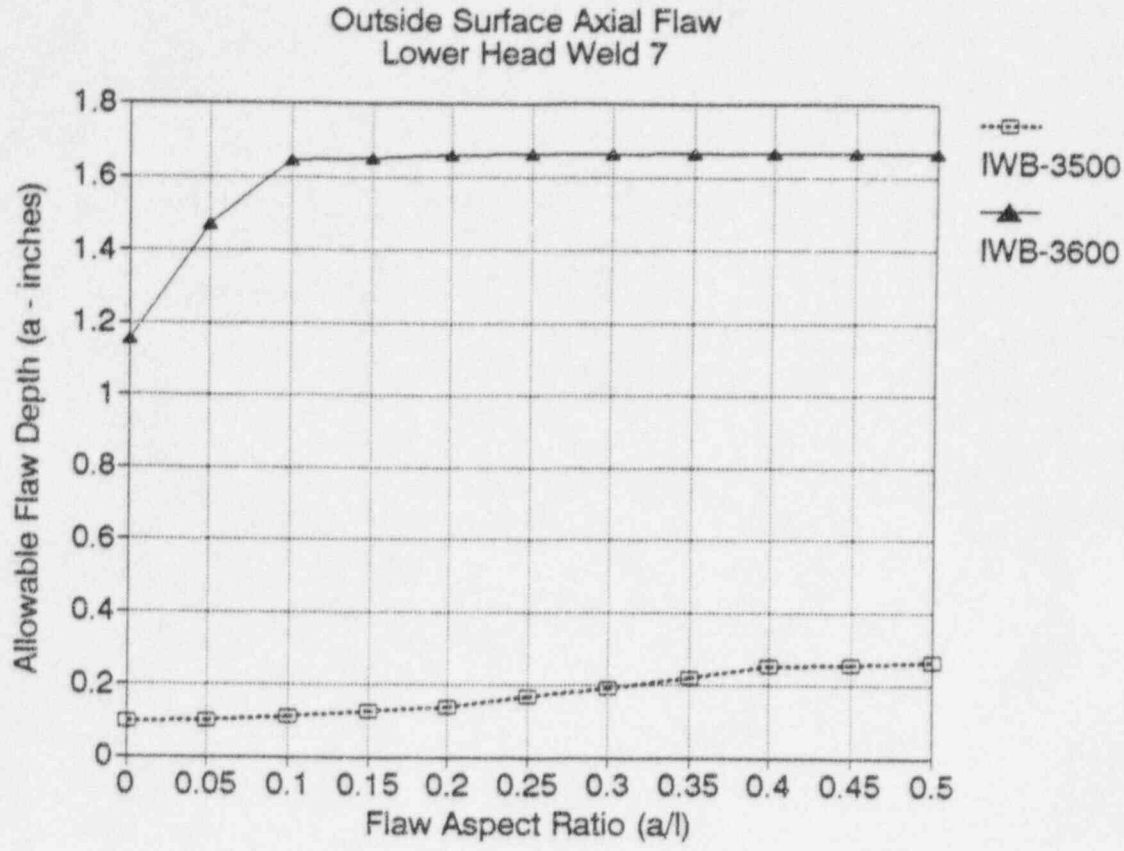

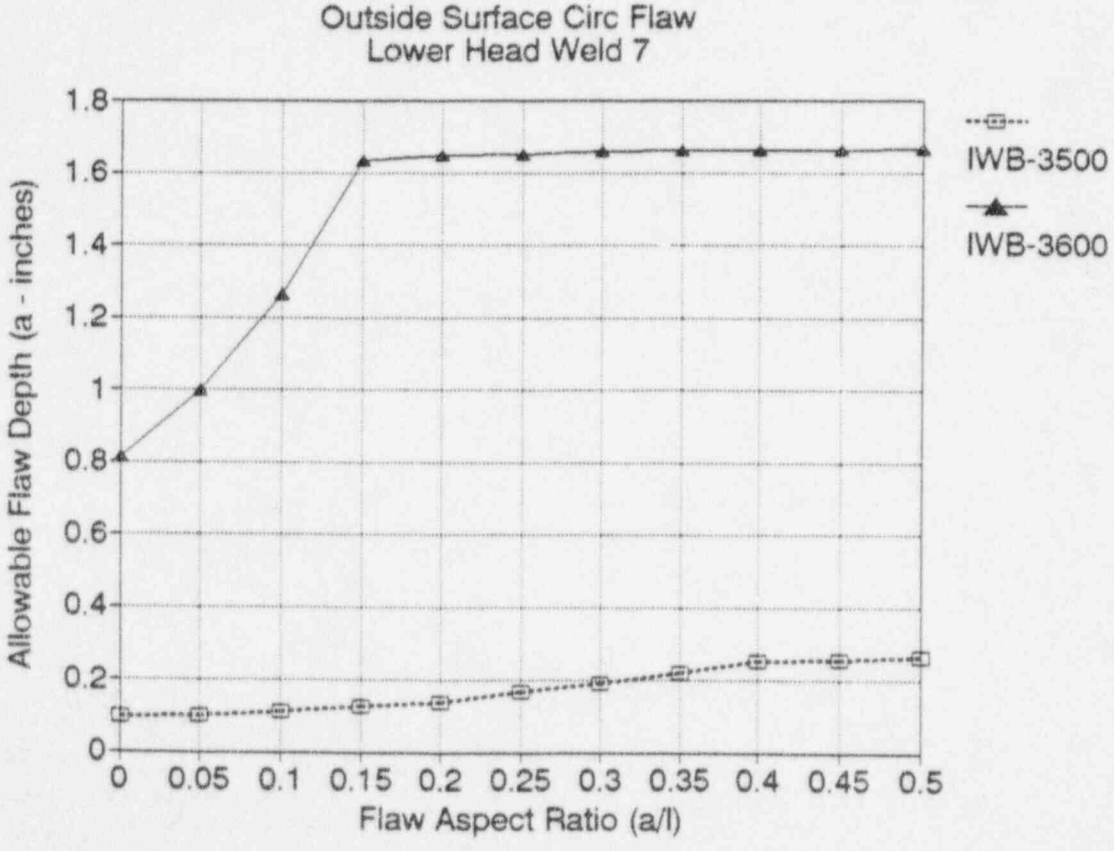

Figure I-2. Flaw Acceptance Diagram for Outside Surface Flaws (Group I)

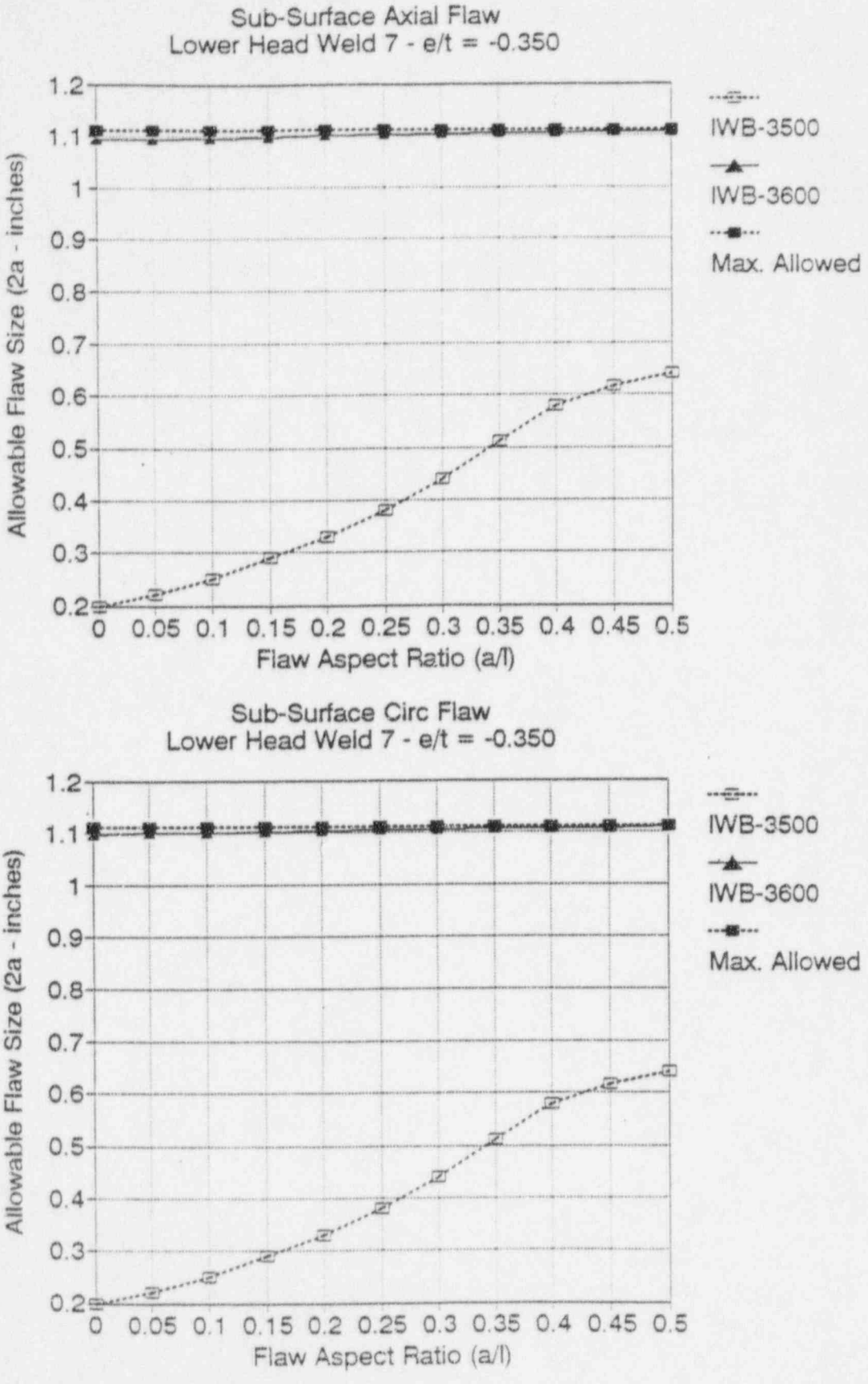

Figure I-3. Flaw Acceptance Diagram for Subsurface Flaws with Eccentricity Ratio of -0.35 (Group I)

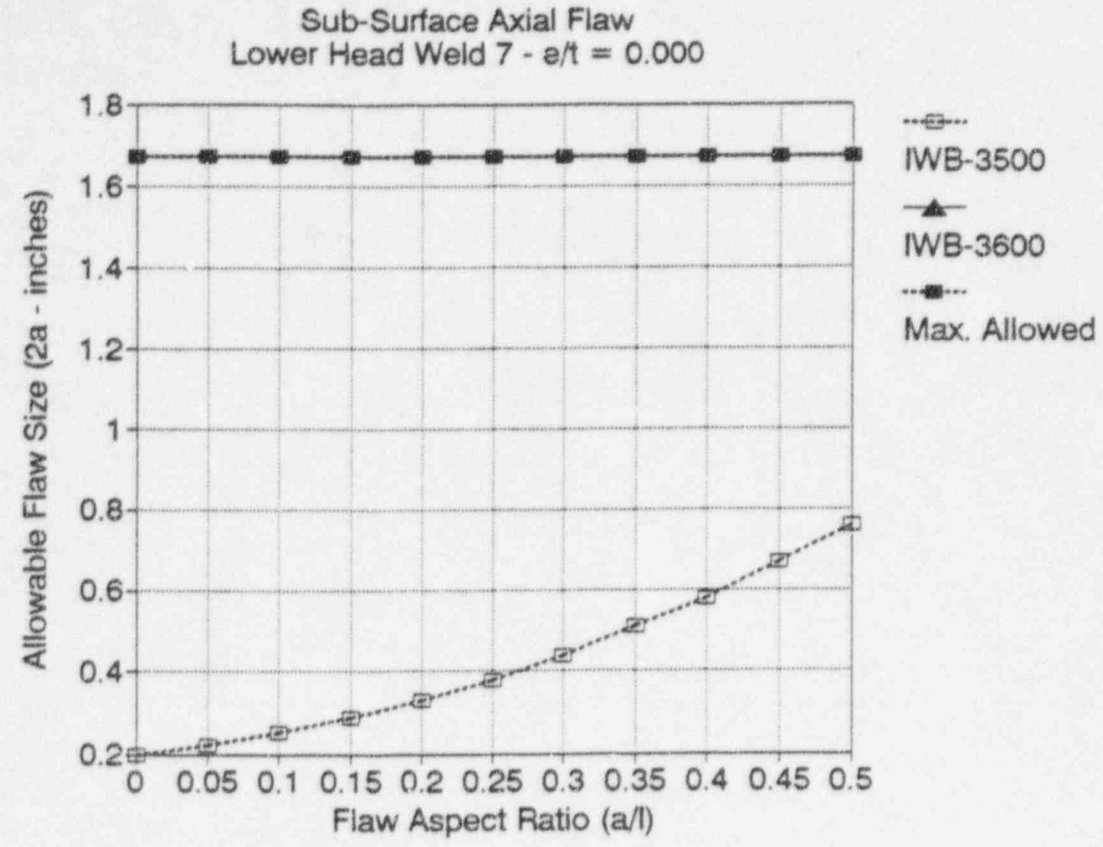

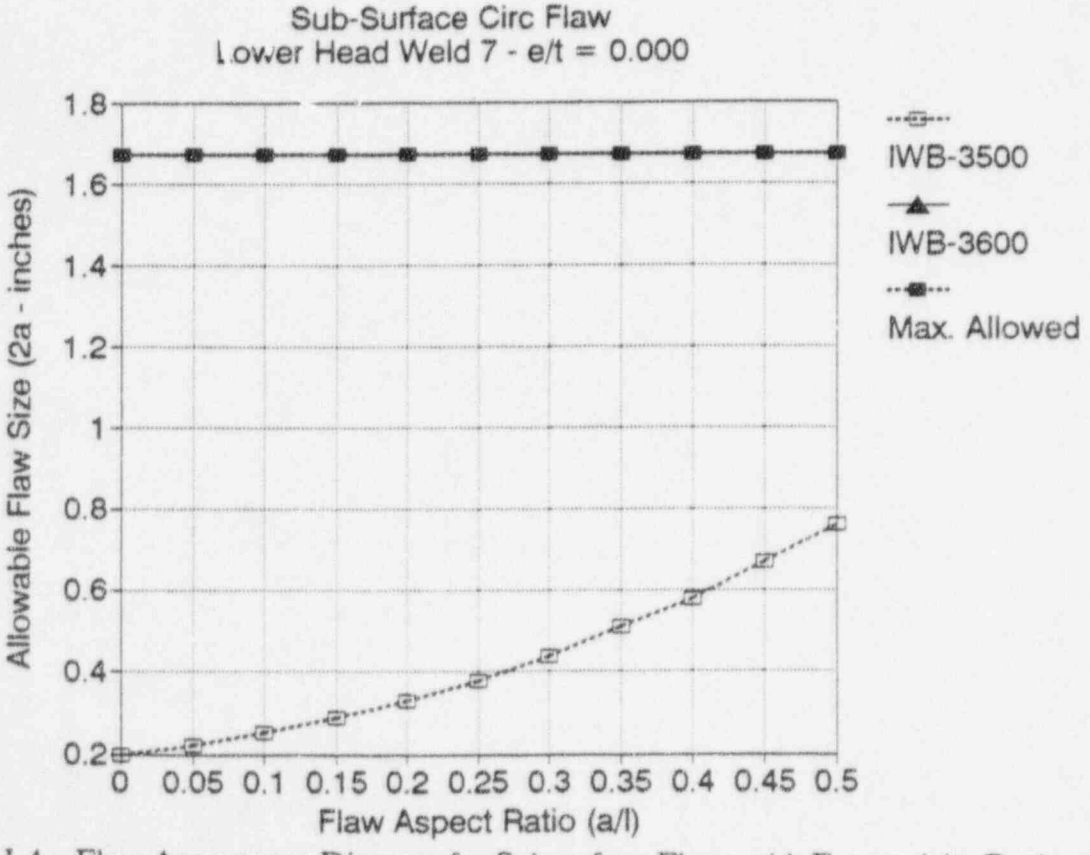

Figure I-4. Flaw Acceptance Diagram for Subsurface Flaws with Eccentricity Ratio of 0.0 (Group I)

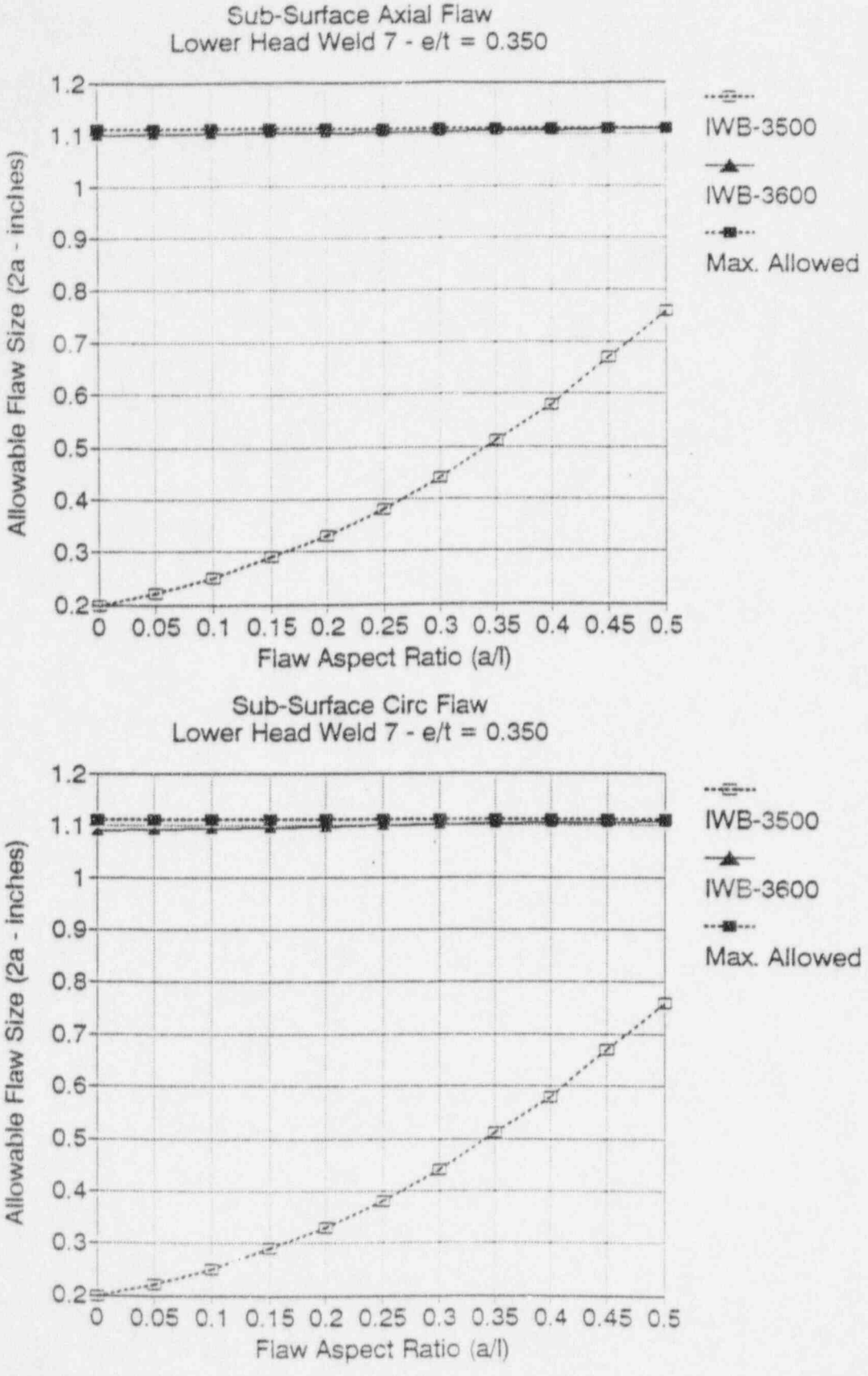

Figure I-5. Flaw Acceptance Diagram for Subsurface Flaws with Eccentricity Ratio of 0.35 (Group I)